

รายงานวิจัยฉบับสมบูรณ์

โครงการ ฤทธิ์ของสารสกัดจากชาเขียวในการป้องกันการเปลี่ยนแปลง ในเซลล์ท่อไตที่เกิดจากการเหนี่ยวนำของอ๊อกซาเลท

โดย ดร.รัตติยาภรณ์ กัลยา

รายงานวิจัยฉบับบสมบูรณ์

โครงการ ฤทธิ์ของสารสกัดจากชาเขียวในการป้องกันการเปลี่ยนแปลง ในเซลล์ท่อไตที่เกิดจากการเหนี่ยวนำของอ๊อกซาเลท

ดร.รัตติยาภรณ์ กัลยา
หน่วยโปรตีโอมิกส์ทางการแพทย์ สถานส่งเสริมการวิจัย
คณะแพทยศาสตร์ศิริราชพยาบาล มหาวิทยาลัยมหิดล

สนับสนุนโดยสำนักงานกองทุนสนับสนุนการวิจัย และมหาวิทยาลัยมหิดล

กิตติกรรมประกาศ

โครงการวิจัยนี้ผู้วิจัยขอขอบพระคุณ ศ.นพ.วิศิษฎ์ ทองบุญเกิด ที่ให้ความกรุณาเป็นอาจารย์ที่ ปรึกษาโครงการและให้คำแนะนำปรึกษาอย่างดียิ่งจนโครงการวิจัยสำเร็จลุล่วงได้ด้วยดี และโครงการวิจัยนี้ ได้รับทุนสนับสนุนการวิจัยจากสำนักงานกองทุนสนับสนุนการวิจัย (สกว.) และทุนอุดหนุนการวิจัยจาก มหาวิทยาลัยมหิดล ผู้วิจัยจึงขอขอบพระคุณเป็นอย่างสูงต่อการสนับสนุนโครงการวิจัยเรื่องฤทธิ์ของสาร สกัดจากชาเขียวในการป้องกันการเปลี่ยนแปลงในเซลล์ท่อไตที่เกิดจากการเหนี่ยวนำของอ๊อกซาเลท จาก สกว.และมหาวิทยาลัยมหิดลมา ณ ที่นี้ด้วย

ดร.รัตติยาภรณ์ กัลยา

Abstract

Project Code: TRG5480005

Project Title: Protective effect of green tea extract against oxalate-induced changes in renal

tubular cells: possibility for prevention of renal fibrosis

Investigator: Rattiyaporn Kanlaya (Ph.D.), Medical Proteomics Unit, Mahidol University

E-mail Address: r.kanlaya@gmail.com

Project Period: 2 years

This study aims to apply a natural compound to prevent the process of epithelial mesenchymal transition (EMT) induced by oxalate treatment. Sodium oxalate was used to induce tubular cell injury and EMT in Mardin-Darby Canine kidney (MDCK) cell line. Oxalate exposure is known to induce cellular injury and presumed to be involved in the pathogenesis of calcium oxalate stone formation. Epigallocatechin gallate (EGCG) extracted from green tea (Camellia Sinensis) was assessed for its anti-fibrotic and anti-oxidative property. EGCG is the most abundant polyphenol compounds found in green tea with high potential anti-oxidative property. Microscopic examination revealed that oxalate could induce morphological change of MDCK from a cobble-stone like into fibroblast-like shap within 24 h. In addition, immunoblotting and indirect immunofluorescence assay confirmed that oxalate-treated cells gained mesenchymal phenotypes by increase expression of vimentin and fibronectin while decrease expression of epithelial markers including, E-cadherin, cytokeratin, occludin, and ZO-1. Interestingly, pretreatment of MDCK cells with 25 µM EGCG could prevent EMT induced by oxalate exposure as it could retain typical epithelial cell morphology as well as epithelial protein markers. The molecular mechanism underlying the prevention of EGCG is most likely by reduction of intracellular reactive oxygen species (ROS) production. Taken together, this study demonstrated a preventive effect of EGCG against oxalate-induced EMT in renal tubular cells which would shed light on the development of novel therapeutics of renal fibrosis in the near future.

Keywords: Epithelial mesenchymal transition, Oxalate, EGCG, Renal fibrosis

บทคัดย่อ

รหัสโครงการ: TRG5480005

ชื่อโครงการ: ฤทธิ์ของสารสกัดจากชาเขียวในการป้องกันการเปลี่ยนแปลงในเซลล์ท่อไตที่เกิดจากการ เหนี่ยวนำของอ๊อกซาเลท

ชื่อนักวิจัย: ดร.รัตติยาภรณ์ กัลยา สังกัดหน่วยโปรตีโอมิกส์ทางการแพทย์ สถานส่งเสริมการวิจัย คณะแพทยศาสตร์ศิริราชพยาบาล มหาวิทยาลัยมหิดล

E-mail Address: r.kanlaya@gmail.com

ระยะเวลาโครงการ: 2 ปี

วัตถุประสงค์ของการศึกษาครั้งนี้เพื่อทดสอบฤทธิ์ของสารสกัดจากธรรมชาติเพื่อใช้ในการป้องกัน การเปลี่ยนแปลงในเซลล์ท่อไตที่เกิดจากการเหนี่ยวนำของอ๊อกซาเลท การศึกษาก่อนหน้านี้รายงานว่าอ๊อก ซาเลทเป็นสารที่สามารถเหนี่ยวนำให้เซลล์บาดเจ็ดได้และคาดว่าภาวะนี้เป็นกลไกหนึ่งที่นำไปสู่การเกิด พยาธิสภาพของโรคนิ่วในไตชนิดแคลเซียมอ๊อกซาเลท ในการศึกษาครั้งนี้จึงใช้โซเดียมอ๊อกซาเลท เหนี่ยวนำให้เซลล์ท่อไตบาดเจ็บและเกิดกระบวนการเปลี่ยนแปลงจาก epithelial ไปเป็น mesenchymal (Epithelial mesenchymal transition หรือ EMT) และทดสอบฤทธิ์ของ Epigallocatechin gallate (EGCG) ซึ่งเป็นสาร polyphenol ที่พบมากในชาเขียว และมีฤทธิ์ต้านอนุมูลอิสระ (Anti-oxidant) ว่าสามารถต้านการ เกิดพังผืด (Anti-fibrotic property) และต้านอนุมูลอิสระในสภาวะนี้ได้หรือไม่ ผลการทดลองพบว่าโซเดียม อ๊อกซาเลทสามารถเหนี่ยวนำให้เกิดการเปลี่ยนแปลงทางสัณฐานวิทยาของเซลล์์ท่อไตให้คล้ายกับเซลล์ fibroblast ได้ภายใน 24 ชั่วโมง นอกจากนี้ผลการแสดงออกของโปรตีนโดยวิธี Immunoblotting และ Indirect immunofluorescence ชี้ให้เห็นว่าเซลล์ท่อไตมีการเปลี่ยนแปลงฟิโนไทป์จาก epithelial cells ไป เป็น mesenchymal cells โดยมีการแสดงออกของโปรตีนที่บ่งชี้ฟิโนไทป์ของ mesenchymal cell เพิ่มขึ้น ได้แก่โปรตีน vimentin และ fibronectin ในขณะที่โปรตีนที่บ่งชี้ฟิโนไทป์ของ epithelial cell ลดลง ได้แก่ โปรตีน E-cadherin, cytokeratin, occludin และ ZO-1 การทดสอบฤทธิ์ของสาร EGCG โดยนำมาเลี้ยง ร่วมกับเซลล์ก่อนการเหนี่ยวนำด้วยโซเดียมอ๊อกซาเลทพบว่า สาร EGCG ที่ความเข้มข้น 25 µM สามารถ ้ต้านการเปลี่ยนแปลงของเซลล์ท่อไตจากการเหนี่ยวนำของอ๊อกซาเลทได้ โดยเซลล์สามารถคงสัณฐานและ ระดับการแสดงออกของโปรตีนที่บ่งชี้ฟิโนไทป์ของ epithelial cellได้ กลไกระดับโมเลกุลที่ทำให้ EGCG สามารถต้านการเกิด EMT ได้น่าจะเป็นเพราะความสามารถในการลดอนุมูลอิสระภายในเซลล์ จากผลการ ทดลองทั้งหมดนี้ชี้ให้เห็นว่าสารสกัด EGCG จากชาเขียวมีฤทธิ์ในการต้านการเกิด EMT ที่เหนี่ยวนำโดย อ๊อกซาเลทได้ ซึ่งความรู้จากการศึกษาครั้งนี้จะนำไปสู่หนทางในการพัฒนาแนวทางการรักษาใหม่สำหรับ การเกิดพังผืดในไตในอนาคต

คำหลัก : การเปลี่ยนแปลงของเซลล์ท่อไต, อ๊อกซาเลท, สารสกัดชาเขียว, การเกิดพังผืดในใต

Introduction

Unsolved chronic kidney diseases (CKD) mostly leads to end-stage renal failure due to kidney fibrosis. Renal fibrosis or scar in the kidney requires a number of cellular events and mediators to act in concert that result in the deterioration of kidney function (1). The risk factors contributing to the development of fibrous kidney can be derived from various primary causes such as hypertension, diabetes mellitus, glomerulopathies and cell injury due to toxic substances, etc (1, 2). Recently, the epithelial plasticity known as epithelial mesenchymal transition (EMT) has been discovered to associate with renal fibrogenesis in injured kidney of adults (3-6). EMT indeed is the important process required during normal embryonic development. EMT process allows the anchored epithelial cells to rearrange into a developing organ (7). During EMT, typical morphology of epithelial cell turns into spindle-shape of fibroblast and the cell lose its polarity (7, 8). Importantly, cells lose their epithelial phenotypes while gain the mesenchymal characteristics. Those include down expression of E-cadherin and tight junction protein ZO-1, resulting in disintegration of cell-cell contact. Cells undergoing EMT up-regulate the mesenchymal marker, including fibroblast-specific protein 1 (FSP1) and vimentin. In addition, over production of extracellular matrix proteins (such as fibronectin and collagen) and metalloproteases was found during EMT induction (7, 9). Moreover, induction of EMT results in actin reorganization and formation of actin stress fiber. Expression of FSP1 was found in acute and chronic injured renal tubular cell, suggested the involvement of EMT in response to tissue repairing (10). Interestingly, study using transgenic mice model that allowed discrimination of the cell origin demonstrated that one third of renal interstitial fibroblasts were derived from tubular epithelial cells underwent EMT (11). Strong association between EMT and renal fibrosis was confirmed in the study provided by Rastaldi et al, (12). They demonstrated that EMT features were observed in 133 human renal biopsies and also correlated with a degree of interstitial damage. In addition, it has been reported that kidney epithelial cells of collecting duct treated with insulin-like growth factors (IGFs) and transforming growth factor-beta 1 (TGB-beta1) were induced to undergo EMT (13). Most recently, EMT marker Twist was evidenced in renal biopsies from nephrolithiasis patients with large calculi (14). These aforementioned studies suggest that renal epithelial cells can transform through EMT mechanism in response to some stimuli and might participate in the pathogenesis of renal fibrosis.

At present, drinking of green tea is more widespread because of the beneficial effects to prevent from lifestyle-related diseases, including cancer and cardiovascular diseases (15-17). Medical studies have demonstrated that green tea contains not only an anti-oxidative but also anti-

allergic, anti-carcinogenic and anti-bacterial effects (15, 18-20). Among the polyphenols found in green tea extract, (-)- epigallocatechin gallate (EGCG) is the major abundant catechins with high potential anti-oxidative property (21, 22). Anti-oxidative effect of green tea was demonstrated in rats with ethylene glycol-induced nephrolithiasis (23). Rats treated with green tea decreased excretion of urinary oxalate and calcium oxalate deposition while increased superoxide dismutase (SOD) activity. Moreover, lower number of cell apoptosis was found when compared to the control group. These findings suggest the inhibitory effect of green tea on calcium oxalate formation by its antioxidative property (23). Accordingly, green tea could attenuate the development of nephrolithiasis induced by oxalate treatment in rats. Green tea could protect the rats from oxalate-induced cytotoxic effect by reducing free radical production and lower number of crystal formation in the kidney (24). In addition, protective effect of green tea against nephrotoxicity of reserpine, the important anti-hypertensive drug was demonstrated in rat model. Administration of green tea extract in rats treated with reserpine showed a significant recovery of kidney proximal tubule cells when compared to the control groups (25). In addition, epigallocatechin gallate (EGCG) could protect human lens epithelial cells from H₂O₂-induced apoptosis through the series of caspases and also modulation of the Bcl-2 family and the MAPK and Akt pathway (22). Recently, anti-fibrotic property of green tea has been demonstrated in an experimental hepatic fibrosis (26) and a pulmonary fibrosis (27). Experimental hepatic fibrosis in rats was induced by dimethylnitrosamine (DMN). However, administration of green tea extract could prevent the rats from development of fibrosis. The histophatological results of kidney tissues revealed that the lower hydroxyproline content was found in green tea treated rats. These results indicated the lower deposition of collagen and down expression of collagen type 1 (26). In addition, administration of EGCG in rat model of bleomycin-induced pulmonary fibrosis demonstrated the involvement of Nrf2-Keap1 signaling to enhance the anti-oxidative activities of phase II enzymes, including glutathione-Stransferase (GST) and NAD(P)H:quinine oxidoreductase 1 (NQO1). This cascade could attenuate the subsequent inflammation. These findings suggest that green tea extract contains the combination of beneficial effects on anti-inflammation, anti-oxidative stress and anti-fibrosis (27).

Therefore, better understanding in the progression of EMT and modulation on this pathogenic mechanism during renal epithelial cell damage would benefit a prevention of fibrosis. This study thus aims to apply a natural compound to reduce or prevent the process of EMT induced by oxalate treatment. In this study, sodium oxalate was used to induce tubular cell injury and EMT in Mardin-Darby Canine kidney (MDCK) cell line. Oxalate exposure is known to induce

cellular injury and presumed to be involved in the pathogenesis of calcium oxalate stone formation (28-30). Epigallocatechin gallate (EGCG), the most abundant polyphenol compounds found in green tea (*Camellia Sinensis*) with high potential anti-oxidative property was assessed for its anti-fibrotic and anti-oxidative property.

Materials and Methods

Cell culture

Mardin-Darby Canine kidney (MDCK), a distal tubular epithelial cell line was cultured in growth Eagle's minimum essential medium (MEM) (Gibco; Grand Island, NY) [MEM supplemented with 10% heat-inactivated fetal bovine serum (FBS) (Gibgo) in the presence of 100 U/ml penicillin G and 100 mg/ml streptomycin (Sigma, St.Louis, MO)]. Cells were maintained in a humidified incubator at 37°C with 5% CO₂.

Cytotoxicity test of EGCG by cell viability assay

MDCK cells were seeded in 24-well plate in growth medium 1 day prior to experiment. Cells were treated with 12, 25 and 50 µM EGCG for 1 h. Cells left untreated were used as a control of treatment. Thereafter, treated cells were detached by trypsinization and determined cell viability by trypan blue exclusion assay.

Induction of epithelial mesenchymal transition (EMT)

MDCK cells were seeded into 6-well plate and cultured in a growth medium for 24 h. Prior to treatment, cells were washed with serum-free medium and then treated with 500 μM sodium oxalate in maintenance MEM medium [MEM supplemented with 1% heat-inactivated FBS] for 24 h.

Morphological study and immunofluorescence microscopy

Cell morphology was observed under a phase contrast microscope (Olympus CKX41; Tokyo, Japan) at the beginning and 24 h after treatment. For immunofluorescence staining, cells were grown on coverslip and EMT was induced as previously described. Cells were processed for immunofluorescence staining of vimentin, fibronectin, cytokeratin, and ZO-1 using corresponding antibodies. In brief, cells were fixed with 3.7% (V/V) formaldehyde in PBS for 10 min and then permeabilized with 0.2% triton X-100 in PBS for 10 min. After washing step, cells were incubated overnight with primary antibody at dilution of 1:50 (in 1%BSA/PBS) at 4°C. Corresponding secondary antibody was used at dilution of 1:2000 (in 1%BSA/PBS) and incubated at RT for 1 h. The nuclei were counterstained with Hoechst dye (Invitrogen/Molecular Probes) at dilution of 1:1000. Thereafter, the cells were extensively washed with PBS and mounted onto a glass slide using ProLong Gold antifade reagent (Invitrogen). The images were captured under the Nikon Eclipse 80i fluorescence microscope (Nikon; Tokyo, Japan).

Prevention of EMT by epigallocatechin gallate (EGCG)

MDCK cells were cultured in growth medium for 24 h and were pretreated with 25 μ M EGCG in maintenance medium (MEM containing 1% heat inactivated FBS) for 1 h followed by sodium oxalate to complete 24 h-incubation. The cells treated with sodium oxalate without EGCG and those left untreated will serve as positive and negative controls, respectively.

Immunoblotting

The cells were induced to undergo EMT as previously described. Cell lysate was prepared in sample buffer (Leammli's buffer) and 30 µg of total protein were resolved by SDSPAGE under reducing and denaturing condition. The resolved protein bands were electrophoretically transferred onto a nitrocellulose membrane and non-specific bindings were blocked by 5% non-fat milk in PBS. The membrane was detected for the expression of vimentin, E-cadherin, occludin, catalase, and GAPDH (as a loading control) using specific antibodies (all was purchased from Santa Cruz Biotechnology, Santa Cruz, CA). After probing with corresponding secondary antibodies, the reactive protein bands were visualized by SuperSignal West Pico chemiluminescence substrate (Pierce Biotechnology, Inc., Rockford, IL) and autoradiography.

Detection of reactive oxygen species (ROS)

ROS production inside the cells was analyzed by flow cytometry. Briefly, the cells were collected as suspension by trypsinization and pretreated with 25 μ M EGCG for 20 min. Thereafter, the cells were loaded with 50 μ M dichlorofluorescein diacetate (DCFH-DA) for 30 min, followed by oxalate exposure for 30 min. The cells left untreated and treated with 0.02%H₂O₂ for were served as negative and positive control, respectively. After complete incubation period, the cells were kept on ice and immediately analyzed by FACScan equipped with CellQuest software (Benton Dickinson; Franklin Lake, NJ).

Statistical analysis

Data were presented as mean ± SD. The significant difference among groups was performed by One-Way ANOVA with Tukey's HSD Post-hoc test using SPSS (version 11.5). Statistical significance was considered at P-value less than 0.05.

Results

Sodium oxalate induced EMT in MDCK cells

MDCK cells were seeded into 6-well plate and cultured in a growth medium for 24 h prior to treat with 500 µM sodium oxalate for 24 h. As expected, Oxalate-treated MDCK cells underwent morphological change into more fibroblast-like in shape within 24 h compared to those left untreated (Figure 1). A number of calcium oxalate monohydrate crystals were observed in the treated condition. To examine whether oxalate exposure could induce EMT in renal epithelial cells, Western blot analysis and indirect immunofluorescence assay (IF) were performed to validate expression of epithelial and mesenchymal protein markers. The results by Western blot analysis revealed that oxalate-treated cells increased expression of vimentin (mesenchymal marker) whereas decreased expression of E-cadherin and occludin (epithelial markers) when compared to those of untreated cells (Figure 2). In according to Western blot results, IF revealed the increased level of vimentin and fibronectin (Figure 3A) while decreased level of cytokeratin, occludin and ZO-1 (Figure 3B). These findings suggest that MDCK were induced to undergo EMT by sodium oxalate exposure within 24 h.

Cytotoxicity test of EGCG in MDCK cells

To examine cytotoxicity of EGCG in MDCK cells, the cells were treated with various dose of EGCG for 1 h and cell viability was determined by trypan blue exclusion assay. The results showed that more than 95% cell viability could be observed in the control cells left untreated. Similar results were obtained when cells were treated with EGCG at 12.5 and 25 μ M. However, incubation with higher concentration of EGCG at 50 μ M could apparently reduce cell survival when compared to the control cells left untreated (92.5% compared to 98.48%; P=0.0543). Percentage of cell viability after EGCG treatment was shown in **Figure 4**. These results suggest that low concentrations of EGCG at 12.5 and 25 μ M for 1 h did not significantly affect to MDCK cell survival. Therefore, pretreatment of cells with 25 μ M for 1 h was used in further experiments.

Preventive effect of EGCG against sodium oxalate-induced EMT

MDCK cells were pretreated with 25 μ M EGCG in maintenance medium (MEM containing 1% heat inactivated FBS) for 1 h followed by 500 μ M sodium oxalate to complete 24 h-incubation. Cells treated with 500 μ M sodium oxalate without EGCG and cells left untreated were served as positive and negative control of EMT induction, respectively. Epithelial and EMT protein markers were evaluated by Western blot analysis and indirect immunofluorescence staining. Western blot

analysis showed a slight increased vimentin expression, while E-cadherin and occludin were decrease when compared to the control cells. However, expression of vimentin, E-cadherin, and occludin was comparable to basal level when cells were pretreated with 25μM EGCG (**Figure 5**). In addition, immunofluorescence assay showed that EMT protein markers including vimentin, and fibronectin expression were obviously induced in MDCK cells treated with sodium oxalate for 24 h compared to control cells left untreated (**Figure 6A**). In contrast, epithelial protein markers including cytokeratin, occludin, and ZO-1 were down-regulated in EMT-induced cells. However, expression of these protein markers were found comparable to those of control cells when cells were pretreated with 25 μM EGCG (**Figure 6B**). These results suggest that pretreatment of cells with 25 μM EGCG could prevent the cells from sodium oxalate-induced EMT process.

Reduction of reactive oxygen species (ROS) by EGCG

Intracellular ROS production was analyzed by flow cytometry. The cells were collected as suspension and incubated with or without EGCG. Thereafter, the cells were loaded with dichlorofluorescein diacetate (DCFH-DA) for 30 min, followed by oxalate exposure. Cells treated with H_2O_2 were served as positive control. Cells left untreated were served as negative control. Intracellular ROS production was basically found in the control cells (less that 5%); however, it was markedly increased when cells were treated with H_2O_2 . Cells underwent EMT process by sodium oxalate induction significantly produced more ROS inside the cells compared to those of control cells. As expected, pretreated the cells with 25 μ M EGCG before sodium oxalate treatment can significantly lower intracellular ROS production (**Figure 7**). The results confirmed the anti-oxidant property of EGCG and it is possible that EGCG might prevent the cells from undergoing EMT by mediated through intracellular ROS production.

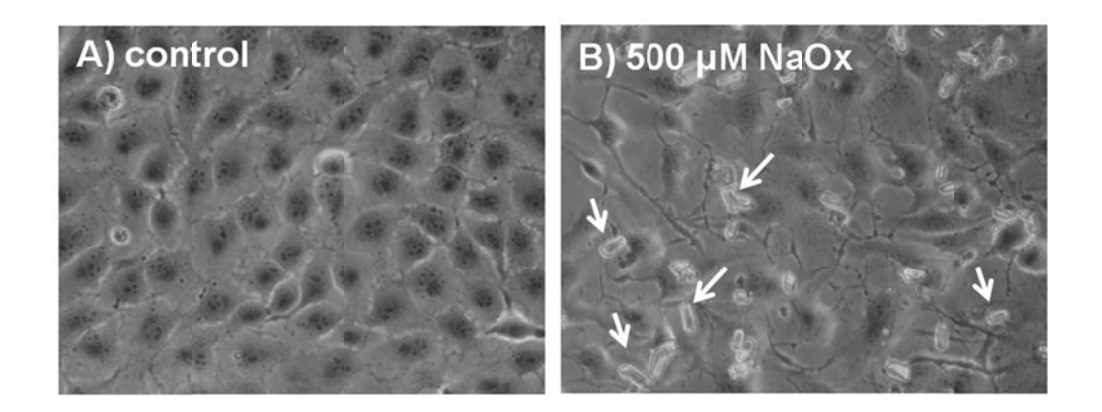


Figure 1. Morphological change induced by oxalate exposure. A) Control MDCK cells left untreated was appeared as a cobble-stone like morphology whereas B) the cells treated with 500 μ M sodium oxalate were induced to undergo morphological change within 24 h as more fibroblast-like in shape have been observed. Calcium oxalate monohydrate crystals (COM), the pathologic crystals were observed under treatment with 500 μ M sodium oxalate as indicated by arrows in B). Original magnification = 400X.

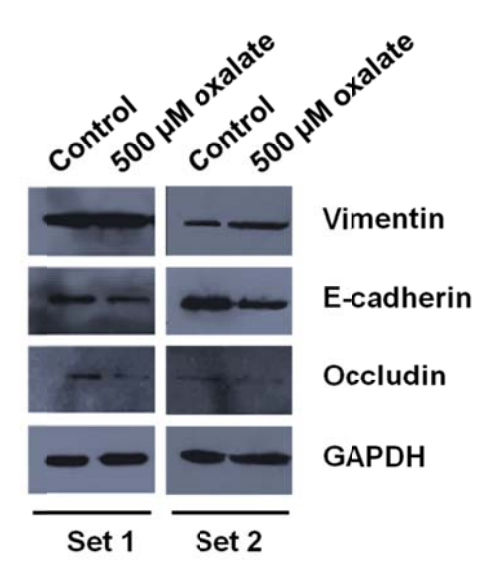


Figure 2. Western blot analysis to detect expression of vimentin (EMT marker), E-cadherin and occludin (epithelial markers). Vimentin was increase while E-cadherin and occludin were decreased in sodium oxalate-treated MDCK cells. GAPDH expression was used to control equal protein loading.

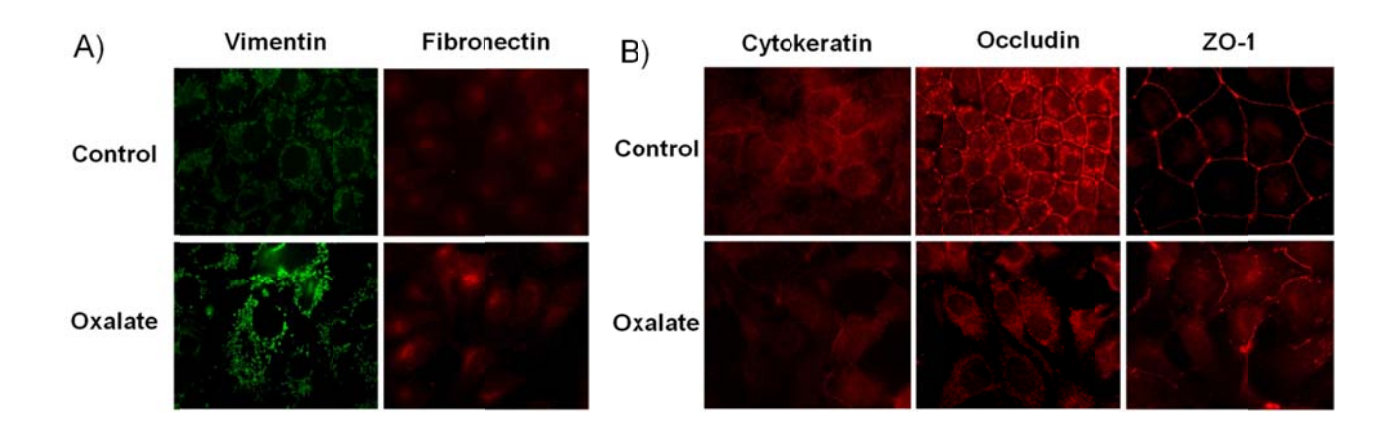


Figure 3. Alterations in expression level of EMT and epithelial markers by indirect immunofluorescence after sodium oxalate exposure. A) Increased level of vimentin and fibronectin (EMT protein markers while B) decreased level of cytokeratin, occludin, and ZO-1 (epithelial protein markers) were observed in sodium oxalate-treated MDCK cells.

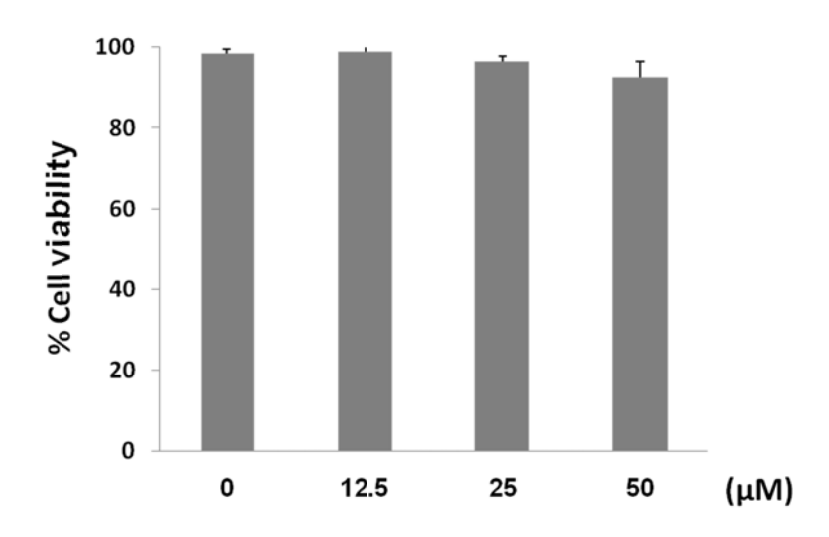


Figure 4. Cytotoxic effect of EGCG to MDCK cells. Cells were treated with various dose of EGCG for 1 h and then trypsinized for determination of cell viability by trypan blue exclusion assay.

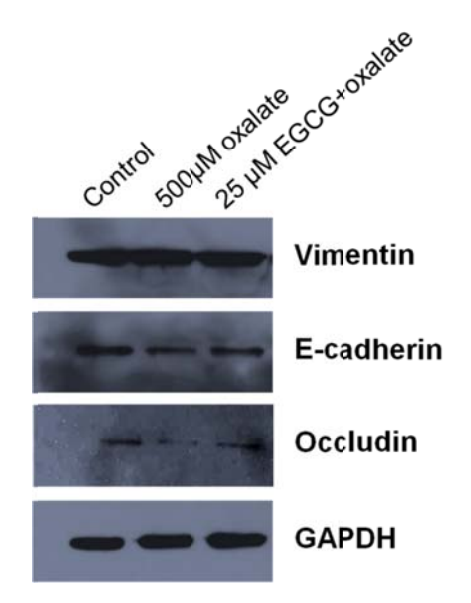


Figure 5. Western blot analysis of EMT and epithelial markers after pretreatment with EGCG. Western blot analysis showed a slight increased vimentin expression, while E-cadherin and occludin were decreased expression when compared to the control cells. Basal level of vimentin, E-cadherin, and occludin was found when cells were pretreated with EGCG. GAPDH expression was used to control equal protein loading

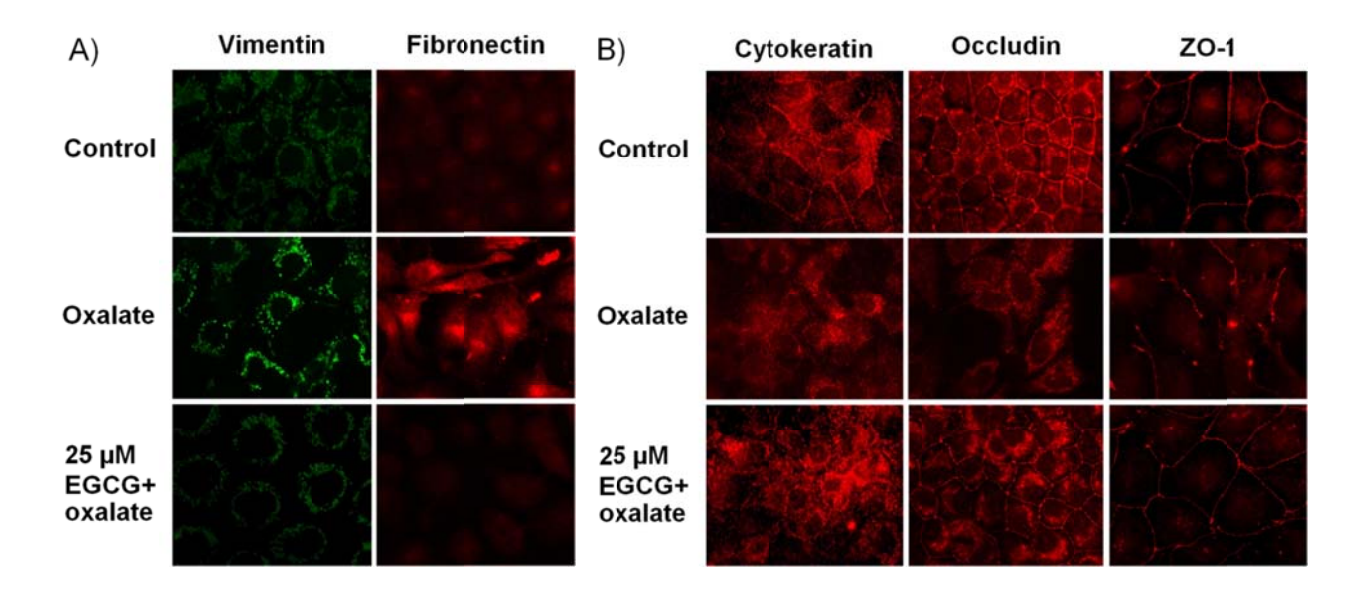


Figure 6. Expression of A) vimentin, fibronectin, B) cytokeratin, occludin, and ZO-1 was comparable to that of control cells when MDCK cells were pretreated with 25μM EGCG for 1 h before sodium oxalate exposure.

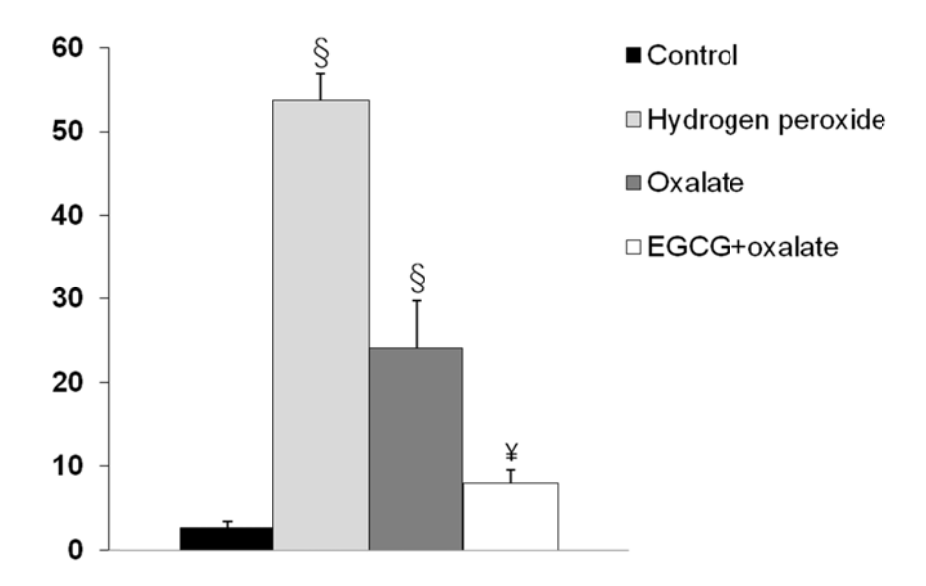


Figure 7. Preventive effect of EGCG by lower production of intracellular reactive oxygen species (ROS). ROS production was measured by DCFH-DA loading and analyzed by flow cytometry. MDCK cells left untreated and treated with hydrogen peroxide were serve as negative and positive control, respectively. Sodium oxalate treatment could induce ROS production significantly compared to the basal stage (*P*<0.0001). Pretreatment with EGCG before sodium oxalate treatment could markedly reduce production of ROS (Oxalate VS EGCG+oxalate, *P*<0.0002). P<0.05 was considered statistical significant. Symbols: §, statistically significant versus control; ¥, statistically significant versus oxalate.

Discussion

There is an increasing evidence for EMT and renal fibrosis over time. Strutz et al, firstly reported the expression of fibroblast-specific protein 1 (FSP-1), which suggest the conversion of epithelial cells into fibroblast type in murine fibrotic kidney (10). In the context of renal stone diseases and EMT, Boonla et al, demonstrated that signs of tubular EMT can be found in nephrolithiasis patients with staghorn calculi. The plausible cause of tubular EMT might be the production of a well-know fibrotic factor TGF-beta 1, which was strongly positive in fibrotic kidney tissues (31). Most recent study in nephrolithiasis patients with large calculi evidenced that the EMT marker Twist was markedly expressed in tubular epithelial cells of kidney biopsies from patients compared to those obtained from normal kidneys. The researchers also demonstrated the inverse correlation of Twist and E-cadherin (epithelial marker) expression and suggested that Twist might be used as an index to predict the progression of renal fibrosis in patients (14). For this reason, it is in need of seeking for the effective therapeutics to prevent the progression of renal fibrosis.

In this study, we thus test the anti-fibrotic property of EGCG against EMT induction by high sodium oxalate. We demonstrated that high concentration of oxalate can induce fibroblast-like feature as shown in Figure 1. Treatment with 500 µM sodium oxalate for 24 h could induce morphological changes of the cells from cobble stone-like into more spindle of fibroblast-like compared to the control cells with unchanged. Interestingly, pretreatment of 25 µM EGCG follow by sodium oxalate could prevent the cells from deteriorate effect. Higher concentration of EGCG at 50 µM; however, did not show protective effect but rather provided cytotoxic effect (data not shown) supporting a number of studies that revealed the pro-oxidative property of EGCG in inbition of cell proliferation and induction of apoptosis (32-34). Previous study reported that EGCG supplementation could attenuate the development of nephrolithiasis in rat by lower number of crystal formation in kidney (23, 35). We also observed a lower number of COM crystals formed under EGCG treated condition compared to those treated with oxalate alone. Interestingly, typical calcium oxalate dihydrate (COD) crystals with octahedral shape could be observed in MDCK cells pretreated with EGCG before oxalate treatment (data not shown). The results suggest that EGCG treatment favors COD crystallization after treatment with high concentration of oxalate. It might be possible that EGCG affect COM crystal formation by shifting pH of the solution to become higher (more basic pH). Retrospective study in renal stone patients revealed that urinary pH could influence the type of crystals formed. They found that COD crystals were common in patients with higher urine pH (36). We observed that MEM containing 25 μM EGCG has higher pH (approx. pH

8) compared to that of MEM (pH 7.4) alone. It is also possible that the formation of COD crystals might a direct consequent of the physicochemical property of EGCG when interacts with ions. The precise mechanism underlying this phenomenon requires further investigations.

We sought to determine whether the change in cell morphology in response to high oxalate was implicated with EMT through examination of mesenchymal and epithelial markers. In according to other studies, oxalate-treated cells lost their epithelial features while gained mesenchymal characteristics. We found decreased expression of E-cadherin the hallmark of EMT in cells treated with oxalate; however E-cadherin expression was retained at basal level when cells were pretreated with EGCG (Figure 5). In addition, the results by indirect immunofluorescence revealed that oxalate-treated cells increased expression of vimentin as well as fibronectin, whilst decreased expression of tight junction proteins, occludin and ZO-1. In addition, occludin and ZO-1 redistribution was observed significantly in oxalate-treated cells. Occludin and ZO-1 were markedly disappeared from the TJ locating at the cell borders into the cytoplasm (Figure 3). Expression of vimentin was up-regulated in oxalate-treated cells but decreased into basal level when cells were pretreated with EGCG followed by oxalate (Figure 6). These findings suggest that TJ disruption occurred when cells were underwent EMT-induced by oxalate. Role of EGCG in protection of tight junction (TJ) barrier has been reported. EGCG can preserve the TJ integrity of the colonic epithelial cells induced by IFN-V via STAT1 independent manner (37, 38). In addition, EGCG could reduce ritonavir-induced endothelial permeability through its effective anti-oxidative property (39). In the present study, both immunofluorescence microscopy and Western blot analysis indicated that EGCG could effectively prevent TJ disassembly induced by oxalate.

Several lines of evidence revealed that oxalate could induce reactive oxygen species (ROS) production in renal epithelial cells. Thamilselvan S, et al. demonstrated that peroxidatve injury initiated by oxalate was involved with the induction of TGF-beta1 and the imbalance of redox reaction by glutathione (GSH) system (40). However, GSH redox status as well as the level of TGF-beta1 was restored to the basal stage by addition of antioxidants, including vitamin E and catalase (40). Evidence from clinical studies indicates that oxidative injury was found in kidney of stone patients with hyperoxaluria (41-43). Several markers indicating the occurrence of oxidative stress and epithelial cell injury were found in the urine of the patients, including higher level of malondialdehyde (MDA), glutathione (GSH), beta-galactosidase (GAL) and N-acetyl-beta-glucosaminidase (NAG) (41, 44, 45). Recent study revealed that administration of green tea can prevent renal tubular microstructure change and oxidative stress induced by glyoxylate in mice

(46). One of a molecular mechanism of oxalate-induced oxidative stress is a production of reactive oxygen species (ROS). Anti-oxidant property of EGCG could protect cell injury by hypoxia-induced oxidative stress in MDCK cells (47). Recent studies showed that regulation of NADPH oxidase, a plasma membrane enzyme generated ROS by the activation of protein kinase C (PKC)-alpha and –delta (48). Importantly, TGF-beta1 a potent fibrotic factor that triggers EMT could also induce a production of intracellular ROS of the rat proximal tubular epithelial cells (49) and MDCK cells (50).

Based on these aforementioned studies, ROS and alterations in redox homeostasis potentially contribute to EMT process. Theoretically, EGCG with highly anti-oxidative activity might control the progression of EMT through the action of ROS scavenger. However, there was no direct evidence to show that ROS generation-induced by oxalate could trigger the process of EMT. In attempt to address this issue, we then assayed for the intracellular ROS after oxalate treatment by pulsing with DCFH-DA and analyzed by flow cytometer. As expected, the results clearly showed that intracellular ROS was significantly elevated when cells were induced to undergo EMT by high oxalate concentration compared to the control cells left untreated. Pretreatment with EGCG markedly reduced ROS production induced by oxalate (Figure 7). In consistent with study of peritoneal fibrosis in a mouse model, EGCG could suppress NF-kB activation and ROS generation and thus prevent from progression of peritoneal fibrosis (51). In addition, although we did not investigate whether TGF-beta1 is mediated in ROS generation and the consequent activation/inactivation of the well-known pathways (i.e. SNAII, GSK-3 β and Wnt/ β catenin) to trigger EMT (49, 52), we showed that oxalate could induce EMT phenotype concomitantly with the increased ROS production. EGCG pretreatment could prevent the conversion of epithelial cells into fibroblast-like cells and reduce intracellular ROS to a greater extent that comparable to the basal level.

To our knowledge, this is the first report to demonstrate that high oxalate concentration could induce alteration in epithelial cell shape to become fibroblast-like morphology through the process so-called EMT and a major component of natural green tea extract, EGCG significantly prevents induction of EMT at least by maintaining cell junctional integrity as well as through its antioxidant property to counteract intracellular ROS production. At present, we provide ongoing effort to study the signaling pathways triggered by EGCG in prevention of oxalate-induced EMT. This would pave the way to the understanding of renal fibrogenesis and ultimate goal in therapeutics of renal fibrosis in chronic kidney diseases.

References

- 1. Vilayur E, Harris DC. Emerging therapies for chronic kidney disease: what is their role? Nat Rev Nephrol. 2009;5(7):375-83.
- 2. Brosnahan G, Fraer M. Chronic kidney disease: whom to screen and how to treat, part 1: definition, epidemiology, and laboratory testing. South Med J. 2010;103(2):140-6.
- 3. Guarino M, Tosoni A, Nebuloni M. Direct contribution of epithelium to organ fibrosis: epithelial-mesenchymal transition. Hum Pathol. 2009;40(10):1365-76.
- Kalluri R, Neilson EG. Epithelial-mesenchymal transition and its implications for fibrosis. J Clin Invest. 2003;112(12):1776-84.
- 5. Zeisberg M, Kalluri R. The role of epithelial-to-mesenchymal transition in renal fibrosis. J Mol Med (Berl). 2004;82(3):175-81.
- 6. Flier SN, Tanjore H, Kokkotou EG, Sugimoto H, Zeisberg M, Kalluri R. Identification of epithelial to mesenchymal transition as a novel source of fibroblasts in intestinal fibrosis. J Biol Chem. 2010;285(26):20202-12.
- 7. Zeisberg M, Neilson EG. Biomarkers for epithelial-mesenchymal transitions. J Clin Invest. 2009;119(6):1429-37.
- 8. Liu Y. Epithelial to mesenchymal transition in renal fibrogenesis: pathologic significance, molecular mechanism, and therapeutic intervention. J Am Soc Nephrol. 2004;15(1):1-12.
- 9. Xu J, Lamouille S, Derynck R. TGF-beta-induced epithelial to mesenchymal transition. Cell Res. 2009;19(2):156-72.
- 10. Strutz F, Okada H, Lo CW, Danoff T, Carone RL, Tomaszewski JE, et al. Identification and characterization of a fibroblast marker: FSP1. J Cell Biol. 1995;130(2):393-405.
- 11. Iwano M, Plieth D, Danoff TM, Xue C, Okada H, Neilson EG. Evidence that fibroblasts derive from epithelium during tissue fibrosis. J Clin Invest. 2002;110(3):341-50.
- 12. Rastaldi MP, Ferrario F, Giardino L, Dell'Antonio G, Grillo C, Grillo P, et al. Epithelial-mesenchymal transition of tubular epithelial cells in human renal biopsies. Kidney Int. 2002;62(1):137-46.
- 13. Ivanova L, Butt MJ, Matsell DG. Mesenchymal transition in kidney collecting duct epithelial cells. Am J Physiol Renal Physiol. 2008;294(5):F1238-48.
- Liu M, Liu YZ, Feng Y, Xu YF, Che JP, Wang GC, et al. Novel evidence demonstrates that epithelial-mesenchymal transition contributes to nephrolithiasis-induced renal fibrosis. J Surg Res. 2013;182(1):146-52.

- 15. Ferrazzano GF, Amato I, Ingenito A, De Natale A, Pollio A. Anti-cariogenic effects of polyphenols from plant stimulant beverages (cocoa, coffee, tea). Fitoterapia. 2009;80(5):255-62.
- 16. Inoue M, Sasazuki S, Wakai K, Suzuki T, Matsuo K, Shimazu T, et al. Green tea consumption and gastric cancer in Japanese: a pooled analysis of six cohort studies. Gut. 2009;58(10):1323-32.
- 17. Lorenz M, Urban J, Engelhardt U, Baumann G, Stangl K, Stangl V. Green and black tea are equally potent stimuli of NO production and vasodilation: new insights into tea ingredients involved. Basic Res Cardiol. 2009;104(1):100-10.
- 18. Hannig C, Sorg J, Spitzmuller B, Hannig M, Al-Ahmad A. Polyphenolic beverages reduce initial bacterial adherence to enamel in situ. J Dent. 2009;37(7):560-6.
- 19. Melgarejo E, Medina MA, Sanchez-Jimenez F, Urdiales JL. Epigallocatechin gallate reduces human monocyte mobility and adhesion in vitro. Br J Pharmacol. 2009;158(7):1705-12.
- 20. Osterburg A, Gardner J, Hyon SH, Neely A, Babcock G. Highly antibiotic-resistant Acinetobacter baumannii clinical isolates are killed by the green tea polyphenol (-)-epigallocatechin-3-gallate (EGCG). Clin Microbiol Infect. 2009;15(4):341-6.
- 21. Arts IC, van De Putte B, Hollman PC. Catechin contents of foods commonly consumed in The Netherlands. 2. Tea, wine, fruit juices, and chocolate milk. J Agric Food Chem. 2000;48(5):1752-7.
- 22. Yao K, Ye P, Zhang L, Tan J, Tang X, Zhang Y. Epigallocatechin gallate protects against oxidative stress-induced mitochondria-dependent apoptosis in human lens epithelial cells. Mol Vis. 2008;14:217-23.
- 23. Itoh Y, Yasui T, Okada A, Tozawa K, Hayashi Y, Kohri K. Preventive effects of green tea on renal stone formation and the role of oxidative stress in nephrolithiasis. J Urol. 2005;173(1):271-5.
- 24. Jeong BC, Kim BS, Kim JI, Kim HH. Effects of green tea on urinary stone formation: an in vivo and in vitro study. J Endourol. 2006;20(5):356-61.
- 25. Abdel-Majeed S, Mohammad A, Shaima AB, Mohammad R, Mousa SA. Inhibition property of green tea extract in relation to reserpine-induced ribosomal strips of rough endoplasmic reticulum (rER) of the rat kidney proximal tubule cells. J Toxicol Sci. 2009;34(6):637-45.
- 26. Kim HK, Yang TH, Cho HY. Antifibrotic effects of green tea on in vitro and in vivo models of liver fibrosis. World J Gastroenterol. 2009;15(41):5200-5.

- 27. Sriram N, Kalayarasan S, Sudhandiran G. Epigallocatechin-3-gallate augments antioxidant activities and inhibits inflammation during bleomycin-induced experimental pulmonary fibrosis through Nrf2-Keap1 signaling. Pulm Pharmacol Ther. 2009;22(3):221-36.
- 28. Jonassen JA, Cao LC, Honeyman T, Scheid CR. Mechanisms mediating oxalate-induced alterations in renal cell functions. Crit Rev Eukaryot Gene Expr. 2003;13(1):55-72.
- 29. Khan SR, Shevock PN, Hackett RL. Acute hyperoxaluria, renal injury and calcium oxalate urolithiasis. J Urol. 1992;147(1):226-30.
- 30. Veena CK, Josephine A, Preetha SP, Varalakshmi P, Sundarapandiyan R. Renal peroxidative changes mediated by oxalate: the protective role of fucoidan. Life Sci. 2006;79(19):1789-95.
- 31. Boonla C, Krieglstein K, Bovornpadungkitti S, Strutz F, Spittau B, Predanon C, et al. Fibrosis and evidence for epithelial-mesenchymal transition in the kidneys of patients with staghorn calculi. BJU Int. 2011;108(8):1336-45.
- 32. Chen R, Wang JB, Zhang XQ, Ren J, Zeng CM. Green tea polyphenol epigallocatechin-3-gallate (EGCG) induced intermolecular cross-linking of membrane proteins. Arch Biochem Biophys. 2011;507(2):343-9.
- 33. Miyamoto Y, Haylor JL, El Nahas AM. Cellular toxicity of catechin analogues containing gallate in opossum kidney proximal tubular (OK) cells. J Toxicol Sci. 2004;29(1):47-52.
- 34. Miyamoto Y, Sano M, Haylor JL, El Nahas AM. (-)-Epigallocatechin 3-O-gallate (EGCG)-induced apoptosis in normal rat kidney interstitial fibroblast (NRK-49F) cells. J Toxicol Sci. 2008;33(3):367-70.
- 35. Jiang YS, Jiang T, Huang B, Chen PS, Ouyang J. Epithelial-mesenchymal transition of renal tubules: Divergent processes of repairing in acute or chronic injury? Med Hypotheses. 2013;81(1):73-5.
- 36. Pierratos AE, Khalaff H, Cheng PT, Psihramis K, Jewett MA. Clinical and biochemical differences in patients with pure calcium oxalate monohydrate and calcium oxalate dihydrate kidney stones. J Urol. 1994;151(3):571-4.
- 37. Watson JL, Ansari S, Cameron H, Wang A, Akhtar M, McKay DM. Green tea polyphenol (-)-epigallocatechin gallate blocks epithelial barrier dysfunction provoked by IFN-gamma but not by IL-4. Am J Physiol Gastrointest Liver Physiol. 2004;287(5):G954-61.
- 38. Suzuki T, Hara H. Role of flavonoids in intestinal tight junction regulation. J Nutr Biochem. 2011;22(5):401-8.

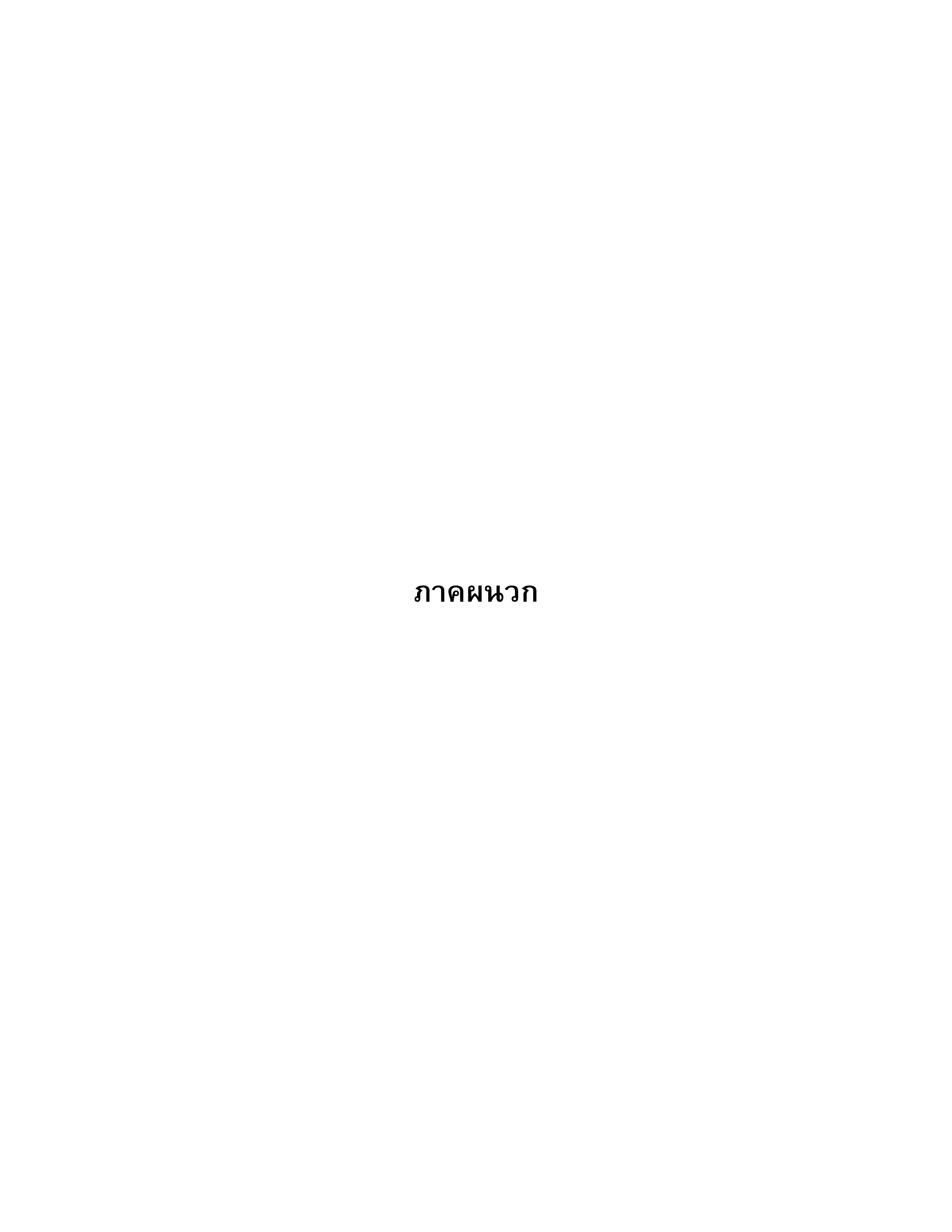
- 39. Chen C, Lu XH, Yan S, Chai H, Yao Q. HIV protease inhibitor ritonavir increases endothelial monolayer permeability. Biochem Biophys Res Commun. 2005;335(3):874-82.
- 40. Rashed T, Menon M, Thamilselvan S. Molecular mechanism of oxalate-induced free radical production and glutathione redox imbalance in renal epithelial cells: effect of antioxidants. Am J Nephrol. 2004;24(5):557-68.
- 41. Khan SR. Hyperoxaluria-induced oxidative stress and antioxidants for renal protection. Urol Res. 2005;33(5):349-57.
- 42. Khan SR. Stress oxidative: nephrolithiasis and chronic kidney diseases. Minerva Med. 2013;104(1):23-30.
- 43. Evan AP, Lingeman JE, Worcester EM, Bledsoe SB, Sommer AJ, Williams JC, Jr., et al. Renal histopathology and crystal deposits in patients with small bowel resection and calcium oxalate stone disease. Kidney Int. 2010;78(3):310-7.
- 44. Huang HS, Ma MC, Chen CF, Chen J. Lipid peroxidation and its correlations with urinary levels of oxalate, citric acid, and osteopontin in patients with renal calcium oxalate stones. Urology. 2003;62(6):1123-8.
- 45. Tungsanga K, Sriboonlue P, Futrakul P, Yachantha C, Tosukhowong P. Renal tubular cell damage and oxidative stress in renal stone patients and the effect of potassium citrate treatment. Urol Res. 2005;33(1):65-9.
- 46. Hirose M, Yasui T, Okada A, Hamamoto S, Shimizu H, Itoh Y, et al. Renal tubular epithelial cell injury and oxidative stress induce calcium oxalate crystal formation in mouse kidney. Int J Urol. 2010;17(1):83-92.
- 47. Itoh Y, Yasui T, Okada A, Tozawa K, Hayashi Y, Kohri K. Examination of the anti-oxidative effect in renal tubular cells and apoptosis by oxidative stress. Urol Res. 2005;33(4):261-6.
- 48. Thamilselvan V, Menon M, Thamilselvan S. Oxalate-induced activation of PKC-alpha and -delta regulates NADPH oxidase-mediated oxidative injury in renal tubular epithelial cells. Am J Physiol Renal Physiol. 2009;297(5):F1399-410.
- 49. Rhyu DY, Yang Y, Ha H, Lee GT, Song JS, Uh ST, et al. Role of reactive oxygen species in TGF-beta1-induced mitogen-activated protein kinase activation and epithelial-mesenchymal transition in renal tubular epithelial cells. J Am Soc Nephrol. 2005;16(3):667-75.
- 50. Zhang A, Dong Z, Yang T. Prostaglandin D2 inhibits TGF-beta1-induced epithelial-to-mesenchymal transition in MDCK cells. Am J Physiol Renal Physiol. 2006;291(6):F1332-42.

- 51. Kitamura M, Nishino T, Obata Y, Furusu A, Hishikawa Y, Koji T, et al. Epigallocatechin gallate suppresses peritoneal fibrosis in mice. Chem Biol Interact. 2012;195(1):95-104.
- 52. Cannito S, Novo E, di Bonzo LV, Busletta C, Colombatto S, Parola M. Epithelial-mesenchymal transition: from molecular mechanisms, redox regulation to implications in human health and disease. Antioxid Redox Signal. 2010;12(12):1383-430.

Output จากโครงการวิจัยที่ได้รับทุนจาก สกว.

- 1. ผลงานตีพิมพ์ในวารสารวิชาการนานาชาติ
 - 1.1 Kanlaya R, Fong-Ngern K, Thongboonkerd V. Cellular adaptive response of distal renal tubular cells to high-oxalate environment highlights surface alpha-enolase as the enhancer of calcium oxalate monohydrate crystal adhesion. J Proteomics. 2013;80C:55-65.
 - 1.2 Kanlaya R, Sintiprungrat K, Chaiyarit S, Thongboonkerd V. Macropinocytosis is the Major Mechanism for Endocytosis of Calcium Oxalate Crystals into Renal Tubular Cells. Cell Biochem Biophys. 2013.
 - 1.3 Kanlaya R, Sintiprungrat K, Thongboonkerd V. Secreted Products of Macrophages Exposed to Calcium Oxalate Crystals Induce Epithelial Mesenchymal Transition of Renal Tubular Cells via RhoA-Dependent TGF-beta1 Pathway. Cell Biochem Biophys. 2013.
 - 1.4 Protective effect of green tea extract against oxalate-induced changes in renal tubular cells: possibility for prevention of renal fibrosis (Manuscript in preparation)
- 2. การนำผลงานวิจัยไปใช้ประโยชน์
 - เชิงพาณิชย์ (มีการนำไปผลิต/ขาย/ก่อให้เกิดรายได้ หรือมีการนำไปประยุกต์ใช้โดยภาค ธุรกิจ/บุคคลทั่วไป)
 - เชิงนโยบาย (มีการกำหนดนโยบายอิงงานวิจัย/เกิดมาตรการใหม่/เปลี่ยนแปลงระเบียบ ข้อบังคับหรือวิธีทำงาน)
 - เชิงสาธารณะ (มีเครือข่ายความร่วมมือ/สร้างกระแสความสนใจในวงกว้าง)
 - เชิงวิชาการ (มีการพัฒนาการเรียนการสอน/สร้างนักวิจัยใหม่)
- 3. อื่นๆ (เช่น หนังสือ การจดสิทธิบัตร)

-

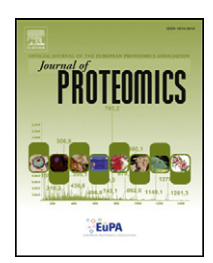




Available online at www.sciencedirect.com

SciVerse ScienceDirect

www.elsevier.com/locate/jprot



Cellular adaptive response of distal renal tubular cells to high-oxalate environment highlights surface alpha-enolase as the enhancer of calcium oxalate monohydrate crystal adhesion

Rattiyaporn Kanlaya, Kedsarin Fong-ngern, Visith Thongboonkerd*

Medical Proteomics Unit, Office for Research and Development, Faculty of Medicine Siriraj Hospital, Mahidol University, Bangkok, Thailand Center for Research in Complex Systems Science, Mahidol University, Bangkok, Thailand

ARTICLE INFO

Article history: Received 26 September 2012 Accepted 7 January 2013 Available online 23 January 2013

Keywords:
Alpha-enolase
Crystal adhesion
Hyperoxaluria
Kidney stone
Oxalate

ABSTRACT

Hyperoxaluria is one of etiologic factors of calcium oxalate kidney stone disease. However, response of renal tubular cells to high-oxalate environment remained largely unknown. We applied a gel-based proteomics approach to characterize changes in cellular proteome of MDCK cells induced by 10 mM sodium oxalate. A total of 14 proteins were detected as differentially expressed proteins. The oxalate-induced up-regulation of alpha-enolase in whole cell lysate was confirmed by 2-D Western blot analysis. Interaction network analysis revealed that cellular adaptive response under high-oxalate condition involved stress response, energy production, metabolism and transcriptional regulation. Down-regulation of RhoA, which was predicted to be associated with the identified proteins, was confirmed by immunoblotting. In addition, the up-regulation of alpha-enolase on apical surface of renal tubular epithelial cells was also confirmed by immunoblotting of the isolated apical membranes and immunofluorescence study. Interestingly, blockage of alpha-enolase expressed on the cell surface by antibody neutralization significantly reduced the number of calcium oxalate monohydrate (COM) crystals adhered on the cells. These results strongly suggest that surface alpha-enolase plays an important role as the enhancer of COM crystal binding. The increase of alpha-enolase expressed on the cell surface may aggravate kidney stone formation in patients with hyperoxaluria.

© 2013 Elsevier B.V. All rights reserved.

1. Introduction

Many attempts have been made to better understand the initiation of kidney stone formation in patients with hyperoxaluria. Because calcium oxalate is the most common type of crystals found in kidney stones, effects of dicarboxylic anion (oxalate) have received wide attention [1,2]. The supersaturation of oxalate ion can initiate crystalline formation and induce renal cell injury, which promotes crystal adhesion on renal cell surface [3,4]. Oxalate exposure can activate several

cellular events, including redistribution of membrane phospholipids, activation of membrane-bound phopholipases, and consequently, lipid signaling that is involved in cellular injury and death [5]. Overloading of oxalate ion can decrease antioxidant activity and increase reactive oxygen species (ROS) production by mitochondria, and ultimately, cell death. However, the increased ROS production and lactate dehydrogenase (LDH) release induced by oxalate are counteracted by several free radical scavengers, including vitamin E, superoxide dismutase (SOD), catalase and iron chelator, suggesting the

E-mail addresses: thongboonkerd@dr.com, vthongbo@yahoo.com (V. Thongboonkerd).

^{*} Corresponding author at: Medical Proteomics Unit, Office for Research and Development, Director of Center for Research in Complex Systems Science (CRCSS), Siriraj Hospital, Mahidol University, 6th Fl-SiMR Bldg., Siriraj Hospital, 2 Prannok Rd., Bangkoknoi, Bangkok 10700, Thailand. Tel.: +66 2 4192850.

promising way to prevent oxidative injury and subsequent crystal nucleation [6]. Moreover, oxalate can induce mitochondrial dysfunction as demonstrated in hyperoxaluric rats induced by ethylene glycol (EG) [7]. The results have shown that oxalate could induce permeability transition in this organelle by decreasing activity of mitochondrial respiratory enzyme complexes and increasing mitochondrial swelling [7]. A recent study by Thamilselvan, et al. [8] has demonstrated for the first time that activation of protein kinase C alpha and delta isoforms is the underlying mechanism for oxalateinduced renal epithelial cell injury through the increased ROS production and LDH release. In addition, oxalate exposure increases the production of urinary modulators, e.g. osteopontin (OPN), that can modulate crystal nucleation, growth and aggregation [9]. Moreover, tubular secretion of oxalate has been considered as the key event resulting to hyperoxaluria in calcium stone formers [10].

Nevertheless, response of renal tubular cells to highoxalate environment remained largely unknown. Daily urinary oxalate excretion can be as high as 0.45-0.50 mg/24 h (equivalent to a concentration of approximately 40-45 mM) in patients with hyperoxaluria [1]. In this study, we investigated the global changes of proteins as a response of distal renal tubular cells under a high-oxalate environment using a gelbased proteomics approach. This in vitro condition mimicked hyperoxaluric feature in patients with hyperoxaluria [1,11]. The interacting protein network was then analyzed to obtain biological meanings of the altered proteins. Our findings highlighted alterations of proteins in many cellular processes for adaptation of distal renal tubular cells under a high-oxalate condition. Thereafter, functional analysis was performed to confirm such biological relevance. The functional data revealed that the increased alpha-enolase on apical cell surface played a significant role in enhancement of crystal adhesion induced by high-oxalate.

2. Materials & methods

2.1. Cell cultivation and high-oxalate treatment

MDCK distal renal tubular cells were maintained in Eagle's minimal essential medium (MEM) (Gibco; Grand Island, NY) containing 10% heat inactivated fetal bovine serum (FBS) (Gibco), 2 mM glutamine (Sigma; St.Louis, MO) in the presence of 100 U/ml penicillin G and 100 mg/ml streptomycin (Sigma). Cells were maintained in a humidified incubator at 37 °C with 5% CO₂. For oxalate treatment, sodium oxalate solution was added into the mentioned growth MEM medium to make a final concentration of 10 mM (in 5 ml total volume). This concentration was based on the findings reported previously by Schepers, et al. [11]. The cells were incubated with or without oxalate treatment in a humidified incubator at 37 °C with 5% CO₂ for 72 h, and were then harvested.

2.2. Protein extraction and two-dimensional polyacrylamide qel electrophoresis (2-D PAGE)

Cellular proteins derived from the controlled and oxalatetreated cells were subjected to 2-D PAGE (n=5 gels derived from 5 independent cultures per group; a total of 10 gels were analyzed). Briefly, the cell monolayers were washed three times with PBS and were gently scraped. Whole cell lysates were obtained using a lysis buffer containing 7 M urea, 2 M thiourea, 40 mg/ml 3-[(3-cholamidopropyl) dimethyl-ammonio]-1-propanesulfonate (CHAPS), 120 mM dithiothreitol (DTT), 2% (v/v) ampholytes pH 3-10, and 40 mM Tris-base) at 4 °C for 30 min. Unsolubilized cellular debris and particles were removed by a centrifugation at 13,000×g and 4 °C for 5 min. Protein concentrations in the clarified supernatants were determined using Bio-Rad Protein Assay (Bio-Rad Laboratories; Hercules, CA) based on the Bradford method. An equal amount of 150 µg proteins recovered from each sample was loaded for 2-D PAGE detailed in "Supplementary methods". The resolved proteins were stained with SYPRO Ruby fluorescence dye (Invitrogen-Molecular Probes; Eugene, OR) and gel images were captured by using a Typhoon laser scanner (GE Healthcare; Uppsala, Sweden).

2.3. Matching and quantitative analysis of protein spots

Image Master 2D Platinum (GE Healthcare) software (version 6.0) was used for matching and analysis of protein spots visualized in individual gels. Details are provided in "Supplementary methods". Intensity volumes of individual spots were obtained and subjected to statistical analysis. Differentially expressed protein spots were subjected to in-gel tryptic digestion and identification by mass spectrometry.

2.4. Protein identification by quadrupole time-of-flight (Q-TOF) mass spectrometry (MS) and tandem MS (MS/MS)

In-gel tryptic digestion was performed as detailed in "Supplementary methods". The proteolytic samples were premixed 1:1 with the matrix solution (5 mg/ml α -cyano-4hydroxycinnamic acid (CHCA) in 50% ACN, 0.1% v/v TFA and 2% w/v ammonium citrate) and spotted onto the 96-well sample stage. The samples were analyzed by the Q-TOF Ultima™ mass spectrometer (Micromass; Manchester, UK) (more details are provided in "Supplementary methods"). The MS peptide masses and MS/MS ions were analyzed by the MASCOT search engine (http://www.matrixscience.com) and queried to the NCBI mammalian protein database, assuming that peptides were monoisotopic, oxidized at methionine residues and carbamidomethylated at cysteine residues. Only 1 missed trypsin cleavage was allowed, and peptide mass tolerances of 100 and 50 ppm were used for MS and MS/MS data, respectively.

2.5. Protein network analysis and subcellular localization

The STRING software [12] was adopted to translate expressional proteomic data into biological relevance. This public database weighs and integrates protein–protein interactions from numerous resources, including experimental repositories, computational prediction and published articles [12]. All the significantly altered proteins identified in oxalate-treated MDCK cells were inputted into STRING 8.3 (http://string-db.org) to retrieve the data of (i) protein function, (ii) subcellular localization and (iii) protein interaction/functional connectivity.

2.6. Western blot analysis

2.6.1. 2-D Western blot analysis

A total of 100 µg proteins derived from whole cell lysate of each sample was dissolved in a 2-D gel as aforementioned. The resolved proteins were electro-transferred onto a nitrocellulose membrane. Non-specific bindings were blocked with 5% skim milk in PBS for 1 h. The membrane was then incubated with rabbit polyclonal anti-enolase antibody (Santa Cruz Biotechnology; Santa Cruz, CA) (1:1000 in 1% skim milk/PBS) at 4 °C for 16 h. After washing, the membrane was incubated with goat anti-rabbit IgG conjugated with horseradish peroxidase (HRP) (DAKO) (1:2000 in 1% skim milk/PBS) at 25 °C for 1 h. Immunoreactive protein spots were visualized by SuperSignal West Pico chemiluminescence substrate (Pierce Biotechnology, Inc.; Rockford, IL) and autoradiography.

2.6.2. 1-D Western blot analysis

For apical membrane proteins, apical membranes were isolated from polarized MDCK cells by peeling method as described with details in our previous study [13] (see also "Supplementary methods"). A total of 50 µg proteins derived from whole cell lysate or apical membrane protein fraction from each sample was resolved by 12% SDS-PAGE and transferred onto a nitrocellulose membrane. After blocking non-specific bindings, the membrane was incubated with mouse monoclonal anti-RhoA antibody (Santa Cruz Biotechnology) or rabbit polyclonal anti-enolase antibody (Santa Cruz Biotechnology) (1:1000 in 1% skim milk in PBS) at 4 °C for 16 h. Mouse monoclonal anti-GAPDH (Santa Cruz Biotechnology) was used to detect GAPDH as the loading control (1:2000 in 1% skim milk/PBS). After washing, the membrane was incubated with corresponding secondary antibody conjugated with horseradish peroxidase (HRP) (DAKO) (1:2000-1:4000 in 1% skim milk/PBS) at 25 °C for 1 h. Immunoreactive protein bands were visualized by SuperSignal West Pico chemiluminescence substrate (Pierce Biotechnology) and autoradiography.

2.7. Laser-scanning confocal microscopic examination of apical membrane enolase

MDCK cells were grown on a coverslip and treated with or without 10 mM sodium oxalate as aforementioned. The cells were rinsed with PBS+ (PBS containing 1 mM MgCl2 and 0.1 mM CaCl₂) and then fixed with 3.7% formaldehyde in PBS+ at 25 °C for 15 min. After washing with PBS+, the cells were incubated with rabbit polyclonal anti-enolase antibody (Santa Cruz Biotechnology) (1:50 in 1% BSA/PBS) at 37 °C for 1 h. Thereafter, the cells were washed with PBS three times and then incubated with anti-rabbit IgG conjugated with Cy3 (Jackson ImmunoResearch Laboratories; West Grove, PA) containing 0.1 µg/ml Hoechst dye (Invitrogen/Molecular Probes) (for nuclear staining) at 37 °C for 1 h. Three-dimensional planes of X-Y, X-Z and Y-Z scanning were captured under a laser-scanning confocal microscope equipped with an LSM5 Image Browser (LSM 510 Meta, Carl Zeiss; Jena, Germany).

2.8. COM crystal adhesion and neutralization assay

COM crystals were prepared as described previously in our previous study [14,15] (see also "Supplementary methods"). MDCK cells were maintained with or without 10 mM sodium oxalate for 72 h as aforementioned. COM crystals were added into the growth medium (100 µg crystals/ml medium) and further incubated with the cells at 37 °C for 30 min. Thereafter, the unbound crystals were removed and the cells were washed three times with PBS. The remaining crystals adhered on the cell surface were counted at 15 randomized high power fields (HPF) under a phase contrast microscope (Olympus CKX41, Olympus Co. Ltd.; Tokyo, Japan). In parallel, the cells that were pre-incubated with 0.2 µg/ml rabbit polyclonal anti-enolase antibody (Santa Cruz Biotechnology) or nonspecific rabbit IgG at 37 °C for 30 min before COM crystal incubation were also evaluated. This experiment was performed in triplicate for all conditions.

2.9. Statistical analysis

Quantitative data are reported as mean±SEM. Comparisons between the two sets of samples (i.e., controlled vs. oxalate-treated) were performed using unpaired Student's t test. P-values less than 0.05 were considered statistically significant.

3. Results

3.1. Proteome changes induced by high-oxalate condition

MDCK cells were maintained with or without 10 mM sodium oxalate for 72 h. Whole cell lysates derived from the controlled (untreated) and oxalate-treated cells were equally loaded (150 μg each) and resolved by 2-D PAGE (n=5 gels derived from 5 independent cultures per group; a total of 10 gels were analyzed). Spot matching and quantitative intensity analysis of the matched spots revealed 14 differentially expressed protein spots between the two groups (Fig. 1). These significantly altered proteins were successfully identified by Q-TOF MS and/or MS/MS (Table 1). Among these, 8 proteins were down-regulated, whereas other 6 proteins were up-regulated by high-oxalate (1 protein spot was expressed only in the high-oxalate condition). 2-D Western blot analysis was performed to confirm the proteomic data, e.g. the increased level of alpha-enolase (spot #354) in the oxalate-treated MDCK cells (Fig. 2). The increased level and locale in the 2-D map of alpha-enolase were confirmed by 2-D Western blot analysis.

3.2. Network analysis and subcellular localization of the significantly altered proteins

The STRING software was employed to translate the significantly altered proteins into the biological relevance by providing the information about their functions, interactions and subcellular localizations (Fig. 3). In addition to the significantly altered proteins induced by high-oxalate identified in this study (labeled as "colored nodes" with upward or downward arrows for up-regulated or down-regulated

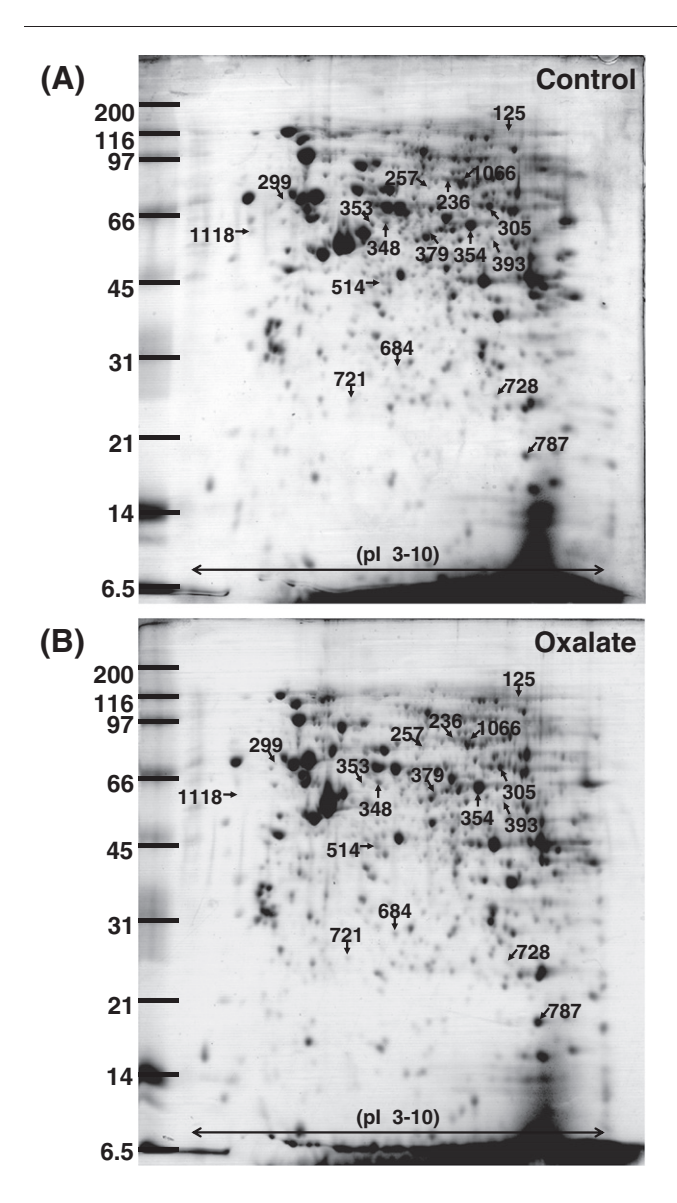


Fig. 1 – Representative 2-D proteome maps of differentially expressed proteins in controlled (A) and oxalate-treated cells (B). MDCK cells were maintained without or with 10 mM sodium oxalate for 72 h and their cellular proteome were analyzed by 2-D PAGE (n=5 gels derived from 5 independent cultures per group; a total of 10 gels were analyzed). Spot matching and quantitative intensity analysis revealed 14 differentially expressed protein spots, which are labeled as numbers corresponding to those reported in Tables 1 and 2.

proteins, respectively), the interacting proteins predicted from literatures and other databases were labeled as the "white nodes" without arrows. Moreover, each protein node was mapped to its major subcellular localization (Table 2), of which the background image was created by the Pathway Builder Online (http://www.proteinlounge.com) (Fig. 3). From this interaction map, RhoA was predicted as an interacting partner of significantly altered proteins identified by proteomic analysis. We then performed 1-D Western blot analysis to examine whether RhoA level was changed by high-oxalate. GAPDH served as the loading control. The data confirmed that

RhoA level was decreased in the oxalate-treated MDCK cells (Fig. 4A).

3.3. Increased surface expression of alpha-enolase induced by high-oxalate

Network analysis and subcellular localization also suggested that the oxalate-induced increase in expression level of alpha-enolase occurred at apical surface of renal tubular cells. To confirm this data, apical membranes were isolated from polarized MDCK renal tubular epithelial cells using a peeling method described previously by our group [13]. This simple and effective method offers a highly purified apical membrane fraction [13]. 1-D Western blot analysis of alphaenolase in this apical membrane fraction confirmed that alpha-enolase was expressed in apical membrane of polarized MDCK renal tubular epithelial cells and its expression was increased in apical membrane after an exposure to highoxalate (Fig. 4B). To further validate this result, immunofluorescence study was performed. The data obtained from laser-scanning confocal microscopy clearly demonstrated that apical surface expression of alpha-enolase was significantly increased in the oxalate-treated cells (Fig. 4C).

3.4. Effects of high-oxalate on COM crystal adhesion and neutralization of surface alpha-enolase

We also evaluated the functional significance of the increased expression level of apical surface of alpha-enolase induced by high-oxalate. We hypothesized that high-oxalate could enhance COM crystal adhesion on the cell surface and that the increased expression level of apical surface of alpha-enolase might play significant role in this phenomenon. Our hypothesis was addressed by COM crystal adhesion assay. The data confirmed that high-oxalate significantly increased the number of adherent COM crystals (Fig. 5). Moreover, the data also revealed that neutralization of surface expression of alphaenolase by specific antibody against this protein dramatically reduced the number of the adherent COM crystals almost to the basal level, whereas neutralization with non-specific IgG derived from the same species as of specific antibody had no effects on the number of adherent COM crystals (Fig. 5).

4. Discussion

Oxalate plays a key role in calcium oxalate kidney stone formation, particularly in hyperoxaluria commonly found in patients with idiopathic calcium oxalate urolithiasis and tubulointerstitial fibrosis [16,17]. However, molecular mechanisms that high-oxalate plays in calcium oxalate kidney stone disease remained unclear. Our present study therefore aimed to characterize changes in cellular proteome of distal renal tubular cells in response to high-oxalate. Our findings have demonstrated that the significantly altered proteins were involved in various biological processes of renal tubular cells, including maintenance of the actin cytoskeletal assembly and nuclear structure (ACTR3, CFL1 and LMNA), signal transduction (PRKAR2A), stress response (HSPB1, ERO1L, SDF2L1 and UQCRC1), energy metabolism (ENO1, GLUD1 and OAT) and

Spot no.	Protein	NCBI entry	Identified by	Identification scores (MS, MS/MS)	%Cov (MS, MS/MS)	No. of matched peptides (MS, MS/MS)	pΙ	MW (kDa)	Intensity level (Mean±SEM)		Ratio (Oxalate/control)	p-value
									Control	Oxalate		
	Up-regulated proteins											
514	60S acidic ribosomal protein P0 (L10E) isoform 8	gi 73994699	MS	70, NA	44, NA	7, NA	5.91	32.09	0.0822±0.0149	0.1291±0.0101	1.57	0.031
348	ARP3 actin-related protein 3 homolog	gi 13542701	MS/MS	NA, 143	NA, 14	NA, 4	5.61	47.78	0.1358±0.0052	0.1802±0.0093	1.33	0.003
787	Cofilin 1, non-muscle (18 kDa phosphoprotein)	gi 15012201	MS/MS	NA, 57	NA, 16	NA, 2	8.22	18.72	0.2424±0.0722	0.4816±0.0447	1.99	0.023
354	Enolase 1, (alpha)	gi 12804749	MS/MS	NA, 265	NA, 13	NA, 4	7.01	47.48	1.0128±0.0703	1.3150±0.0502	1.30	0.008
684	Heat shock 27 kDa protein 1	gi 50979116	MS/MS	NA, 87	NA, 20	NA, 3	6.23	22.93	0.0303±0.0187	0.0878±0.0085	2.90	0.023
	Down-regulated proteins											
257	ERO-1like protein alpha precursor (ERO-1lalpha) (Oxidoreductin 1-lalpha)	gi 73963815	MS	108, NA	36, NA	11, NA	5.97	55.18	0.0610±0.0046	0.0336±0.0061	0.55	0.007
305	Glutamate dehydrogenase 1	gi 6980956	MS/MS	NA, 85	NA, 5	NA, 2	8.05	61.72	0.4839±0.0394	0.3107±0.0392	0.64	0.014
236	Lamin A/C	gi 13111979	MS	106, NA	31, NA	13, NA	6.40	65.15	0.1633 ± 0.0331 0.1422 ± 0.0235	0.0810 ± 0.0032	0.57	0.011
379	Ornithine aminotransferase, mitochondrial precursor	gi 73998802	MS/MS	NA, 155	NA, 13	NA, 4	6.44	48.75	0.0874±0.0043	0.0656±0.0078	0.75	0.039
1066	Paraspeckle protein 1	gi 20071204	MS/MS	NA, 34	NA, 2	NA, 1	6.26	58.54	0.1041 ± 0.0144	0.0602 ± 0.0082	0.58	0.029
728	Stromal cell-derived factor 2-like protein 1 precursor (SDF2 like protein 1) (PWP1-interacting protein 8)	gi 73996025	MS/MS	NA, 71	NA, 19	NA, 3	10.04	36.73	0.0906±0.0117	0.0330±0.0156	0.36	0.018
393	Thyroid receptor interactor	gi 695370	MS/MS	NA, 83	NA, 8	NA, 2	7.70	45.78	0.0978 ± 0.0063	0.0634 ± 0.0089	0.65	0.013
353	Ubiquinol-cytochrome c reductase core protein I isoform 2	gi 73985642	MS	102, NA	38, NA	11, NA	6.04	53.54	0.1498±0.0124	0.0730±0.0110	0.49	0.002
200	Newly expressed proteins	ail10E107	MC/MC	NA 60	NIA 2	NIA 1	4.90	4E 20	0.0000 + 0.0000	0.0016 + 0.0015	Divided by 0	-0.001
299	cAMP-dependent protein kinase type II-alpha regulatory subunit	gi 125197	MS/MS	NA, 60	NA, 3	NA, 1	4.80	45.28	0.0000±0.0000	0.0216±0.0015	Divided by 0	<0.001

%Cov = %sequence coverage = [(number of the matched residues/total number of residues in the entire sequence) × 100%]. NA = not applicable.

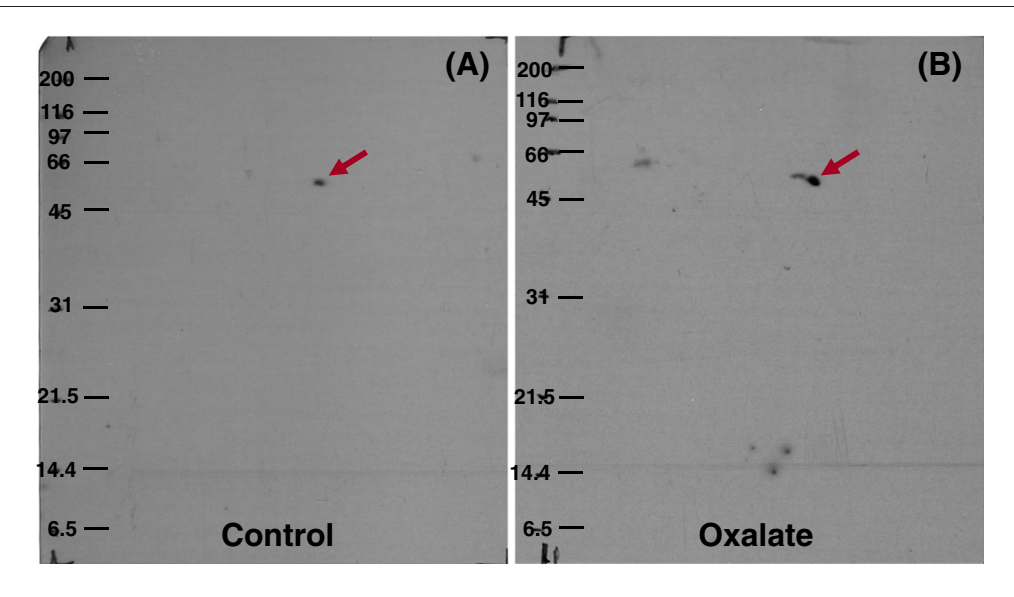


Fig. 2 – Confirmation of the proteome data by 2-D Western blot analysis. Proteins (with an equal amount of 100 μ g) derived from whole cell lysate of the controlled (A) and oxalate-treated (B) MDCK cells were resolved by 2-D PAGE and subjected to 2-D Western blot analysis. Primary antibody was rabbit polyclonal anti-enolase antibody (Santa Cruz Biotechnology) (1:1000 in 1% skim milk/PBS), whereas secondary antibody was goat anti-rabbit IgG conjugated with horseradish peroxidase (HRP) (DAKO) (1:2000 in 1% skim milk/PBS).

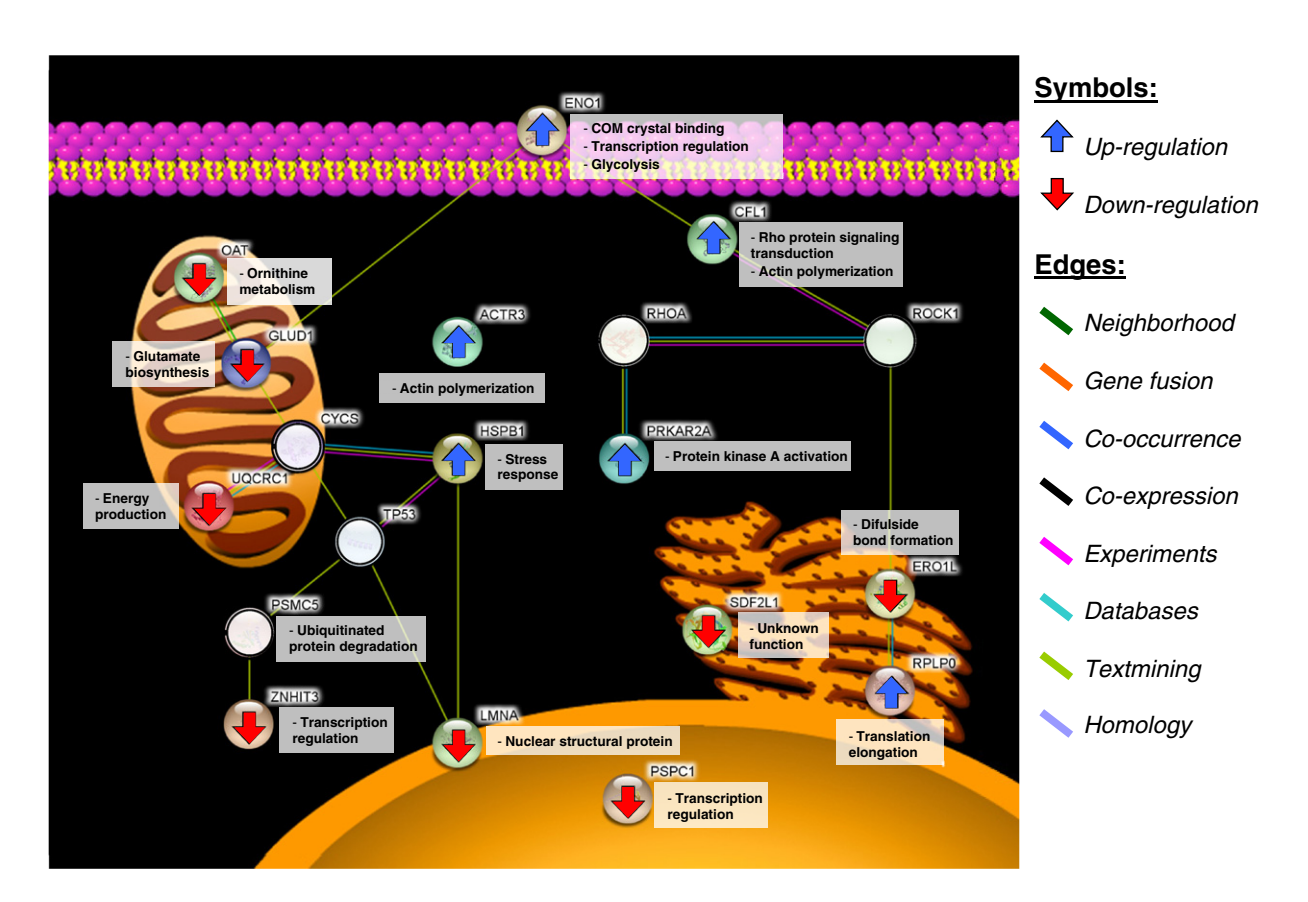


Fig. 3 – Network analysis and subcellular localizations of the significantly altered proteins. Integration of all the significantly altered proteins into the relevant biological meanings was performed by using the STRING software. The network analysis reveals the interactions among proteins, their functions, and subcellular localizations. The "colored nodes" with upward or downward arrows depict the up-regulated or down-regulated proteins, respectively, whereas the "white nodes" without arrows indicate the interacting proteins predicted from literatures and other databases.

Table 2 – Functional classification and subcellular localization of significantly altered proteins in response to high-oxalate exposure and their predicted interacting partners.

Spot no.	Abbreviation	Full protein name	Function(s)	Subcellular localization(s)
Up-reg	ulated proteins			
514	RPLP0	60S acidic ribosomal protein P0 (L10E) isoform 8	Ribosome biogenesis; translational elongation	Cytoplasm; nucleus
348	ACTR3	ARP3 actin-related protein 3 homolog	Actin polymerization	Cytoplasm
787	CFL1	Cofilin 1	Rho protein signaling transduction; actin polymerization	Cytoplasm; nucleus
354	ENO1	Enolase 1	COM crystal binding; transcription regulation; glycolysis	Plasma membrane; cytoplasm; nucleus
684	HSPB1	Heat shock 27 kDa protein 1	Stress response	Cytoplasm; nucleus
299	PRKAR2A	cAMP-dependent protein kinase type II -alpha regulatory subunit	Protein kinase A activation	Cytoplasm
Down-	regulated proteins	3		
257	ERO1L	ERO-1 like protein alpha presursor (ERO-1lalpha)	Disulfide bond formation of proteins	Endoplasmic reticulum
305	GLUD1	Glutamate dehydrogenase 1	Glutamate biosynthesis	Mitochondria
236	LMNA	Lamin A/C	Nuclear structural protein	Nuclear membrane
379	OAT	Ornithine aminotransferase, mitochondrial precursor	Ornithine metabolism	Mitochondria
1066	PSPC1	Paraspeckle protein 1	Transcription regulation	Nucleus
728	SDF2L1	Stromal cell-derived factor 2-like protein 1 precursor	ER stress response	Endoplasmic reticulum
393	ZNHIT3	Thyroid receptor interacting protein 3	Transcription regulation	Cytoplasm
353	UQCRC1	Ubiquinol-cytochrome c reductase core protein I isoform 2	Stress response; Energy metabolism	Mitochondria
Predict	ed interacting pro	teins *		
	RHOA	RhoA protein	Rho protein signaling transduction; actin polymerization	Cytoplasm; plasma membrane
	ROCK1	Rho-associated protein kinase 1	Rho protein signaling transduction; actin polymerization	Cytoplasm
	PSPC5	26S protease regulatory subunit 8	Protein degradation by proteasome	Cytoplasm
	CYCS	Cytochrome C	Electron transport chain	Mitochondria
	TP53	Tumor antigen p53	Pro-apoptosis; anti-proliferation	Cytoplasm

transcriptional regulation (PSPC1 and ZNHIT3). The possibilities that these significantly altered proteins played in calcium oxalate kidney stone formation and disease progression are discussed as follows.

Proteins involved in the dynamics of actin cytoskeletal assembly were increased in response to high-oxalate condition. Actin-related protein 3 (ACTR3) is well-characterized as a major component of the ARP2/3 complex lining the cell surface that is essential for maintaining cell shape and motility through actin polymerization. Cofilin1 is necessary for maintaining architecture of podocytes during cell injury [18]. It has been reported that cofilin could interact with ClC-5 and regulates albumin uptake in proximal tubular cells. Phosphorylation of cofilin results in stabilization of actin cytoskeleton and thus inhibits albumin uptake [19]. We hypothesized that the increased levels of ACTR3 and cofilin 1 might be involved in actin remodeling in response to oxalate-induced injury. In contrast, we found the decreased level of a nucleoskeletal protein, lamin A/C, which is the constituent of the nuclear matrix. Hypertonicity could induce expression of lamin A/C and its distribution in the nucleoplasm. Moreover, lamin A/C serves as a scaffold protein by interacting with TonEBP, a transcriptional regulator of gene

cassettes contributing in protection against hyperosmolarity [20,21]. We assumed that the decreased level of lamin A/C reflected that the cells might fail to cope with the deteriorate effects induced by high-oxalate.

Type II-alpha regulatory subunit of cAMP-dependent protein kinase (PRKAR2A) was newly expressed under the high-oxalate environment. This protein is involved in signal transduction through protein kinase A (PKA) activation. This regulatory subunit has been shown to regulate protein transport from endosomes to golgi apparatus and endoplasmic reticulum [22]. PRKAR2A also mediates membrane association by binding to a group of PKA anchoring proteins (AKAPs) [23]. Unlike type I PKA, which is highly expressed in proliferating cells, type II PKA is preferentially expressed in the cells that underwent growth arrest [24]. Activation of PKA contributes to oxidative stress found in diabetic rat kidney [25]. Moreover, up-regulation of PRKAR1A has been found in nodular hyperplasia of parathyroid glands in patients with chronic renal failure [26]. Therefore, it is likely that the increase in regulatory subunit of the PKA found in our present study might reflect growth retardation of the cells and oxidative stress induced by PKA activation under the high-oxalate condition.

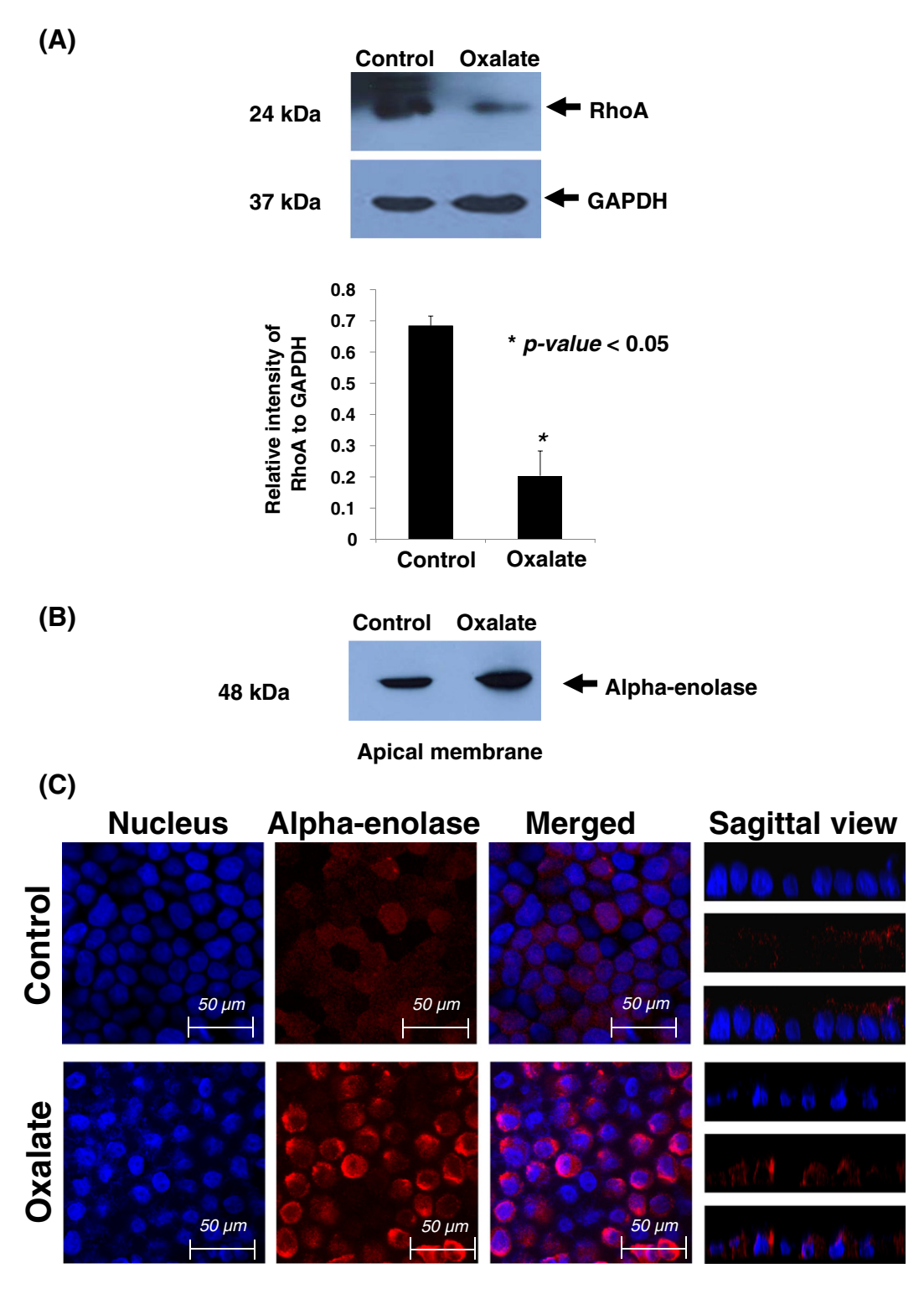


Fig. 4 – Confirmation of the data predicted from network analysis and subcellular localizations using the STRING tool. The decreased level of cytosolic RhoA in oxalate-treated cells was confirmed in whole cell lysate by 1-D Western blot analysis, in which GAPDH served as a loading control (A). 1-D Western blotting was also employed to confirm the increased level of alpha-enolase apical membrane fraction of oxalate-treated cells (B). The latter was also confirmed by immunofluorescence study (C). The fluorescence images were captured under a laser-scanning confocal microscope with 6300× original magnification power (Carl Zeiss; Jena, Germany).

Adaptive response to protect cells during chronic hyperoxaluria by up-regulation of HSP70 has been reported previously [2]. In the present study, we found the increased level

of a small heat shock protein. HSP27 (also known as HSPB1 or HSP25) is a small protein with chaperone activity involving in a variety of cellular functions, including thermoresistance,

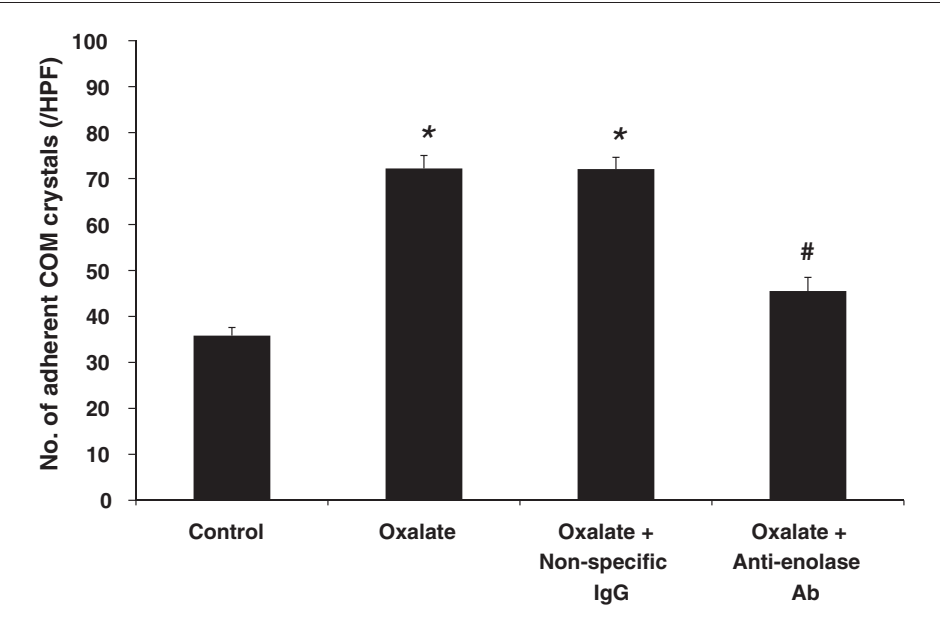


Fig. 5 – COM crystal adhesion and neutralization assay. After MDCK cells were maintained with or without 10 mM sodium oxalate for 72 h, COM crystals were added into the growth medium (100 μ g crystals/ml medium) and further incubated with the cells at 37 °C for 30 min. After removing the unbound crystals, the remaining crystals adhered on the cell surface were counted at 15 randomized high power fields (HPF) under a phase contrast microscope (Olympus CKX41). In parallel, the cells that were pre-incubated with 0.2 μ g/ml rabbit polyclonal anti-enolase antibody (Santa Cruz Biotechnology) or non-specific rabbit IgG at 37 °C for 30 min before COM crystal incubation were also evaluated. Each bar was constructed from 3 independent experiments. *=p<0.05 vs. control; #=p<0.05 vs. oxalate-treated cells (without or with non-specific rabbit IgG pretreatment).

inhibition of apoptosis, cell differentiation and signal transduction [27]. A variety of stresses can result to up-regulation of HSP27. We hypothesized that the increase of HSP27 might reflect cellular adaptive response to protect the cells from high-oxalate-induced cell death. In contrast, we also observed the decreased levels of ERO-1 like protein (ERO1L) and stromal cell-derived factor 2-like protein 1 (SDF2L1). ERO1L is an enzyme responsible for disulfide bond formation of proteins [28], whereas SDF2L1 is a component of the endoplasmic reticulum involved in folding of nascent polypeptides in cooperation with other chaperones and members of protein-disulfide family to correct protein folding [29]. Within the endoplasmic reticulum, ERO1 protein family is required for the catalytic activity of protein disulfide isomerase (PDI) [30]. Therefore, the decreased levels of ERO1L and SDF2L1 might aggravate deteriorate effects in the oxalate-treated cells due to accumulation of the misfolded proteins. Another evidence to confirm the induction of oxidative stress response to high-oxalate was the decrease in expression of ubiquinol cytochrome c reductase (UQCRC1 or Cytochrome bc1 complex), which is a subunit of complex III respiratory chain protein with the role in energy production. The loss of UQCRC1 in epithelial cells exposed to H_2O_2 has been reported to worsen cellular oxidative stress through mitochondrial dysfunction [31]. We thus presumed that the reduced UQCRC1 found in our present study reflected mitochondrial dysfunction upon high-oxalate treatment.

The highlight of findings in the present study was the up-regulation of alpha-enolase (enolase 1; ENO1), one of the key glycolytic enzymes. Interestingly, it has been demonstrated that alpha-enolase plays another important role as a plasminogen receptor on many cell types, including monocytes, epithelial

cells, and endothelial cells [31-33]. Because plasminogen/plasmin plays a crucial role in extracellular matrix degradation, the up-regulation of alpha-enolase (as a plasminogen receptor) on the cell surface might aggravate crystal invasion under the high-oxalate environment. Network analysis and subcellular localization using the STRING tool revealed that the increased level of alpha-enolase was localized at apical membranes (Fig. 3). Its increased expression at apical membranes was nicely confirmed by Western blot analysis of apical membrane fraction and by immunofluorescence study using laser-scanning confocal microscopic examination (Fig. 4B and C). In addition, our previous study also identified alpha-enolase as one of COM crystal-binding proteins on apical membranes of polarized MDCK cells [34]. Therefore, it is plausible that the increased surface expression of alpha-enolase, as a COM crystal-binding protein, was related to the enhancement of COM crystal adhesion onto renal tubular epithelial cells upon high-oxalate exposure. Our hypothesis was nicely confirmed by a functional assay, which demonstrated that high-oxalate significantly induced COM crystal adhesion and neutralization of surface expression of alpha-enolase successfully prevented such enhancement (Fig. 5).

Our findings indicated that alpha-enolase not only plays a role in regulation of cellular energy but also serves as the binding molecule for COM crystals to enhance COM crystal adhesion under the high-oxalate condition. It would be best to also validate our results in a kidney tissue from hyperoxaluric patients. However, the lack of such tissue is a major limitation in our present study. Moreover, the results also suggested that molecular blocking of surface molecules on renal tubular cells involved in crystal binding may be an effective way to prevent

progression of kidney stone formation in patients with hyperoxaluria. Further clinical studies are required to address this novel therapeutic approach.

In summary, we report herein the adaptive response of distal renal tubular cells to high-oxalate environment. The results revealed that such condition induced many deteriorate effects to the cells. In order to complement and maintain several biological functions, the cells altered a set of proteins to cope with this situation. We also demonstrated that high-oxalate could induce surface expression of alpha-enolase to enhance COM crystal adhesion on the cell surface. These data enlighten that the increased expression of alpha-enolase on apical membranes is, at least in part, a crucial mechanism beneath kidney stone formation in patients with hyperoxaluria.

Supplementary data to this article can be found online at http://dx.doi.org/10.1016/j.jprot.2013.01.001.

Acknowledgments

We thank Prof. Shui-Tein Chen, Supachok Sinchaikul and Somchai Chutipongtanate for their technical assistance. This study was supported by the Thailand Research Fund (TRF) (RTA5380005 and TRG5480005), Office of the Higher Education Commission and Mahidol University under the National Research Universities Initiative, and Faculty of Medicine Siriraj Hospital. K.F. was supported by Royal Golden Jubilee Ph.D. Program scholarship, whereas V.T. is also supported by "Chalermphrakiat" Grant, Faculty of Medicine Siriraj Hospital.

REFERENCES

- Marengo SR, Romani AM. Oxalate in renal stone disease: the terminal metabolite that just won't go away. Nat Clin Pract Nephrol 2008;4:368–77.
- [2] Greene EL, Farell G, Yu S, Matthews T, Kumar V, Lieske JC. Renal cell adaptation to oxalate. Urol Res 2005;33:340–8.
- [3] Evan AP. Physiopathology and etiology of stone formation in the kidney and the urinary tract. Pediatr Nephrol 2010;25: 831–41.
- [4] Khan SR. Renal tubular damage/dysfunction: key to the formation of kidney stones. Urol Res 2006;34:86–91.
- [5] Jonassen JA, Cao LC, Honeyman T, Scheid CR. Intracellular events in the initiation of calcium oxalate stones. Nephron Exp Nephrol 2004;98:e61–4.
- [6] Thamilselvan S, Khan SR, Menon M. Oxalate and calcium oxalate mediated free radical toxicity in renal epithelial cells: effect of antioxidants. Urol Res 2003;31:3–9.
- [7] Veena CK, Josephine A, Preetha SP, Rajesh NG, Varalakshmi P. Mitochondrial dysfunction in an animal model of hyperoxaluria: a prophylactic approach with fucoidan. Eur J Pharmacol 2008;579:330–6.
- [8] Thamilselvan V, Menon M, Thamilselvan S. Oxalate-induced activation of PKC-alpha and -delta regulates NADPH oxidase-mediated oxidative injury in renal tubular epithelial cells. Am J Physiol Renal Physiol 2009;297: F1399–410.
- [9] Mazzali M, Kipari T, Ophascharoensuk V, Wesson JA, Johnson R, Hughes J. Osteopontin—a molecule for all seasons. QJM 2002;95:3–13.
- [10] Bergsland KJ, Zisman AL, Asplin JR, Worcester EM, Coe FL. Evidence for net renal tubule oxalate secretion in patients

- with calcium kidney stones. Am J Physiol Renal Physiol 2011:300:F311–8.
- [11] Schepers MS, van Ballegooijen ES, Bangma CH, Verkoelen CF. Oxalate is toxic to renal tubular cells only at supraphysiologic concentrations. Kidney Int 2005;68:1660–9.
- [12] Jensen LJ, Kuhn M, Stark M, Chaffron S, Creevey C, Muller J, et al. STRING 8—a global view on proteins and their functional interactions in 630 organisms. Nucleic Acids Res 2009;37:D412–6.
- [13] Fong-ngern K, Chiangjong W, Thongboonkerd V. Peeling as a novel, simple, and effective method for isolation of apical membrane from intact polarized epithelial cells. Anal Biochem 2009;395:25–32.
- [14] Thongboonkerd V, Semangoen T, Chutipongtanate S. Factors determining types and morphologies of calcium oxalate crystals: molar concentrations, buffering, pH, stirring and temperature. Clin Chim Acta 2006;367: 120–31.
- [15] Thongboonkerd V, Chutipongtanate S, Semangoen T, Malasit P. Urinary trefoil factor 1 is a novel potent inhibitor of calcium oxalate crystal growth and aggregation. J Urol 2008;179: 1615–9.
- [16] Smith LH. Diet and hyperoxaluria in the syndrome of idiopathic calcium oxalate urolithiasis. Am J Kidney Dis 1991;17:370–5.
- [17] Khan SR. Pathogenesis of oxalate urolithiasis: lessons from experimental studies with rats. Am J Kidney Dis 1991;17: 398–401.
- [18] Garg P, Verma R, Cook L, Soofi A, Venkatareddy M, George B, et al. Actin-depolymerizing factor cofilin-1 is necessary in maintaining mature podocyte architecture. J Biol Chem 2010;285:22676–88.
- [19] Hryciw DH, Wang Y, Devuyst O, Pollock CA, Poronnik P, Guggino WB. Cofilin interacts with ClC-5 and regulates albumin uptake in proximal tubule cell lines. J Biol Chem 2003;278:40169–76.
- [20] Jeon US, Kim JA, Sheen MR, Kwon HM. How tonicity regulates genes: story of TonEBP transcriptional activator. Acta Physiol (Oxf) 2006;187:241–7.
- [21] Favale NO, Sterin Speziale NB, Fernandez Tome MC. Hypertonic-induced lamin A/C synthesis and distribution to nucleoplasmic speckles is mediated by TonEBP/NFAT5 transcriptional activator. Biochem Biophys Res Commun 2007;364:443–9.
- [22] Wojtal KA, Hoekstra D, van Ijzendoorn SC. Anchoring of protein kinase A-regulatory subunit IIalpha to subapically positioned centrosomes mediates apical bile canalicular lumen development in response to oncostatin M but not cAMP. Mol Biol Cell 2007;18:2745–54.
- [23] Foss KB, Solberg R, Simard J, Myklebust F, Hansson V, Jahnsen T, et al. Molecular cloning, upstream sequence and promoter studies of the human gene for the regulatory subunit RII alpha of cAMP-dependent protein kinase. Biochim Biophys Acta 1997;1350:98–108.
- [24] Cho-Chung YS. Antisense protein kinase A RI alpha-induced tumor reversion: portrait of a microarray. Biochim Biophys Acta 2004:1697:71–9.
- [25] Xu Y, Osborne BW, Stanton RC. Diabetes causes inhibition of glucose-6-phosphate dehydrogenase via activation of PKA, which contributes to oxidative stress in rat kidney cortex. Am J Physiol Renal Physiol 2005;289:F1040–7.
- [26] Hibi Y, Kambe F, Tominaga Y, Mizuno Y, Kobayashi H, Iwase K, et al. Up-regulation of the gene encoding protein kinase A type I alpha regulatory subunit in nodular hyperplasia of parathyroid glands in patients with chronic renal failure. J Clin Endocrinol Metab 2006;91:563–8.
- [27] de Graauw M, Tijdens I, Cramer R, Corless S, Timms JF, van de WB. Heat shock protein 27 is the major differentially phosphorylated protein involved in renal epithelial cellular

- stress response and controls focal adhesion organization and apoptosis. J Biol Chem 2005;280:29885–98.
- [28] Sevier CS, Kaiser CA. Ero1 and redox homeostasis in the endoplasmic reticulum. Biochim Biophys Acta 2008;1783: 549-56.
- [29] Tongaonkar P, Selsted ME. SDF2L1, a component of the endoplasmic reticulum chaperone complex, differentially interacts with {alpha}-, {beta}-, and {theta}-defensin propeptides. J Biol Chem 2009;284:5602–9.
- [30] Shibanuma M, Inoue A, Ushida K, Uchida T, Ishikawa F, Mori K, et al. Importance of mitochondrial dysfunction in oxidative stress response: a comparative study of gene expression profiles. Free Radic Res 2011;45:672–80.
- [31] Plow EF, Das R. Enolase-1 as a plasminogen receptor. Blood 2009;113:5371–2.
- [32] Seweryn E, Pietkiewicz J, Bednarz-Misa IS, Ceremuga I, Saczko J, Kulbacka J, et al. Localization of enolase in the subfractions of a breast cancer cell line. Z Naturforsch C 2009;64:754–8.
- [33] Pancholi V. Multifunctional alpha-enolase: its role in diseases. Cell Mol Life Sci 2001;58:902–20.
- [34] Fong-ngern K, Peerapen P, Sinchaikul S, Chen ST, Thongboonkerd V. Large-scale identification of calcium oxalate monohydrate crystal-binding proteins on apical membrane of distal renal tubular epithelial cells. J Proteome Res 2011;10:4463–77.

ORIGINAL PAPER

Macropinocytosis is the Major Mechanism for Endocytosis of Calcium Oxalate Crystals into Renal Tubular Cells

Rattiyaporn Kanlaya · Kitisak Sintiprungrat · Sakdithep Chaiyarit · Visith Thongboonkerd

© Springer Science+Business Media New York 2013

Abstract During an initial phase of kidney stone formation, the internalization of calcium oxalate (CaOx) crystals by renal tubular cells has been thought to occur via endocytosis. However, the precise mechanism of CaOx crystal endocytosis remained unclear. In the present study, MDCK renal tubular cells were pretreated with inhibitors specific to individual endocytic pathways, including nystatin (lipid raft/caveolae-mediated), cytochalasin D (actindependent or macropinocytosis), and chlorpromazine (CPZ; clathrin-mediated) before exposure to plain (non-labeled), or fluorescence-labeled CaOx monohydrate (COM) crystals. Ouantitative analysis by flow cytometry revealed that pretreatment with nystatin and CPZ slightly decreased the crystal internalization, whereas the cytochalasin D pretreatment caused a marked decrease in crystal uptake. Immunofluorescence study and laser-scanning confocal microscopic examination confirmed that the cytochalasin D-pretreated cells had dramatic decrease of the internalized crystals, whereas the total number of crystals interacted with the cells was unchanged (crystals could adhere but were not internalized). These data have demonstrated for the first time that renal tubular cells endocytose COM crystals mainly via macropinocytosis. These novel findings will be useful for

Electronic supplementary material The online version of this article (doi:10.1007/s12013-013-9630-8) contains supplementary material, which is available to authorized users.

R. Kanlaya · K. Sintiprungrat · S. Chaiyarit · V. Thongboonkerd (☒)
Medical Proteomics Unit, Office for Research and
Development, Faculty of Medicine, Siriraj Hospital, and Center
for Research in Complex Systems Science (CRCSS), Mahidol
University, 6th Floor SiMR Building, 2 Prannok Road,
Bangkoknoi, Bangkok 10700, Thailand
e-mail: thongboonkerd@dr.com; vthongbo@yahoo.com

Published online: 22 May 2013

further tracking the endocytosed crystals inside the cells during the course of kidney stone formation.

Keywords Calcium oxalate · Crystal · Endocytosis · Internalization · Macropinocytosis

Introduction

Calcium oxalate (CaOx) is the major causative crystalline composition of kidney stones, which lead to a common health problem around the globe [1]. Many lines of evidence from in vivo investigations and clinical studies have demonstrated that CaOx crystals can deposit inside tubular lumen [2] and renal interstitium [3, 4] during the course of kidney stone development and then aggravate renal tissue injury and dysfunction [5]. By adhesion, crystals can be retained on apical surface of renal tubular cells, which subsequently internalize the adherent crystals most likely by endocytosis [6, 7]. The internalized or endocytosed crystals are then translocated to basolateral site of renal tubular cells and finally to the interstitial space, leading to interstitial plaque formation [8, 9]. This plaque has been thought to serve as a crucial site for the stone development [10]. Despite this background, the precise mechanism for endocytosis of CaOx crystals by renal tubular cells had never been investigated previously and thus remained unknown.

Endocytosis is a common cellular function pivotal for nutrient uptake, receptor recycling, regulation of cell shape for mitosis, antigen presentation, and cell migration [11]. Major endocytic mechanisms can be divided into three distinct pathways with differential sensitivities to chemical inhibitors [12]. These include (i) lipid raft/caveolae-mediated endocytosis, (ii) macropinocytosis/phagocytosis, and



(iii) clathrin-mediated endocytosis [12, 13]. Lipid raft/caveolae-mediated pathway causes engulfment of cholesterol-enriched microdomains (also known as lipid rafts) of the plasma membranes containing glycosylphosphatidylinositol-anchored proteins [14, 15]. Macropinocytosis/phagocytosis is initiated by changes in the dynamics of cortical actin in order to uptake particles or aqueous solutions via pseudo-podium formation. The plasma membranes from two sides of pseudopodia can fuse together to engulf such particles or foreign bodies into a specialized structure namely "phago-some" (mainly used for typical phagocytes) or "macropinosome" (used for non-phagocytes) [16]. Clathrin-mediated endocytosis is a result of clathrin-coated protein assembly beneath inner leaflet of the plasma membranes, which then form clathrin-coated pits [17].

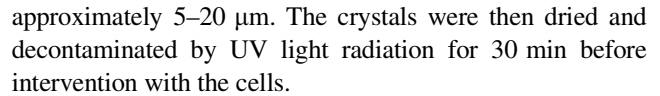
Several chemical inhibitors have been employed to evaluate specific endocytic pathways in various models of in vitro and in vivo studies [12]. Nystatin can bind with cholesterol in plasma membranes and then alters the membrane function, including caveolae formation, thus can inhibit lipid raft engulfment [18]. Cytochalasin D is used as a specific inhibitor for macropinocytosis by binding to actin filaments, thus can interfere with actin polymerization and assembly [19]. Chlorpromazine (CPZ) is widely used as an inhibitor of clathrin-mediated endocytosis because it can be incorporated into lipid bilayers and later causes defective invagination of plasma membranes [20].

In this study, we aimed to define the specific endocytic pathways that renal tubular epithelial cells used to internalize CaOx crystals into the cells. Specific inhibitors for all three major endocytic pathways together and recently established fluorescence-labeled CaOx monohydrate (COM) crystals [21] were employed for quantitative analysis using flow cytometry. Moreover, immunofluorescence staining followed by laser-scanning confocal microscopic examinations were performed to confirm the flow cytometric data.

Materials and Methods

Preparation of Plain (Non-labeled) and Fluorescence-Labeled COM Crystals

Plain COM crystals were prepared as described previously [22, 23]. Briefly, 10 mM calcium chloride was mixed with 10 mM sodium oxalate to achieve final concentrations of 5 mM and 0.5 mM, respectively, in a buffer containing 90 mM Tris–HCl (pH 7.4) and 10 mM NaCl. The mixture was incubated at room temperature (RT) overnight and the COM crystals were harvested by a centrifugation at 3,000 rpm for 5 min. The crystal pellet was washed in absolute methanol and then collected by another centrifugation at 3,000 rpm for 5 min. The size of crystals generated by this protocol was



The fluorescence-labeled COM crystals were generated according to the protocol recently reported by our group [21]. Briefly, the crystals were prepared as aforementioned but in the presence of 10 μl of rabbit anti-mouse IgG conjugated with FITC (DAKO; Glostrup, Denmark) during the initial reaction between calcium chloride and sodium oxalate. The mixture was incubated at RT overnight in the dark and the crystals were harvested, followed by washing, drying, and decontaminating steps as for preparation of the plain COM crystals. The size of fluorescence-labeled crystals obtained was the same as of plain crystals.

Cell Cultivation and COM Crystal Treatment

MDCK renal tubular cells were cultivated in a growth medium [Eagle's minimum essential medium (MEM; Gibco, Grand Island, NY) supplemented with 10 % fetal bovine serum (FBS) (Gibco), 1.2 % penicillin-G/streptomycin, and 2 mM L-glutamine (Sigma; St. Louis, MO)]. The cells were maintained in a humidified incubator at 37 °C with 5 % CO₂. For crystal intervention, the cells (approximately 8×10^4 cells) were seeded in each well of a 24-well plate containing a maintenance medium (MEM supplemented with 1 % heat-inactivated FBS). After 24-h incubation, the cells were washed twice with plain medium and then pretreated with 50 µM nystatin, cytochalasin D, or CPZ in the maintenance medium for 15 min. After the pretreatment, the inhibitors were discarded and the cells were rinsed twice with plain medium. The cells were further incubated with plain (non-labeled) or fluorescencelabeled COM crystals at a dosage of 500 µg crystals/ml culture medium at 37 °C with 5 % CO₂. At 1, 2, and 6 h post-incubation with crystals, the cells were subjected to the flow cytometric measurements (as detailed below). The cells without crystal intervention served as the controls.

Quantitative Analysis of Endocytosis by Flow Cytometry

At 1, 2, and 6 h post-incubation with plain (non-labeled) or fluorescence-labeled crystals with or without the inhibitor pretreatment, the cells at indicated time-points were rinsed with PBS (to eliminate the unbound crystals) followed by trypsinization. The adherent crystals were then eliminated (dissolved) by 5 mM EDTA in PBS for 5 min. The cells with internalized crystals were then quantitated using a flow cytometer (FACScan, Becton-Dickinson Immunocytometry System; San Jose, CA). Quantitation of the internalized plain crystals was performed by analyzing side scattered (SSC) light parameter. Briefly, cell population



was gated by forward-scattered (FSC) and SSC lights, which reflected cell size and granularity, respectively. The controlled cells without any treatment were used to determine the cut-off level of normal cell granularity. The cells with SSC shift-up above this cut-off value were counted as the ones with internalized crystals. For FITC-labeled crystals, the cells with positive FITC signal were directly counted as those with internalized crystals.

Immunofluorescence Staining and Imaging by Laser-Scanning Confocal Microscopy

MDCK cells were cultivated on cover slips (cleaved mica disk diameter: 9.5 mm, SPI Supplies; Toronto, Canada) for 24 h. The cells were rinsed with plain medium before pretreatment with or without 50 µM cytochalasin D for 15 min followed by incubation with 500 µg/ml COM crystals in the maintenance medium for 2 h. After washing with PBS, the cells were fixed with 3.7 % formaldehyde for 10 min and permeabilized with 0.1 % Triton X-100 for another 10 min. After another wash with PBS, the cells were incubated with Phalloidin conjugated with Oregon Green (Invitrogen/Molecular Probes; Burlington, Canada) to stain F-actin (at a dilution of 1:50 in 1 % BSA/ PBS) at 37 °C for 1 h. The nuclei were counterstained by Hoechst dye (Invitrogen/Molecular Probes) (at a dilution of 1:2,000 in 1 % BSA/PBS) at RT for 5 min. The cover slips were then mounted with 50 % glycerol/PBS and the cells were visualized using a laser-scanning confocal microscope equipped with LSM5 Image Browser (LSM 510 META, Carl Zeiss; Oberkochen, Germany). COM crystals adhered on the cell surface or internalized into the cells were visualized by light reflection (in red) at $\lambda = 633$ nm ($\lambda 633$ nm) of the Kr laser as described elsewhere [21, 24]. The intracellular (endocytosed) crystals were also imaged along the vertical axis (Z-axis).

Statistical Analysis

All the aforementioned experiments were performed in triplicate and all the quantitative data are presented as mean \pm SEM unless stated otherwise. Comparisons between two sets of the data were performed using unpaired Student's t test. Multiple-comparisons were performed by ANOVA with Tukey's HSD post-hoc test. P values <0.05 were considered statistically significant.

Results

In previous studies, electron microscopic examination had demonstrated that COM crystals could be internalized into MDCK renal tubular cells by endosome formation [6, 7, 25]. On this basis, the endocytosed COM crystals should

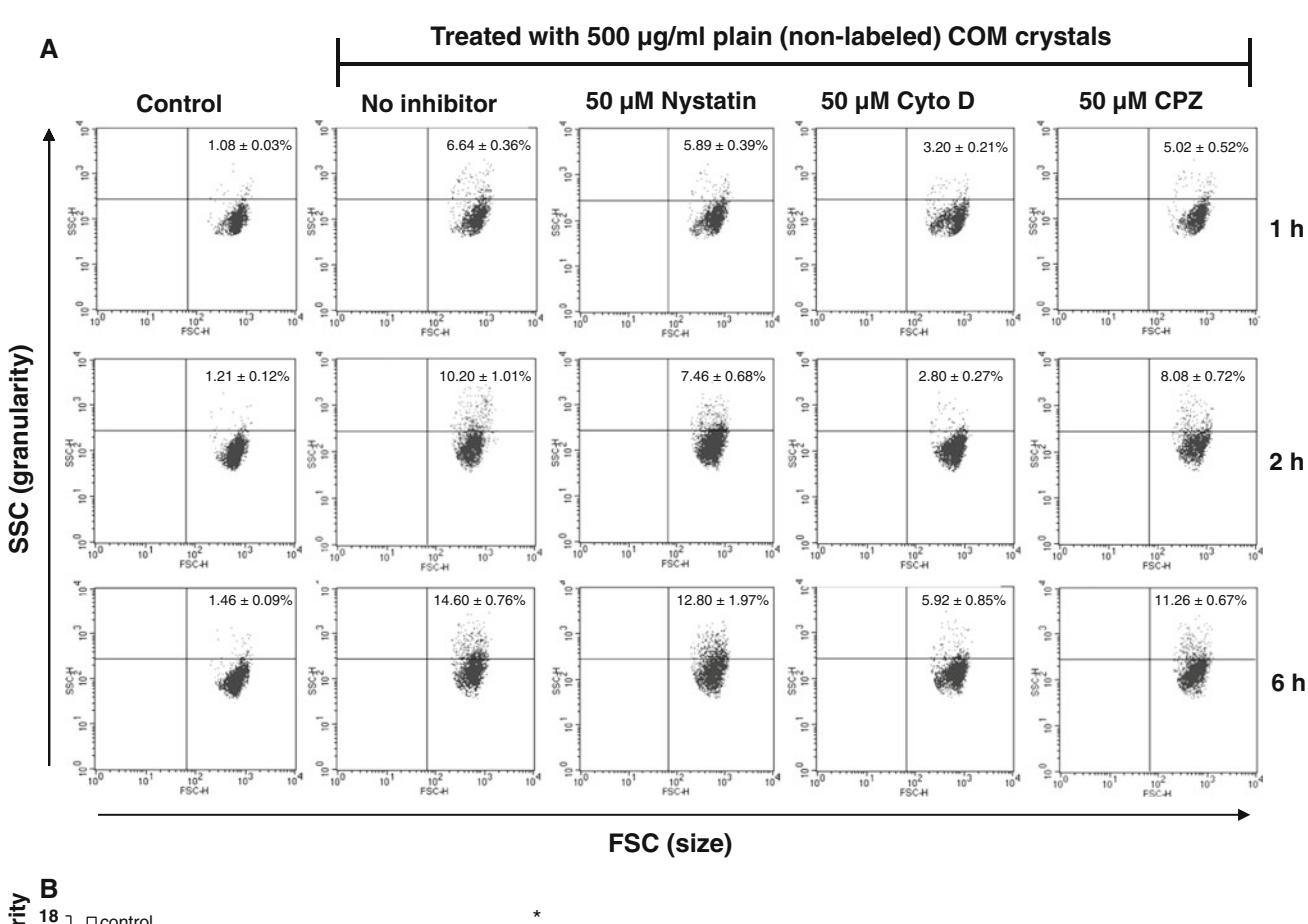
result in the increase of cellular granularity because of the formed endosomes and crystalline compositions inside the cells. To address this point, we applied quantitative flow cytometric analysis to determine changes in cellular granularity after MDCK cells were incubated with or without plain (non-labeled) COM crystals at a dosage of 500 μ g/ml. At 1, 2, and 6 h post-incubation, the cells incubated with COM crystals had marked increase of cellular granularity as compared to the controlled cells (Fig. 1). The data also showed that the increase of cellular granularity of the COM-exposed MDCK cells was time dependent (i.e., the degree of increase was greatest at 6 h).

To investigate specific endocytic pathway of COM crystal uptake into renal tubular cells, MDCK cells were pretreated with each of specific inhibitors for the three main endocytic pathways (including nystatin, cytochalasin D, and CPZ) before incubation with plain COM crystals. The results showed that the increase of cellular granularity induced by plain COM crystals was modestly reduced (or even unaffected in some conditions) by the pretreatment with nystatin and CPZ (Fig. 1). However, the COM crystal-induced increase of cellular granularity was dramatically decreased by the pretreatment with cytochalasin D (Fig. 1), suggesting that macropinocytosis might be the major pathway for endocytosis of COM crystals by renal tubular cells.

Since apoptotic cell death might also lead to the increase of cell granularity and could interfere with data interpretation, we thus performed trypan blue exclusion assay to determine cell viability after treatment with crystals and inhibitors. The results showed that >95 % of the cells remained survived under our experimental conditions. COM crystals at a dosage of 500 µg crystals/ml culture medium and 6-h incubation did not affect the cell survival. Additionally, there were no significant differences by using various inhibitors (Supplementary Methods and Fig. S1). We therefore assumed that changes in cell granularity observed was due to modifications of crystal internalization into the cells and was not caused by potential toxic effects of chemicals and inhibitors.

In addition to the increase of cellular granularity induced by plain COM crystals, flow cytometric quantification of the internalized fluorescence-labeled COM crystals was also performed. This recently established technique, based on the direct quantification of fluorescence signals inside the cells, allows more accurate quantification of the internalized COM crystals [21]. In concordance with the data obtained from the plain COM crystals, the cells incubated with fluorescence-labeled COM crystals had marked increase in percentage of FITC-positive cells, which indicated the internalized crystals, in a time-dependent manner (Fig. 2). Also, pretreatment with nystatin and CPZ slightly decreased the number of the FITC-positive cells with internalized crystals. However,





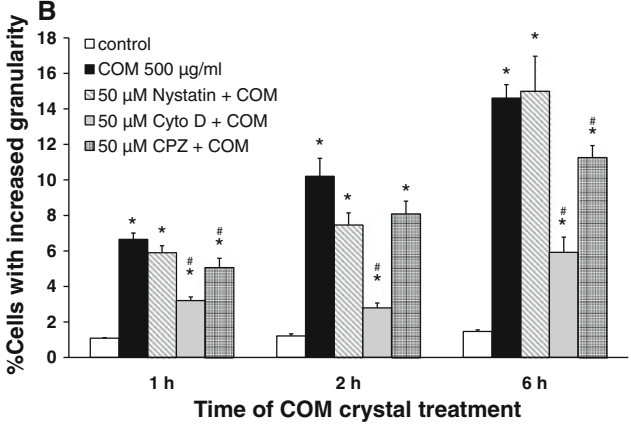


Fig. 1 Flow cytometric analysis of cellular granularity of MDCK cells incubated with plain (non-labeled) COM crystals. Before incubation with or without 500 μg/ml plain COM crystals, MDCK cells were pretreated with 50 μM nystatin, cytochalasin D, or CPZ for 15 min. After 1–6 h of incubation with crystals, the cells were harvested and analyzed by flow cytometry. Dot-plot analysis of

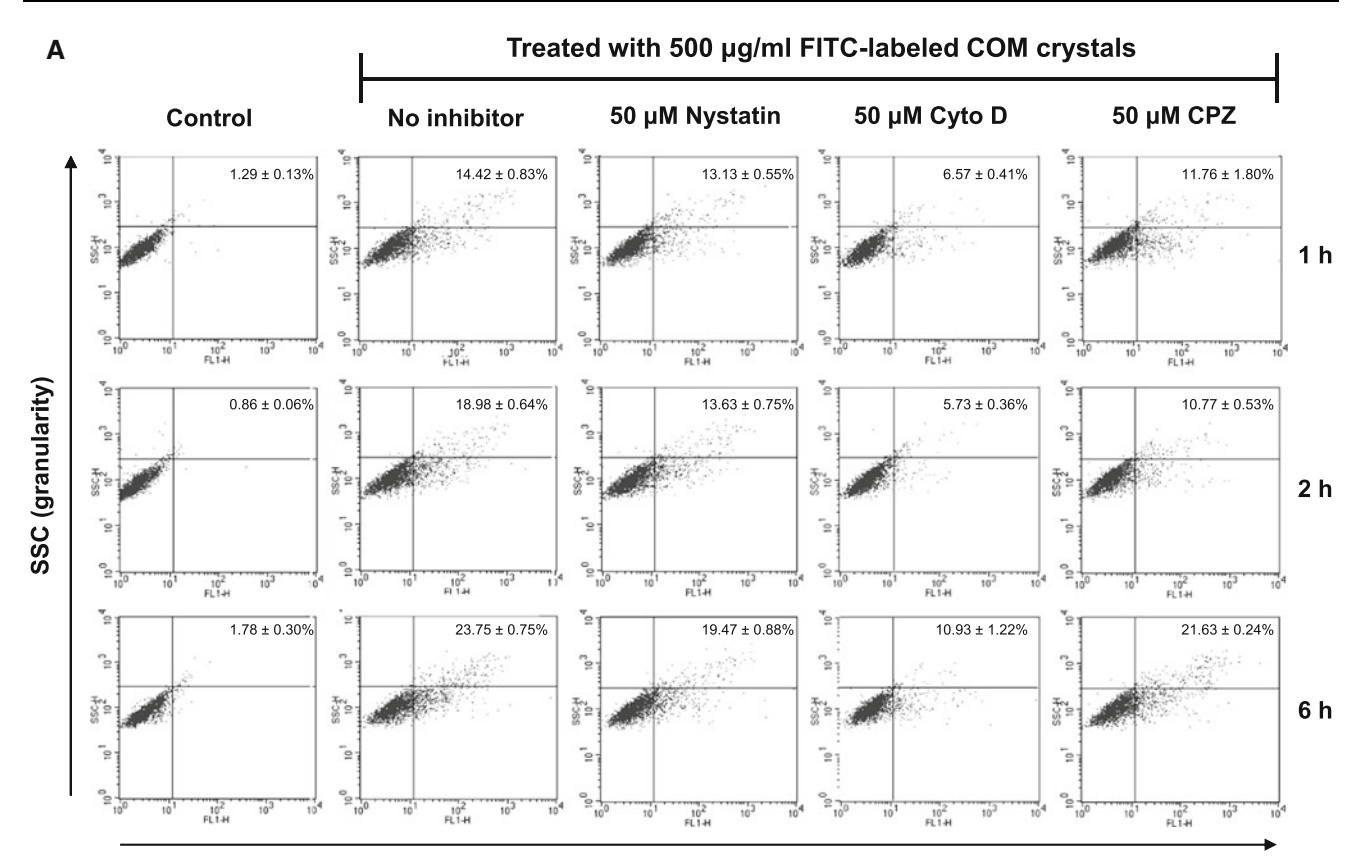
granularity (SSC; y-axis) and size (FSC; x-axis) of the cells is demonstrated in (a), whereas statistical analysis of the percentage of cells with increased granularity is shown in (b). Each *bar* was derived from 3 independent experiments. *P < 0.05 vs. controls; *P < 0.05 vs. COM-treated cells without inhibitor pretreatment

pretreatment with cytochalasin D dramatically reduced the number of FITC-positive cells with internalized crystals (Fig. 2). These results strongly suggested that COM crystals were internalized into renal tubular cells mainly through macropinocytosis.

To confirm the flow cytometric data, we performed immunofluorescence staining followed by laser-scanning

confocal microscopy to directly visualize the endocytosed COM crystals with or without a specific inhibitor of macropinocytosis, cytochalasin D. This experiment was also to address whether cytochalasin D affected crystal adhesion or not. The data obtained from top-view captures revealed that the total number of crystals (adhered onto the cell surface and/or internalized into the cells) remained





FL1-H (mean fluorescence intensity)

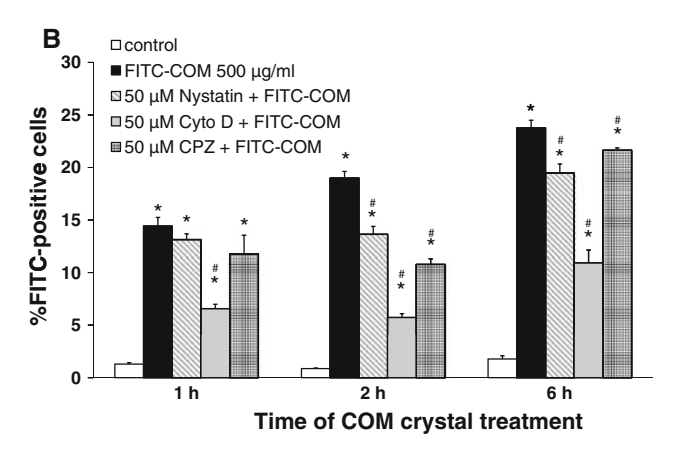


Fig. 2 Quantitative assay of the COM crystal endocytosis in MDCK cells using fluorescence-labeled crystals. Before incubation with or without 500 $\mu g/ml$ FITC-labeled COM crystals, MDCK cells were pretreated with 50 μM nystatin, cytochalasin D, or CPZ for 15 min. After 1–6 h of incubation with crystals, the cells were harvested and analyzed by flow cytometry. Dot-plot analysis of granularity (SSC;

unchanged by cytochalasin D (Fig. 3a, b). This data indicated that the inhibitory effect of cytochalasin D on endocytosis (macropinocytosis) was not a result of reduction of total number of crystals interacted with the cells, but was really a result of the specific inhibition of macropinocytosis. Similar results on number of adhered and/or internalized crystals were observed when the cells were

y-axis) and mean fluorescence intensity (FL1-H; x-axis) of the cells is demonstrated in (a), whereas statistical analysis of the percentage of FITC-positive cells is shown in (b). Each bar was derived from 3 independent experiments. *P < 0.05 vs. controls; *P < 0.05 vs. COM-treated cells without inhibitor pretreatment

treated with nystatin and CPZ (Supplementary Fig. S2A and S2B, respectively).

Consistently, the depth- and sagittal-views showed that the cells pretreated with cytochalasin D had the COM crystals mostly at their apical surfaces with rare crystals found inside the cells, whereas the cells without inhibitor pretreatment demonstrated many of the internalized



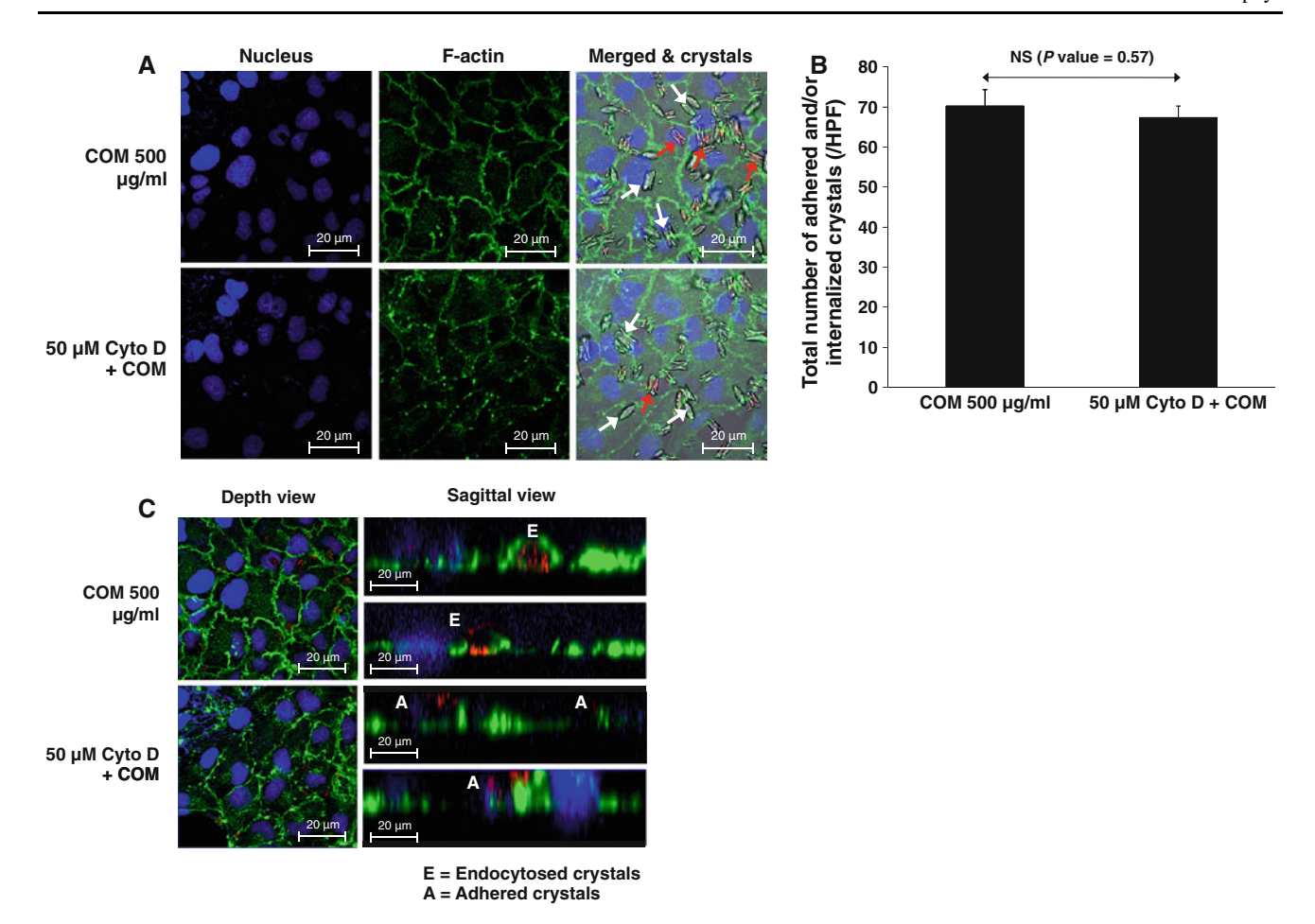


Fig. 3 Confirmation of the inhibitory effects of cytochalasin D on COM crystal endocytosis. MDCK cells grown on cover slips were pretreated with or without 50 μM cytochalasin D for 15 min before incubation with COM crystals for 2 h. **a** F-actin was stained in *green* with Oregon Green-conjugated phalloidin, whereas nuclei were counterstained with Hoechst dye. The images were taken by *topview*. The *last column* shows merged view of bright field and fluorescence staining. The internalized crystals are shown in red color (by using light reflection at λ 633 nm) and marked with *red arrows*, whereas the adhered crystals (by bright field) on cell surfaces are

crystals (Fig. 3c). These findings indicated that cytochalasin D pretreatment did not interfere with crystal adhesion on the cell surface (which is a crucial step required before crystal internalization) and confirmed the flow cytometric data that cytochalasin D dramatically prevented the cells to internalize COM crystals.

Discussion

Nephrolithiasis (kidney stone disease) is a common disease affecting general adult population worldwide. Although physicochemical mechanisms of stone formation have been partially described, little is known for the interaction between renal tubular cells and crystalline compound of the stones. To unravel pathogenic mechanisms of the disease,

located with white arrows. **b** Quantitative data and statistical analysis of the total number of COM crystals interacted with MDCK cells by adhesion and/or internalization. Each bar was derived from 3 independent experiments (HPF high-power field). **c** Depth- and sagittal-views of cells with adhered (labeled as "A") or endocytosed (labeled as "E") crystals. The images were captured under a laser-scanning confocal microscope at an original magnification of $\times 630$. COM crystals were visualized in red by a light reflection at $\lambda 633$ nm using the Kr laser (Color figure online)

the interaction between renal tubular cells and crystals has become one of major research topics of this field during the past decade. The fixed-particle model of the disease has suggested that crystal retention is an important step prior to the stone development [26, 27]. Several macromolecules (in free forms or anchored on the cell surfaces) have been demonstrated to involve in this step [26]. Subsequently, the crystals are rapidly engulfed or endocytosed into renal tubular cells. The endocytosis of crystals has been shown to be a crucial step during the stone initiation [6, 7, 28]. In many previous studies, animal models of kidney stone disease and clinical samples obtained from stone formers have demonstrated that CaOx crystals can be found inside renal tubular cells [29, 30]. In addition, several in vitro studies on renal tubular cell lines exposed to COM crystals have shown that the crystals could adhere on microvilli of



the cell surface and were sequentially internalized into the cells within an hour [6, 7, 25, 31]. The term "endocytosis" has been generally used for internalization or engulfment of the crystals adhered on the cell surface. However, there had been no available data to address molecular pathway underlying crystal internalization through endocytosis.

Several methods have been used for the investigations of COM crystal endocytosis. The simplest one is using a phase contrast microscope. Nevertheless, the data obtained are not reliable since this technique cannot distinguish the internalized crystals from those adhered on the cell surface. Therefore, most of the studies have employed [14C]-labeled COM crystals to determine the cells with the engulfed crystals [6, 32]. Although it provides higher sensitivity, this method may be hazardous to health and environment. Another approach is to distinguish cell size and granularity between the controlled cells and those with endocytosed crystals. Flow cytometry allows for such discrimination by using FSC and SSC signals, which correlate very well with the cell size and the complexity inside the cells (e.g., granules, vesicles), respectively. The granularity of cells with endocytosed crystals was expected to increase compared to the controlled cells [33]. Furthermore, we have recently established a novel non-radioactive method based on fluorescence labeling for visualizing and tracking the crystals [21].

In the present study, we applied both flow cytometry and fluorescence-labeled crystals for the investigations of COM crystal endocytosis in renal tubular cells. It has been hypothesized that distal nephron was the priming site for stone nidus formation. Therefore, MDCK cells, which were derived from normal canine kidneys (particularly from distal renal tubule and collecting duct [34]), were employed in the present study. We first used the plain or non-labeled COM crystals and found the increased granularity of the cells with endocytosed crystals (Fig. 1). However, the obtained data could not be referred directly to the cells with the endocytosed or internalized crystals. We then employed the FITClabeled COM crystals in combination with flow cytometry for the more reliable analyses [21]. To avoid the false positive generated by the adhered crystals, we completely dissolved such adherent crystals by using EDTA before the analysis [32]. Thus, the positive signals would directly refer to the engulfed COM crystals inside the cells. The results showed that the data obtained from fluorescence-labeled COM crystals (Fig. 2) were consistent with those obtained from the plain COM crystals (Fig. 1).

The analysis revealed that pretreatment with cytochalasin D provided the greatest degree of reduction of the endocytosed crystals, whereas nystatin and CPZ had only modest degree of such inhibition (Figs. 1, 2). However, higher degree of inhibition was observed when using fluorescence-labeled crystals. The reason behind was that detection of changes in fluorescence signal (%FITC-

positive cells) is more sensitive as compared to the detection of changes in cell granularity. This means that under the same situation, if the cell engulfed only a tiny fluorescence-labeled crystal, it could be counted as a FITC-positive cell although such uptake might not affect the cell granularity.

Various drugs and chemical reagents were used to define the specific mechanisms involved in COM crystal endocytosis by MDCK cells. Previous findings suggested that increased intracellular calcium concentration, blockade of actin polymerization, inhibition of protein kinase C, and cyclo-oxygenase activity were involved in the reduction of COM crystal uptake [35]. We obtained similar findings that cytochalasin D significantly reduced the number of crystals uptake most likely via inhibition of actin polymerization. In concordance with others [6, 25], using laser-scanning confocal microscopy, we found that more than one crystal could be engulfed into the cell. Microscopic examination revealed that microvilli of the cells played a key role in crystal internalization process [36]. Lieske et al. [6] demonstrated that the adhered crystals were engulfed into vesicles by the cellular projection. Using laser-scanning confocal microscope, we also observed that the endocytosed crystals were surrounded by actin vesicles. Pretreatment with cytochalasin D did not affect crystal adhesion on MDCK cell surface. As macropinosomes were derived from actin-rich plasma membranes, so called ruffles, it was unsurprising that disruption by cytochalasin D markedly inhibited COM crystal uptake.

Although macropinosome shared some features with other organelles, e.g., endosome, lysosome, and phagolysosome, however, it has distinct organization process. While phagosome formation is initiated and maintained by interaction between Fc receptors and the internalized particles (opsonized particles), macropinosome formation is rather independent of the external stimuli [16]. In addition, maturation of macropinosome requires the exchange of membrane components with those of other organelles, including endolysosomal system (i.e., Rab7), making it more difficult to define the unique molecular markers of this process [37, 38].

Finally, it should be emphasized that the inhibition of crystal endocytosis using cytochalasin D to block macropinocytosis was not perfectly complete. This might be simply explained that endocytosis of COM crystals by renal tubular cells was also mediated partially through lipid raft/caveolae- and clathrin-dependent pathways (as the minor or alternative mechanisms to uptake COM crystals) (Figs. 1, 2). Theoretically, using inhibitors specific to all three endocytic pathways should completely inhibit the crystal uptake. However, it may not be practical because overdose of inhibitors will cause cytotoxicity and ultimately cell death, which affects interpretation of the



results. Also, the experimental condition used in our study might not be optimal to completely inhibit the COM crystal uptake. However, these findings could highlight that endocytosis of COM crystals by MDCK renal tubular cells was mainly actin cytoskeleton-dependent process (i.e., macropinocytosis).

In summary, we report herein for the first time that renal tubular cells endocytose COM crystals mainly via macropinocytosis. These novel findings will pave the way for further tracking the endocytosed crystals inside renal tubular cells during the course of kidney stone formation. Further in-depth studies on subsequent signal transduction cascade following macropinocytosis of COM crystals and the fate of the endocytosed crystals after such uptake will definitely provide valuable information to better understand the precise mechanisms of kidney stone formation.

Acknowledgments This study was supported by Office of the Higher Education Commission and Mahidol University under the National Research Universities Initiative, The Thailand Research Funds (RTA5380005, TRG5480005, and TRG5480008), and Faculty of Medicine Siriraj Hospital. KS is supported by the Royal Golden Jubilee PhD Program, whereas VT is also supported by the "Chalermphrakiat" Grant, Faculty of Medicine Siriraj Hospital.

References

- Moe, O. W. (2006). Kidney stones: Pathophysiology and medical management. *Lancet*, 367, 333–344.
- 2. Khan, S. R., & Hackett, R. L. (1991). Retention of calcium oxalate crystals in renal tubules. *Scanning Microscopy*, *5*, 707–711.
- 3. De Bruijn, W. C., Boeve, E. R., van Run, P. R., van Miert, P. P., de Water, R., Romijn, J. C., et al. (1995). Etiology of calcium oxalate nephrolithiasis in rats. I. Can this be a model for human stone formation? *Scanning Microscopy*, *9*, 103–114.
- de Water, R., Noordermeer, C., van der Kwast, T. H., Nizze, H., Boeve, E. R., Kok, D. J., et al. (1999). Calcium oxalate nephrolithiasis: Effect of renal crystal deposition on the cellular composition of the renal interstitium. *American Journal of Kidney Diseases*, 33, 761–771.
- Tsujihata, M. (2008). Mechanism of calcium oxalate renal stone formation and renal tubular cell injury. *International Journal of Urology*, 15, 115–120.
- Lieske, J. C., Swift, H., Martin, T., Patterson, B., & Toback, F. G. (1994). Renal epithelial cells rapidly bind and internalize calcium oxalate monohydrate crystals. *Proceedings of the National Academy of Sciences USA*, 91, 6987–6991.
- Schepers, M. S., Duim, R. A., Asselman, M., Romijn, J. C., Schroder, F. H., & Verkoelen, C. F. (2003). Internalization of calcium oxalate crystals by renal tubular cells: A nephron segment-specific process? *Kidney International*, 64, 493–500.
- 8. Evan, A. P., Lingeman, J. E., Coe, F. L., Parks, J. H., Bledsoe, S. B., Shao, Y., et al. (2003). Randall's plaque of patients with nephrolithiasis begins in basement membranes of thin loops of Henle. *The Journal of Clinical Investigation*, 111, 607–616.
- Kumar, V., Farell, G., Yu, S., Harrington, S., Fitzpatrick, L., Rzewuska, E., et al. (2006). Cell biology of pathologic renal calcification: Contribution of crystal transcytosis, cell-mediated calcification, and nanoparticles. *Journal of Investigative Medicine*, 54, 412–424.

- Evan, A. P., Coe, F. L., Lingeman, J. E., Shao, Y., Sommer, A. J., Bledsoe, S. B., et al. (2007). Mechanism of formation of human calcium oxalate renal stones on Randall's plaque. *The Anatomical Record (Hoboken)*, 290, 1315–1323.
- Doherty, G. J., & McMahon, H. T. (2009). Mechanisms of endocytosis. *Annual Review of Biochemistry*, 78, 857–902.
- Ivanov, A. I. (2008). Pharmacological inhibition of endocytic pathways: Is it specific enough to be useful? *Methods in Molecular Biology*, 440, 15–33.
- Seto, E. S., Bellen, H. J., & Lloyd, T. E. (2002). When cell biology meets development: Endocytic regulation of signaling pathways. *Genes & Development*, 16, 1314–1336.
- Parton, R. G., & Richards, A. A. (2003). Lipid rafts and caveolae as portals for endocytosis: New insights and common mechanisms. *Traffic*, 4, 724–738.
- Vassilieva, E. V., Gerner-Smidt, K., Ivanov, A. I., & Nusrat, A. (2008). Lipid rafts mediate internalization of beta1-integrin in migrating intestinal epithelial cells. *American Journal of Physiology Gastrointestinal and Liver Physiology*, 295, G965–G976.
- Kerr, M. C., & Teasdale, R. D. (2009). Defining macropinocytosis. *Traffic*, 10, 364–371.
- Sorkin, A. (2004). Cargo recognition during clathrin-mediated endocytosis: A team effort. Current Opinion in Cell Biology, 16, 392–399.
- Ros-Baro, A., Lopez-Iglesias, C., Peiro, S., Bellido, D., Palacin, M., Zorzano, A., et al. (2001). Lipid rafts are required for GLUT4 internalization in adipose cells. *Proceedings of the National Academy of Sciences USA*, 98, 12050–12055.
- Peterson, J. R., & Mitchison, T. J. (2002). Small molecules, big impact: A history of chemical inhibitors and the cytoskeleton. *Chemistry & Biology*, 9, 1275–1285.
- Inal, J., Miot, S., & Schifferli, J. A. (2005). The complement inhibitor, CRIT, undergoes clathrin-dependent endocytosis. *Experimental Cell Research*, 310, 54–65.
- Chaiyarit, S., Mungdee, S., & Thongboonkerd, V. (2010). Nonradioactive labelling of calcium oxalate crystals for investigations of crystal-cell interaction and internalization. *Analytical Methods*, 2, 1536–1541.
- Thongboonkerd, V., Semangoen, T., Sinchaikul, S., & Chen, S. T. (2008). Proteomic analysis of calcium oxalate monohydrate crystal-induced cytotoxicity in distal renal tubular cells. *Journal* of Proteome Research, 7, 4689–4700.
- Semangoen, T., Sinchaikul, S., Chen, S. T., & Thongboonkerd, V. (2008). Proteomic analysis of altered proteins in distal renal tubular cells in response to calcium oxalate monohydrate crystal adhesion: Implications for kidney stone disease. *Proteomics Clinical Applications*, 2, 1099–1109.
- Verkoelen, C. F., van der Boom, B. G., Houtsmuller, A. B., Schroder, F. H., & Romijn, J. C. (1998). Increased calcium oxalate monohydrate crystal binding to injured renal tubular epithelial cells in culture. *American Journal of Physiology*, 274, F958–F965.
- Kohjimoto, Y., Ebisuno, S., Tamura, M., & Ohkawa, T. (1996).
 Interactions between calcium oxalate monohydrate crystals and Madin–Darby canine kidney cells: Endocytosis and cell proliferation. *Urological Research*, 24, 193–199.
- Verkoelen, C. F., & Verhulst, A. (2007). Proposed mechanisms in renal tubular crystal retention. *Kidney International*, 72, 13–18.
- Kok, D. J., & Khan, S. R. (1994). Calcium oxalate nephrolithiasis, a free or fixed particle disease. *Kidney International*, 46, 847–854.
- Lieske, J. C., & Toback, F. G. (1993). Regulation of renal epithelial cell endocytosis of calcium oxalate monohydrate crystals. *American Journal of Physiology*, 264, F800–F807.
- Ebisuno, S., Kohjimoto, Y., Tamura, M., Inagaki, T., & Ohkawa,
 T. (1997). Histological observations of the adhesion and



- endocytosis of calcium oxalate crystals in MDCK cells and in rat and human kidney. *Urologia Internationalis*, 58, 227–231.
- Khan, S. R. (1995). Calcium oxalate crystal interaction with renal tubular epithelium, mechanism of crystal adhesion and its impact on stone development. *Urological Research*, 23, 71–79.
- Lieske, J. C., Norris, R., Swift, H., & Toback, F. G. (1997).
 Adhesion, internalization and metabolism of calcium oxalate monohydrate crystals by renal epithelial cells. *Kidney International*, 52, 1291–1301.
- Hovda, K. E., Guo, C., Austin, R., & McMartin, K. E. (2010).
 Renal toxicity of ethylene glycol results from internalization of calcium oxalate crystals by proximal tubule cells. *Toxicology Letters*, 192, 365–372.
- Borges, F. T., Michelacci, Y. M., Aguiar, J. A., Dalboni, M. A., Garofalo, A. S., & Schor, N. (2005). Characterization of glycosaminoglycans in tubular epithelial cells: Calcium oxalate and oxalate ions effects. *Kidney International*, 68, 1630–1642.

- Dukes, J. D., Whitley, P., & Chalmers, A. D. (2011). The MDCK variety pack: Choosing the right strain. BMC Cell Biology, 12, 43
- Campos, A. H., & Schor, N. (2000). Mechanisms involved in calcium oxalate endocytosis by Madin–Darby canine kidney cells. *Brazilian Journal of Medical and Biological Research*, 33, 111–118
- Kohjimoto, Y., Ebisuno, S., Tamura, M., & Ohkawa, T. (1996).
 Adhesion and endocytosis of calcium oxalate crystals on renal tubular cells. *Scanning Microscopy*, 10, 459–468.
- Racoosin, E. L., & Swanson, J. A. (1993). Macropinosome maturation and fusion with tubular lysosomes in macrophages. *Journal of Cell Biology*, 121, 1011–1020.
- 38. Kerr, M. C., Lindsay, M. R., Luetterforst, R., Hamilton, N., Simpson, F., Parton, R. G., et al. (2006). Visualisation of macropinosome maturation by the recruitment of sorting nexins. *Journal of Cell Science*, 119, 3967–3980.



ORIGINAL PAPER

Secreted Products of Macrophages Exposed to Calcium Oxalate Crystals Induce Epithelial Mesenchymal Transition of Renal Tubular Cells via RhoA-Dependent TGF-\(\beta\)1 Pathway

Rattiyaporn Kanlaya · Kitisak Sintiprungrat · Visith Thongboonkerd

© Springer Science+Business Media New York 2013

Abstract Kidney stone disease is associated with renal fibrosis by the unclear mechanisms. We hypothesized that calcium oxalate (CaOx), a major crystalline component of kidney stones, could induce secretion of fibrotic factors from macrophages leading to "epithelial mesenchymal transition/transdifferentiation" (EMT) of renal tubular cells. Western blot analysis revealed an increased level of vimentin (mesenchymal marker) but decreased levels of E-cadherin and cytokeratin (epithelial markers) in MDCK cells treated with "secreted products from CaOx-exposed macrophages" (CaOx-M-Sup). Immunofluorescence study confirmed the increased level of vimentin and decreased level of cytokeratin, and also revealed the increased level of fibronectin (another mesenchymal marker). The data also showed decreased levels and disorganization of F-actin (cytoskeletal marker) and zonula occludens-1 (ZO-1) (tight junction marker) induced by CaOx-M-Sup. ELISA demonstrated the increased level of transforming growth factor-β1 (TGF-β1), the well-defined EMT inducer, in CaOx-M-Sup. Downstream signaling of TGF-β1 was involved as demonstrated by the decreased level of RhoA. Interestingly, pretreatment with a proteasome inhibitor (MG132) could restore RhoA to its basal level, most likely

through ubiquitin-proteasome pathway (UPP). Moreover, MG132 successfully sustained cytoskeletal assembly and tight junction, and could prevent the cells from EMT. Altogether, these data demonstrate for the first time that CaOx-M-Sup could induce EMT in renal tubular cells by TGF- β 1 signaling cascade via RhoA and UPP. This may be, at least in part, the underlying mechanism for renal fibrosis in kidney stone disease.

Keywords Calcium oxalate · Epithelial mesenchymal transition (EMT) · RhoA · Secretome · Tubular cells

Introduction

Many studies have demonstrated the association between kidney stone disease (nephrolithiasis/urolithiasis) and renal fibrosis [1, 2]. Unlike other types of chronic kidney disease (CKD) (e.g., diabetic nephropathy, glomerulopathies) in which mechanisms underlying renal fibrotic changes have been extensively investigated and some of them are well accepted, the mechanisms underlying renal fibrosis in kidney stone disease remain largely unknown. In general, a process called "epithelial mesenchymal transition/transdifferentiation" (EMT) plays a crucial role in many models of renal fibrosis [3, 4]. Typical morphology and polarity of tubular epithelial cells are lost during EMT, and the cells transform to fibroblasts with spindle shape [5, 6]. With this transition, the cells acquire mesenchymal characteristics, including down-regulation of epithelial markers, i.e., E-cadherin, cytokeratin, and tight junction protein zonula occludens-1 (ZO-1), resulting to disintegration and loss of the cell contact. On the other hand, the cells undergoing EMT up-regulates mesenchymal markers, i.e., vimentin and fibroblast-specific protein 1 (FSP1). Over-production

R. Kanlaya · K. Sintiprungrat · V. Thongboonkerd (☒)
Medical Proteomics Unit, Office for Research and Development,
Faculty of Medicine Siriraj Hospital, and Center for Research
in Complex Systems Science, Mahidol University, 6th Floor,
SiMR Building, 2 Prannok Road, Bangkoknoi,
Bangkok 10700, Thailand

e-mail: thongboonkerd@dr.com; vthongbo@yahoo.com

Published online: 23 May 2013



of extracellular matrix proteins (e.g., fibronectin, collagen, matrix metalloproteinases (MMPs)) has been also found during the EMT induction [5, 7]. Moreover, EMT can induce actin disorganization or reorganization into the actin stress fiber.

In a previous study by Iwano et al. [8] using chimeric bone marrow and transgenic murine model, approximately one third of renal interstitial fibroblasts have been found to be derived from tubular epithelial cells by the EMT process. In another study by Rastaldi et al. [4], 133 human renal biopsies from patients with various kidney diseases have shown EMT characteristics correlated with the degree of interstitial damage. Transforming growth factor-\(\beta\)1 (TGF-β1) is the well-known proinflammatory cytokine that plays a crucial role in the induction of EMT [3] and has been reported to be associated with CKD [9]. A recent study has shown that renal tubular epithelial cells derived from collecting duct treated with insulin-like growth factors and TGF-β1 turned to fibroblasts by EMT [10]. These aforementioned studies suggest that renal tubular epithelial cells can be transformed via EMT mechanism in response to some stimuli and may, in turn, participate in the pathogenesis of renal fibrosis. Hence, the investigations of underlying mechanisms that regulate EMT in combination with the studies to search for novel inhibitors that can prevent or limit EMT process are of great importance.

In a rat model of kidney stone disease, macrophages have been found to accumulate at the site of calcium oxalate (CaOx) crystal deposition [11, 12]. It has been generally presumed that these cells play important roles in the elimination of CaOx crystals by phagocytosis. Moreover, the activated macrophages can also produce proinflammatory cytokines, which in turn may stimulate production of other various cytokines in response to the inflammation [13–15]. Consequently, progressive inflammation develops and can amplify the tubulointerstitium damage because of the synergistic effects of the leukocyte recruitment and the secreted products derived from the activated macrophages to initiate tissue fibrosis [15, 16].

In this study, we hypothesized that the secreted products derived from macrophages exposed to CaOx, a major causative crystalline component of kidney stones, could induce secretion of fibrotic factors from macrophages leading to EMT of renal tubular cells. EMT markers were examined by Western blot analysis and immunofluorescence study. Level of TGF-β1 in the "secreted products of CaOx-exposed macrophages" (CaOx-M-Sup) and cellular levels of the cascade signaling molecule RhoA as well as the ubiquitinated proteins were measured. Finally, a proteasome inhibitor (MG132) was applied to examine whether the intervention of ubiquitin-proteasome pathway (UPP) could prevent EMT and changes in RhoA induced by CaOx-M-Sup.



Macrophage Cultivation, Intervention by CaOx Crystals, and Collection of CaOx-M-Sup

Human monocytic cell line U937 was grown in complete RPMI medium (Gibco; Grand Island, NY) supplemented with 10 % (v/v) heat-inactivated fetal bovine serum (FBS) (Gibco), 100 U/ml penicillin G and 100 mg/ml streptomycin (Sigma; St.Louis, MO). The cells were maintained in a humidified incubator at 37 °C with 5 % CO₂. U937 cells were derived to human macrophages by incubation with 100 ng/ml phorbol 12-myristate 13-acetate (PMA) for 48 h, and the biology and characteristics of macrophages were confirmed as previously described [17]. During PMA treatment, the cells were refreshed with growth RPMI medium every 24 h. Thereafter, macrophages were treated with 100 µg/ml CaOx crystals (prepared as described in our previous studies [18, 19]) in complete RPMI without FBS supplementation for 48 h and the culture supernatant was then harvested. The collected supernatant (CaOx-M-Sup) was clarified by a centrifugation at 3,500 rpm at 4 °C for 15 min and kept as aliquots at -80 °C until used.

Cultivation of Distal Renal Tubular Cells and Induction of EMT by CaOx-M-Sup

Mardin-Darby Canine Kidney (MDCK), a distal renal tubular epithelial cell line, was cultivated in a growth medium (Eagle's minimum essential medium (MEM) (Gibco) supplemented with 10 % (v/v) heat-inactivated FBS (Gibco), 100 U/ml penicillin G and 100 mg/ml streptomycin (Sigma)). The cells were maintained in a humidified incubator at 37 °C with 5 % CO₂. MDCK cells were seeded into six-well plate at 4 × 10⁴ cells/well and further maintained in the growth medium for 24 h. Thereafter, the cells were washed with serum-free medium and then incubated in CaOx-M-Sup mixed 1:1 with a maintenance medium (MEM supplemented with 1 % heat-inactivated FBS) for 24 h. The cells incubated with plain MEM mixed with a maintenance medium (1:1) served as the controls.

Prevention of EMT by a Proteasome Inhibitor

MDCK cells were seeded into six-well plate at 4×10^4 cells/well and further maintained in the growth medium for 24 h, the cells were pretreated with either dimethyl sulf-oxide (DMSO; as a chemical control for inhibitory effect) or 0.1 μ M MG132 (a specific proteasome inhibitor) (Tocris Bioscience; Bristol, UK) for 2 h before incubation with or without CaOx-M-Sup for 24 h as aforementioned. The cells were then subjected to morphological analysis,



immunofluorescence study and Western blot analyses as follows.

Morphological Study and Immunofluorescence Stainings

Cell morphology was observed under a phase contrast microscope (Olympus CKX41; Tokyo, Japan) at 24 h after treatment with or without CaOx-M-Sup. For immunofluorescence stainings, the cells were grown on a coverslip and EMT was induced by CaOx-M-Sup as aforementioned. The cells were then processed for immunofluorescence stainings of vimentin, fibronectin, cytokeratin, F-actin and ZO-1. In brief, the cells were washed once with PBS and then fixed with 3.7 % formaldehyde in PBS at room temperature (RT) for 10 min and permeabilized with 1 % triton x-100 in PBS at RT for another 10 min. After washing, the cells were incubated with anti-vimentin conjugated with Alexa Fluor 488 (Invitrogen; Eugene, OR) or other specific primary antibody (anti-fibronectin, anti-cytokeratin, or anti-ZO-1) (Santa Cruz Biotechnology; Santa Cruz, CA), all at a dilution of 1:50 in 1 % BSA/PBS at 37 °C for 1 h. F-actin was stained by Oregon Green labeled-phalloidin (Invitrogen) at a dilution of 1:50 in 1 % BSA/PBS at 37 °C for 1 h. The cells were then extensively washed with PBS. Except for stainings of vimentin and F-actin, the cells were further incubated with respective secondary antibody conjugated with Cy3 (Dako; Glostrup, Denmark) at a dilution of 1:2,500 in 1 % BSA/PBS at RT for 1 h. After the final washing step, the cells were mounted onto a glass slide using ProLong Gold antifade reagent (Invitrogen) and images were captured under the Nikon Eclipse 80i fluorescence microscope (Nikon; Tokyo, Japan).

Western Blot Analyses

Proteins were extracted from the whole cells using Laemmli's buffer and concentrations of proteins derived from individual samples were obtained using the Bio-Rad Protein Assay (Bio-Rad Laboratories; Hercules, CA) based on the Bradford method. An equal amount of 20 µg proteins derived from each sample was resolved by 12 % SDS-PAGE. The resolved proteins were transferred onto a nitrocellulose membrane and then incubated with specific primary antibody (anti-vimentin, anti-E-cadherin, anticytokeratin, anti-RhoA, anti-ubiquitin, or anti-GAPDH) (Santa Cruz Biotechnology) at a dilution of 1:1,000 in 1 % skim milk/PBS at 4 °C overnight. Note that GAPDH served as the equal loading control. After washing, the membrane was further incubated with corresponding secondary antibody conjugated with horseradish peroxidase (HRP) (Dako) at a dilution of 1:2,000 in 1 % skim milk/ PBS at RT for 1 h. Finally, the reactive protein bands were visualized by SuperSignal West Pico chemiluminescence substrate (Pierce Biotechnology, Inc., Rockford, IL) and autoradiography. Band intensity data were obtained using ImageQuant software (GE Healthcare; Uppsala, Sweden).

ELISA

Level of TGF- β 1 in CaOx-M-Sup was measured by a commercially available ELISA kit (RayBiotech; Singapore). The procedures were performed according to the protocol provided by the manufacturer.

Statistical Analysis

Quantitative data are reported as mean \pm SEM. Comparisons of the data between the two sets of samples were performed using unpaired Student's t test. P values less than 0.05 were considered statistically significant.

Results

Induction of EMT in Renal Tubular Cells by CaOx-M-Sup

MDCK cells were maintained in CaOx-M-Sup mixed 1:1 with a maintenance medium. After 24 h of such treatment, the cells with typical epithelial-like morphology turned into the fibroblast-like cells with spindle shape (Fig. 1a). We then performed Western blot analysis to examine for markers of the transition of epithelial cells to mesenchymal cells, including the up-regulation of mesenchymal marker (vimentin) and down-regulation of epithelial markers (E-cadherin and cytokeratin). In concordance to the morphological changes, Western blot data showed significant increase in vimentin level and decreases in levels of E-cadherin and cytokeratin as compared to the controlled cells (Fig. 1b, c). In addition, the induction of EMT by CaOx-M-Sup was also confirmed by immunofluorescence study, which revealed increased expression levels of vimentin and fibronectin (mesenchymal markers), whereas expression level of cytokeratin (epithelial marker) was decreased (Fig. 1d). Moreover, the data also showed the decreased levels and disorganization of F-actin and tight junction protein zonula occludens-1 (ZO-1) (Fig. 1d).

Induction of EMT by CaOx-M-Sup was Controlled by TGF-β1-Induced RhoA Degradation through Ubiquitin-Proteasome Pathway (UPP)

Because the proinflammatory cytokine TGF- β 1 has been recognized as the key factor for induction of EMT, we thus measured level of TGF- β 1 in CaOx-M-Sup using ELISA.



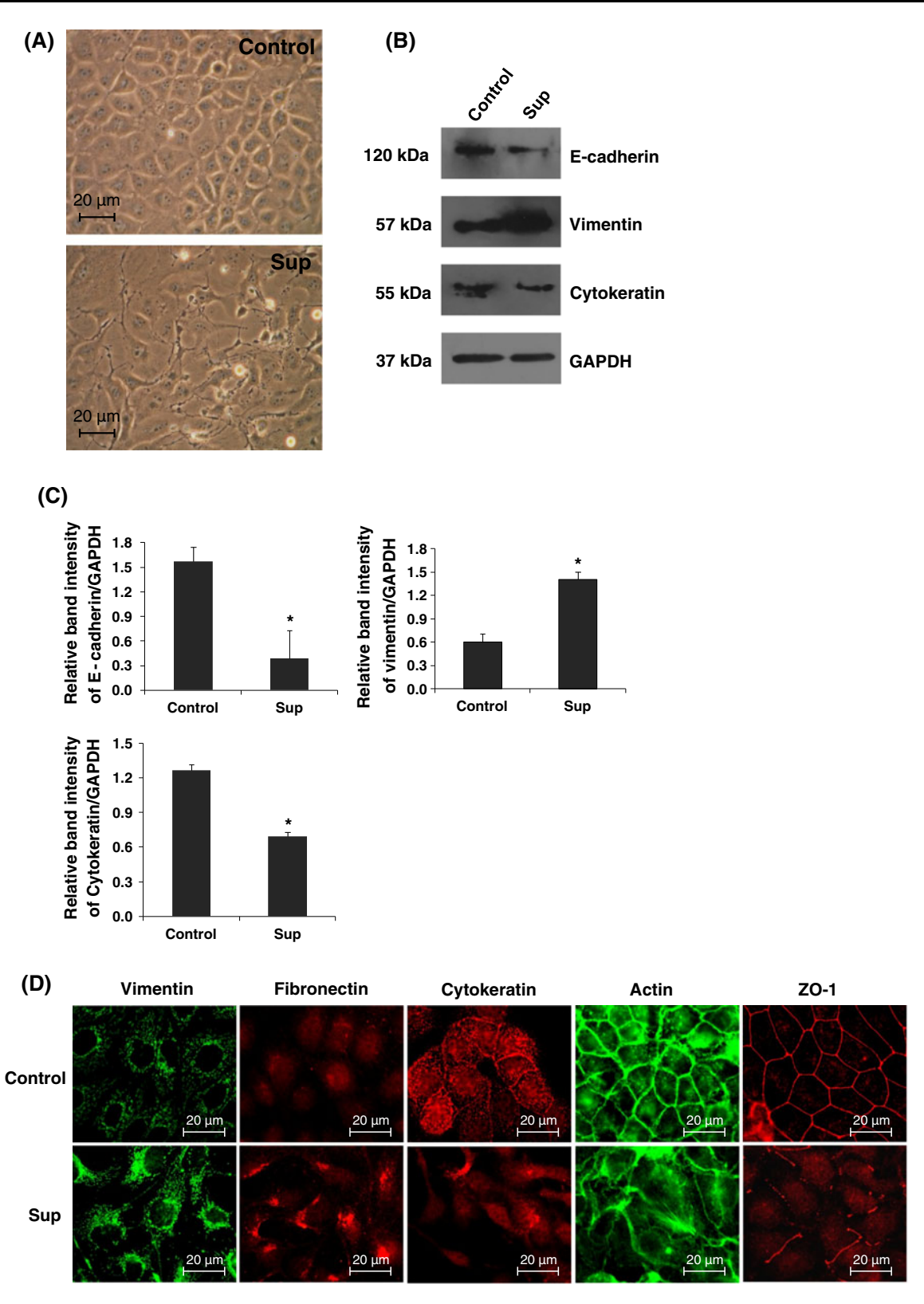


Fig. 1 Induction of EMT in MDCK cells by secreted products from CaOx-exposed macrophages (CaOx-M-Sup). The cells were cultivated with the controlled maintenance medium or with CaOx-M-Sup mixed 1:1 with the maintenance medium for 24 h and were then subjected to morphological study (a). Western blot analysis was performed (b) and

band intensity data were obtained from 3 independent experiments and normalized with GAPDH, which served as the loading control (c). Immunofluorescence study was performed for staining mesenchymal markers (vimentin and fibronectin) and epithelial markers (E-cadherin, cytokeratin, F-actin and ZO-1) (d). *p < 0.05 versus control



The results showed that level of TGF-\(\beta\)1 in CaOx-M-Sup was significantly greater than that of the controlled medium (Fig. 2a). Recent lines of evidence have reported that RhoA might be a cascade signaling molecule responsible for TGF-β1-induced EMT [3–10]. Once triggered by TGFβ1, RhoA would be degraded by UPP. To examine the involvement of RhoA and UPP in EMT in our model, we performed Western blot analysis to determine cellular level of RhoA (Fig. 2b). The data showed that RhoA was significantly reduced in MDCK cells treated with CaOx-M-Sup as compared to the controls. Interestingly, pretreatment of the cells with a proteasome inhibitor (MG132) prior to EMT induction successfully restored RhoA to its basal level, whereas pretreatment with DMSO (as a chemical control for inhibitory effect) had no influence on RhoA level (Fig. 2b). In parallel, we also determined levels of ubiquitin-tagged proteins using an antibody specific ubiquitin molecules. As expected, levels of the ubiquitinated proteins were significantly increased in the cells pretreated with MG132 prior to the induction of EMT, whereas their levels were comparable among the controlled cells, CaOx-M-Sup-treated cells, and CaOx-M-Sup-treated cells pretreated with DMSO (Fig. 2c, d). Taken together, these data implicated that the decreased RhoA level in CaOx-M-Sup-treated cells was most likely due to the UPP-mediated degradation.

Disorganization of the Actin Cytoskeletal Assembly and ZO-1 Induced by CaOx-M-Sup was Successfully Prevented by a Specific Proteasome Inhibitor

We next examined whether MG132 could prevent disorganization of the actin cytoskeletal assembly and the tight junction protein ZO-1 upon the induction of EMT by CaOx-M-Sup. Immunofluorescence study revealed that the decreased levels and disorganization of actin and ZO-1

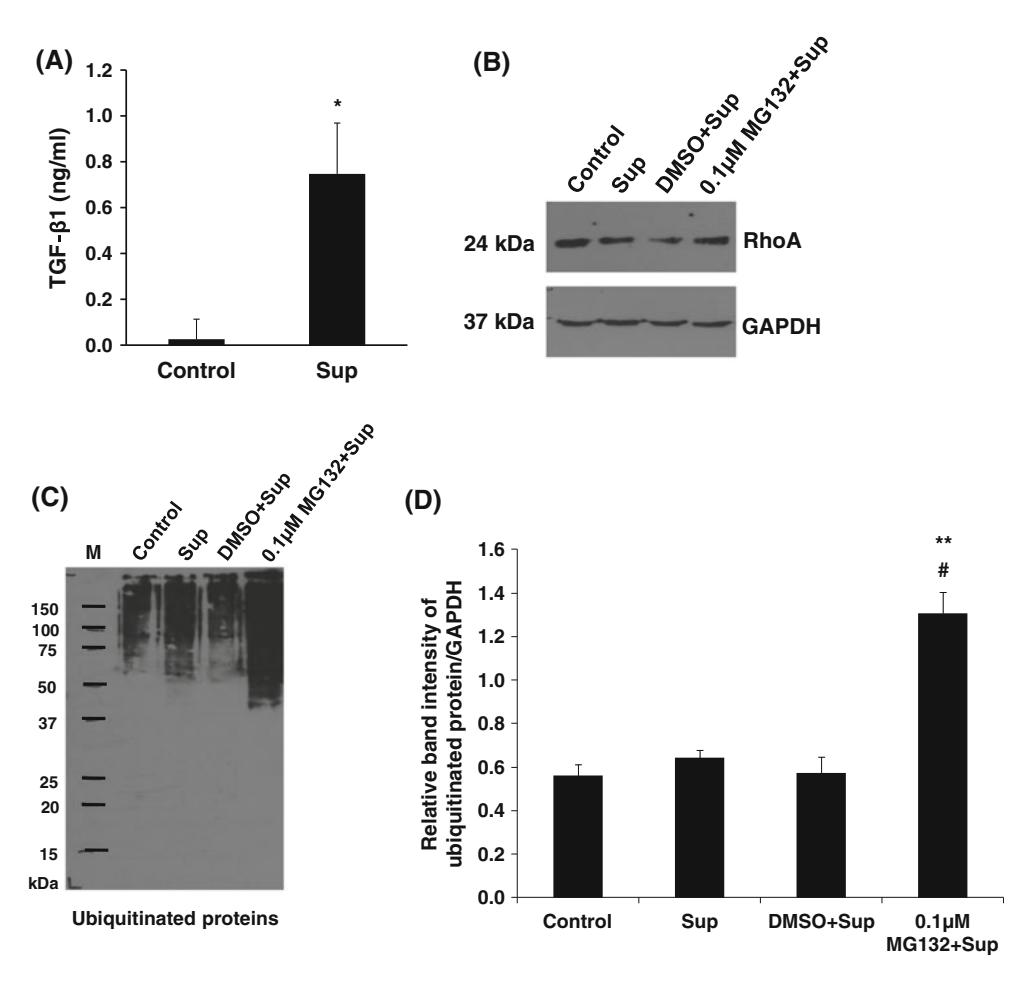


Fig. 2 Measurements of TGF-β1 level in CaOx-M-Sup and cellular levels of RhoA and ubiquitinated proteins in MDCK cells. The level of TGF-β1 in CaOx-M-Sup was measured by ELISA (a), whereas the cellular levels of RhoA (b) and ubiquitinated proteins (c) in MDCK cells were evaluated by Western blot analyses. Band intensity data of ubiquitinated proteins were obtained from 3 independent experiments

and normalized with GAPDH, which served as the loading control (d). A specific proteasome inhibitor MG132 was employed to demonstrate the significant role of UPP in RhoA degradation. DMSO served as the chemical control of the inhibitory effects by MG132. *p < 0.02 versus control; **p < 0.05 versus control; *p < 0.05 versus control; *p < 0.05 versus CaOx-M-Sup group



were successfully prevented by the MG132 pretreatment, not by DMSO pretreatment (Fig. 3a).

Restoration of Epithelial Marker and Suppression of Mesenchymal Marker by MG132

Our findings suggested the significant role of the proteasome inhibitor MG132 in the prevention of EMT induced by CaOx-M-Sup. We finally examined whether MG132 could restore the epithelial marker, while suppressed the mesenchymal marker. The results confirmed that pretreatment with MG132 successfully prevented the induction of EMT as demonstrated by the restoration of the epithelial

protein E-cadherin and suppression of the mesenchymal protein vimentin to their basal levels (Fig. 3b, c).

Discussion

The common manifestation of CKD is characterized by renal fibrosis, of which pathology can be found in both glomerulus (glomerulosclerosis) and tubulointerstitium (tubulointerstitial fibrosis). Although the pathogenic mechanisms leading to renal fibrosis remains hazy, transformation of epithelial cells to fibroblasts (also known as EMT) has been implicated as a crucial mechanism underlying renal

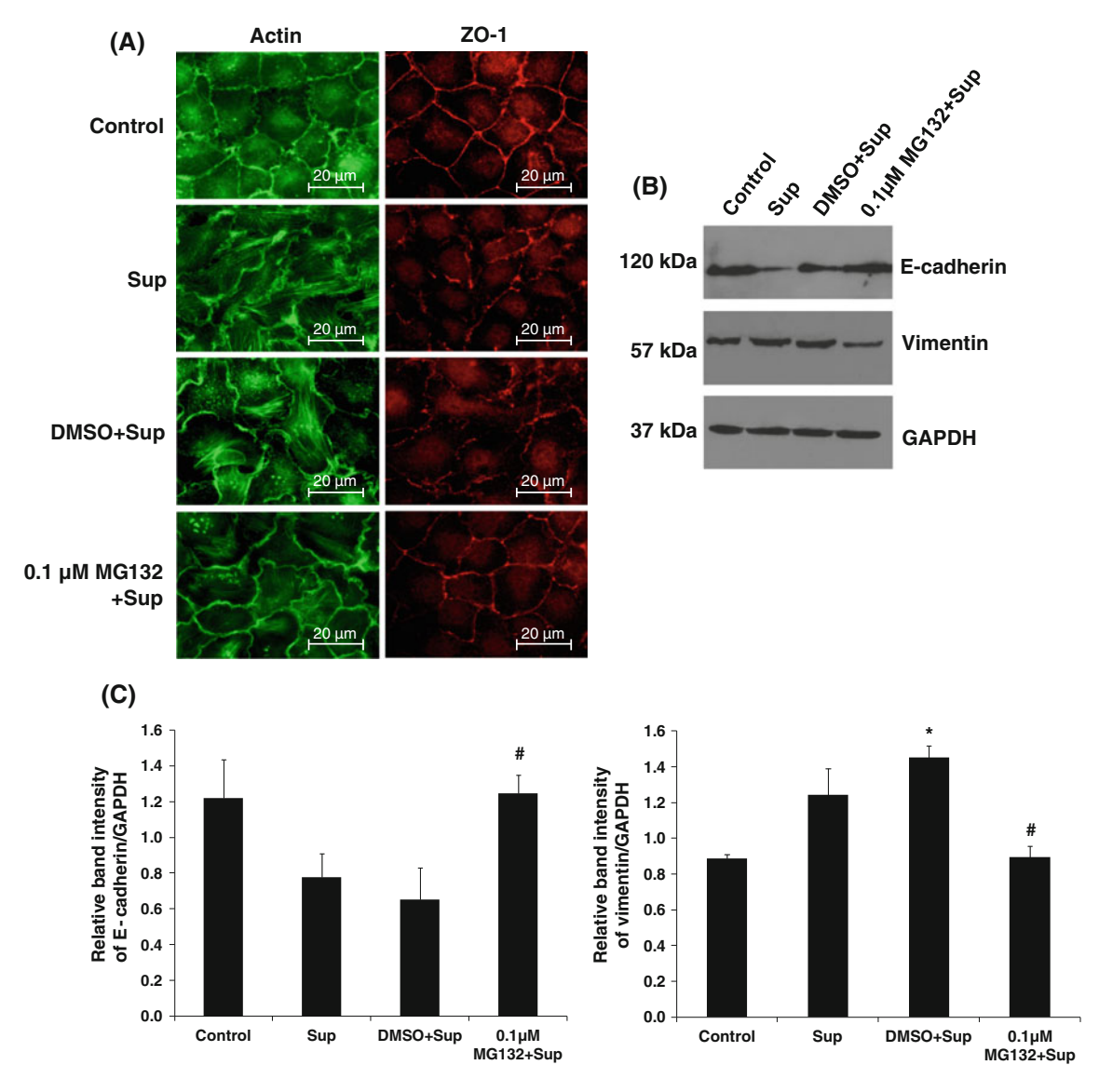


Fig. 3 Effects of the specific proteasome inhibitor MG132 on EMT induced by CaOx-M-Sup. Immunofluorescence study was performed to determine the effects of MG132 on restoration of F-actin cytoskeletal assembly and tight junction complex (a). Western blot analysis was done to demonstrate the effects of MG132 on

epithelial marker (E-cadherin) and mesenchymal marker (vimentin) (b). Band intensity data were obtained from 3 independent experiments and normalized with GAPDH, which served as the loading control (c). *p < 0.05 versus control; *p < 0.05 versus CaOx-M-Sup group



fibrosis [3–10]. Many lines of evidence have demonstrated the important role of macrophages in inflammatory response of renal tissues as well as the initiation of renal injury in CKD [12, 15, 16, 20]. Macrophages represent the predominant interstitial leukocytes in the diseased kidney. Once interstitial inflammation occurs, both activated residential and infiltrating macrophages produce various secretory products, including cytotoxic factors (e.g., reactive oxygen species, nitric oxide, etc.), angiogenesis factors (e.g., thrombospodin-1, angiotensin-II, endothelin, vascular endothelial growth factor, etc.), and fibrotic factors (e.g., TGF- β , platelet-derived growth factor, tumor necrosis factor- α , tissue inhibitor of MMPs, etc.) that not only aggravate the tissue injury but also promote the organ fibrosis [15].

In kidney stone disease, CaOx crystals are predominate as the major crystalline composition in the stone matrix. During the initiation of stone formation, CaOx crystals have undergone crystal growth, aggregation and adhesion to renal tubular epithelial cells [11, 21]. In addition, CaOx crystals have been thought to participate in the renal interstitial inflammation by interacting with tissue macrophages [11-13]. A previous study has demonstrated that upon interaction with CaOx crystals, macrophages had increased secretion of the proinflammatory cytokines, including tumor necrosis factor-α and interleukin-6, in response to binding and phagocytosis of CaOx crystals [13]. Based on these backgrounds, we thus hypothesized that the "secreted products of macrophages exposed to CaOx" (CaOx-M-Sup) might contain some factors that contributed to the interstitial fibrosis through the induction of EMT.

To address our hypothesis, we first confirmed that MDCK cells switched-on mesenchymal features while the epithelial phenotypes were switched-off upon treatment with CaOx-M-Sup. In concordance with other studies [22, 23], we found the increased expression levels of mesenchymal markers, including vimentin and fibronectin, as well as the decreased expression levels of epithelial markers, including E-cadherin, cytokeratin, F-actin, and ZO-1, by immunoblotting and immunofluorescence stainings (Fig. 1). Our findings suggested that CaOx-M-Sup contained some particular fibrotic factors that could induce the cells to undergo EMT. As TGF-β1 is the well-defined factor that plays a prominent role in the regulation of EMT, both at transcription and translation levels [7, 24, 25], we then measured the TGF-\beta1 level in CaOx-M-Sup. The striking results obtained from ELISA confirmed the markedly increased level of TGF-β1 in CaOx-M-Sup (Fig. 2a).

The increase of TGF- β 1 in CaOx-M-Sup raised our attention to the Rho family, the small GTPase that is recognized as the downstream effector during TGF- β 1-

induced EMT [26]. Each isoform of Rho (RhoA, RhoB and RhoC) displays unique function during the progression of EMT in renal proximal tubular cells [27]. Among these, RhoA seems to be the most important isoform in TGF-β1induced EMT [27]. Accordingly, TGF-\u03b31-mediated EMT has been proven to be a RhoA-dependent mechanism in a previous study, which showed that inactivation of RhoA or its downstream effector successfully inhibited the conversion of EMT in a mammary epithelial cell line (NMuMG) [28]. On the other hand, RhoA is a small GTPase playing multiple roles through interactions with various partners. It also plays an important role for maintaining cell polarity, junctions, and migration [29]. A previous study by Ozdamar et al. [30] has demonstrated that RhoA turnover is required for TGF-β1-dependent EMT. They have shown the role of TGF-β-Par6 signaling in regulation of tight junction disruption during EMT process. After binding with its ligand, TGF-β receptor type II (TGFβRII) phosphorylates the preformed complex Par6-TGFβRI (TGF-β receptor type I), which then stimulates the binding of Par6 to ubiquitin E3, Smurf1 [30]. These bindings lead to RhoA degradation via UPP, resulting to the disruption of tight junction [7, 30, 31].

We then examined the potential role of RhoA in maintenance of cellular integrity and junctional protein complexes. The early event of EMT requires the disruption of epithelial integrity, particularly the tight junction complex [7] and also the reorganization of the cytoskeletal assembly [32]. ZO-1 is associated with actin filament and functions to maintain the strength of the tight junction. The significant role of RhoA in CaOx-M-Sup-induced EMT in MDCK cells has been confirmed in our present study as demonstrated in Fig. 2b. In concordance with previous studies, RhoA expression level was reduced during TGF-βinduced EMT [30, 31, 33]. In addition, targeting RhoA for degradation is required in regulation of cell polarity and protrusion [31]. Interestingly, pretreatment of the cells with a specific proteasome inhibitor MG132 successfully prevented the decrease in RhoA level in the CaOx-M-Suptreated cells. The data also confirmed that such prevention of RhoA degradation by MG132 was most likely through UPP (Fig. 2b-d). In this study, we demonstrated that both F-actin cytoskeletal assembly and ZO-1 were disorganized and disrupted upon CaOx-M-Sup-induced EMT in MDCK cells (Fig. 1d). Using the specific proteasome inhibitor MG132, we could successfully prevent the CaOx-M-Supinduced disorganization of both F-actin and ZO-1 (Fig. 3a). Moreover, we could successfully restore the expression of E-cadherin and attenuate the increase in vimentin expression to their basal levels using the specific proteasome inhibitor MG132 (Fig. 3b, c). Our findings suggest that maintaining the RhoA expression by inhibition of



proteasome-mediated degradation of RhoA during EMT could reserve cellular junctions and prevent reorganization of actin cytoskeleton from stress fiber formation.

It should be noted that not only TGF-β1 but also other pro-fibrotic factors that might be present in CaOx-M-Sup. Thus, other mechanisms, e.g., oxidative stress [34, 35] and disruption of basement membrane via overproduction of MMPs [36], should be taken into account for the CaOx-M-Sup-induced EMT. A recent study has revealed the presence of MMPs in conditioned medium derived from lipopolysaccharide-activated macrophages that could induce EMT in both C1.1 cells and primary tubular epithelial cells [36]. Moreover, TGF-β1 has several signaling cascades, e.g., through Smad, PI3K/Akt-mTOR, Wnt, and the Notch-activated signaling pathways [37–41]. Therefore, it is not surprising that the pretreatment with a proteasome inhibitor MG132 might not completely prevent the EMT induction by CaOx-M-Sup.

In summary, we have demonstrated herein for the first time that CaOx-M-Sup could induce EMT in renal tubular cells by TGF- $\beta1$ signaling cascade via targeting RhoA to proteasome degradation. In addition, a proteasome inhibitor MG132 could successfully prevent such phenomenon via UPP-dependent prevention of RhoA degradation. The TGF- $\beta1$ signaling cascade via RhoA may be, at least in part, the underlying mechanism for renal fibrosis in kidney stone disease.

Acknowledgments We thank Ms. Paleerath Peerapen for her technical assistance. This study was supported by The Thailand Research Fund (RTA5380005 and TRG5480005), Office of the Higher Education Commission and Mahidol University under the National Research Universities Initiative, and Faculty of Medicine Siriraj Hospital. KS is supported by the Royal Golden Jubilee PhD Program, whereas VT is also supported by the "Chalermphrakiat" Grant, Faculty of Medicine Siriraj Hospital.

References

- Saucier, N. A., Sinha, M. K., Liang, K. V., Krambeck, A. E., Weaver, A. L., Bergstralh, E. J., et al. (2010). Risk factors for CKD in persons with kidney stones: A case-control study in Olmsted County, Minnesota. *American Journal of Kidney Dis*eases, 55, 61-68.
- Iseki, K. (2008). Chronic kidney disease in Japan. *Internal Medicine*, 47, 681–689.
- 3. Iwano, M. (2010). EMT and TGF-beta in renal fibrosis. *Frontiers in Bioscience (Scholar edition)*, 2, 229–238.
- 4. Rastaldi, M. P., Ferrario, F., Giardino, L., Dell'Antonio, G., Grillo, C., Grillo, P., et al. (2002). Epithelial–mesenchymal transition of tubular epithelial cells in human renal biopsies. *Kidney International*, 62, 137–146.
- Zeisberg, M., & Neilson, E. G. (2009). Biomarkers for epithelialmesenchymal transitions. *Journal of Clinical Investigation*, 119, 1429–1437.
- Liu, Y. (2004). Epithelial to mesenchymal transition in renal fibrogenesis: Pathologic significance, molecular mechanism, and

- therapeutic intervention. Journal of the American Society of Nephrology, 15, 1–12.
- 7. Xu, J., Lamouille, S., & Derynck, R. (2009). TGF-beta-induced epithelial to mesenchymal transition. *Cell Research*, 19, 156–172.
- Iwano, M., Plieth, D., Danoff, T. M., Xue, C., Okada, H., & Neilson, E. G. (2002). Evidence that fibroblasts derive from epithelium during tissue fibrosis. *Journal of Clinical Investiga*tion, 110, 341–350.
- Garcia-Sanchez, O., Lopez-Hernandez, F. J., & Lopez-Novoa, J. M. (2010). An integrative view on the role of TGF-beta in the progressive tubular deletion associated with chronic kidney disease. *Kidney International*, 77, 950–955.
- Ivanova, L., Butt, M. J., & Matsell, D. G. (2008). Mesenchymal transition in kidney collecting duct epithelial cells. *American Journal of Physiology-Renal Physiology*, 294, F1238–F1248.
- de Water, R., Noordermeer, C., van der Kwast, T. H., Nizze, H., Boeve, E. R., Kok, D. J., et al. (1999). Calcium oxalate nephrolithiasis: Effect of renal crystal deposition on the cellular composition of the renal interstitium. *American Journal of Kidney Diseases*, 33, 761–771.
- de Water, R., Noordermeer, C., Houtsmuller, A. B., Nigg, A. L., Stijnen, T., Schroder, F. H., et al. (2000). Role of macrophages in nephrolithiasis in rats: An analysis of the renal interstitium. *American Journal of Kidney Diseases*, 36, 615–625.
- de Water, R., Leenen, P. J., Noordermeer, C., Nigg, A. L., Houtsmuller, A. B., Kok, D. J., et al. (2001). Cytokine production induced by binding and processing of calcium oxalate crystals in cultured macrophages. *American Journal of Kidney Diseases*, 38, 331–338.
- Leonard, M., Ryan, M. P., Watson, A. J., Schramek, H., & Healy, E. (1999). Role of MAP kinase pathways in mediating IL-6 production in human primary mesangial and proximal tubular cells. *Kidney International*, 56, 1366–1377.
- Sean, E. K., & Cockwell, P. (2005). Macrophages and progressive tubulointerstitial disease. *Kidney International*, 68, 437–455.
- Wilson, H. M., Walbaum, D., & Rees, A. J. (2004). Macrophages and the kidney. Current Opinion in Nephrology and Hypertension, 13, 285–290.
- Sintiprungrat, K., Singhto, N., Sinchaikul, S., Chen, S. T., & Thongboonkerd, V. (2010). Alterations in cellular proteome and secretome upon differentiation from monocyte to macrophage by treatment with phorbol myristate acetate: Insights into biological processes. *Journal of Proteomics*, 73, 602–618.
- Semangoen, T., Sinchaikul, S., Chen, S. T., & Thongboonkerd, V. (2008). Proteomic analysis of altered proteins in distal renal tubular cells in response to calcium oxalate monohydrate crystal adhesion: Implications for kidney stone disease. *Proteomics Clinical Applications*, 2, 1099–1109.
- Thongboonkerd, V., Semangoen, T., Sinchaikul, S., & Chen, S. T. (2008). Proteomic analysis of calcium oxalate monohydrate crystal-induced cytotoxicity in distal renal tubular cells. *Journal* of *Proteome Research*, 7, 4689–4700.
- Kinsey, G. R., Li, L., & Okusa, M. D. (2008). Inflammation in acute kidney injury. *Nephron Experimental Nephrology*, 109, e102–e107.
- Coe, F. L., Evan, A., & Worcester, E. (2005). Kidney stone disease. *Journal of Clinical Investigation*, 115, 2598–2608.
- Das, S., Becker, B. N., Hoffmann, F. M., & Mertz, J. E. (2009).
 Complete reversal of epithelial to mesenchymal transition requires inhibition of both ZEB expression and the Rho pathway.
 BMC Cell Biology, 10, 94.
- Mathias, R. A., Wang, B., Ji, H., Kapp, E. A., Moritz, R. L., Zhu, H. J., et al. (2009). Secretome-based proteomic profiling of Rastransformed MDCK cells reveals extracellular modulators of epithelial–mesenchymal transition. *Journal of Proteome Research*, 8, 2827–2837.



- Hills, C. E., & Squires, P. E. (2010). TGF-beta1-induced epithelial-to-mesenchymal transition and therapeutic intervention in diabetic nephropathy. *American Journal of Nephrology*, 31, 68–74.
- Campanaro, S., Picelli, S., Torregrossa, R., Colluto, L., Ceol, M., Del Prete, D., et al. (2007). Genes involved in TGF beta1-driven epithelial–mesenchymal transition of renal epithelial cells are topologically related in the human interactome map. *BMC Genomics*, 8, 383.
- Bishop, A. L., & Hall, A. (2000). Rho GTPases and their effector proteins. *Biochemical Journal*, 348(2), 241–255.
- Hutchison, N., Hendry, B. M., & Sharpe, C. C. (2009). Rho isoforms have distinct and specific functions in the process of epithelial to mesenchymal transition in renal proximal tubular cells. *Cellular Signalling*, 21, 1522–1531.
- Bhowmick, N. A., Ghiassi, M., Bakin, A., Aakre, M., Lundquist, C. A., Engel, M. E., et al. (2001). Transforming growth factorbeta1 mediates epithelial to mesenchymal transdifferentiation through a RhoA-dependent mechanism. *Molecular Biology of the* Cell, 12, 27–36.
- Fukata, M., Nakagawa, M., & Kaibuchi, K. (2003). Roles of Rhofamily GTPases in cell polarisation and directional migration. *Current Opinion in Cell Biology*, 15, 590–597.
- Ozdamar, B., Bose, R., Barrios-Rodiles, M., Wang, H. R., Zhang, Y., & Wrana, J. L. (2005). Regulation of the polarity protein Par6 by TGFbeta receptors controls epithelial cell plasticity. *Science*, 307, 1603–1609.
- Wang, H. R., Zhang, Y., Ozdamar, B., Ogunjimi, A. A., Alexandrova, E., Thomsen, G. H., et al. (2003). Regulation of cell polarity and protrusion formation by targeting RhoA for degradation. *Science*, 302, 1775–1779.
- Pellegrin, S., & Mellor, H. (2007). Actin stress fibres. *Journal of Cell Science*, 120, 3491–3499.

- Gunaratne, A., Thai, B. L., & Di Guglielmo, G. M. (2013).
 Atypical protein kinase C phosphorylates Par6 and facilitates transforming growth factor beta-induced epithelial-to-mesenchymal transition. *Molecular and Cellular Biology*, 33, 874–886.
- 34. Rodriguez-Iturbe, B., & Garcia, G. G. (2010). The role of tubulointerstitial inflammation in the progression of chronic renal failure. *Nephron Clinical Practice*, 116, c81–c88.
- 35. Xie, P., Sun, L., Nayak, B., Haruna, Y., Liu, F. Y., Kashihara, N., et al. (2009). C/EBP-beta modulates transcription of tubulointerstitial nephritis antigen in obstructive uropathy. *Journal of the American Society of Nephrology*, 20, 807–819.
- 36. Tan, T. K., Zheng, G., Hsu, T. T., Wang, Y., Lee, V. W., Tian, X., et al. (2010). Macrophage matrix metalloproteinase-9 mediates epithelial–mesenchymal transition in vitro in murine renal tubular cells. *American Journal of Pathology*, 176, 1256–1270.
- Nelson, W. J., & Nusse, R. (2004). Convergence of Wnt, betacatenin, and cadherin pathways. Science, 303, 1483–1487.
- Zavadil, J., Cermak, L., Soto-Nieves, N., & Bottinger, E. P. (2004). Integration of TGF-beta/Smad and Jagged1/Notch signalling in epithelial-to-mesenchymal transition. *EMBO Journal*, 23, 1155–1165.
- Kattla, J. J., Carew, R. M., Heljic, M., Godson, C., & Brazil, D. P. (2008). Protein kinase B/Akt activity is involved in renal TGFbeta1-driven epithelial-mesenchymal transition in vitro and in vivo. American Journal of Physiology-Renal Physiology, 295, F215–F225.
- 40. Liu, Y. (2006). Renal fibrosis: New insights into the pathogenesis and therapeutics. *Kidney International*, 69, 213–217.
- Saad, S., Stanners, S. R., Yong, R., Tang, O., & Pollock, C. A. (2010). Notch mediated epithelial to mesenchymal transformation is associated with increased expression of the Snail transcription factor. *International Journal of Biochemistry & Cell Biology*, 42, 1115–1122.



Protective effect of green tea extract against oxalate-induced changes in renal tubular cells: possibility for prevention of renal fibrosis

Rattiyaporn Kanlaya^{1,2} and Visith Thongboonkerd^{1,2*}

¹Medical Proteomics Unit, Office for Research and Development, Faculty of Medicine Siriraj Hospital, Mahidol University, Bangkok, THAILAND

² Siriraj Hospital, and Center for Research in Complex Systems Science (CRCSS), Mahidol University, Bangkok, THAILAND

Running Title: Protective role of EGCG against oxalate-induced EMT

*Correspondence to:

Visith Thongboonkerd, MD, FRCPT

Medical Proteomics Unit, Office for Research and Development,

Siriraj Hospital, and Center for Research in Complex Systems Science

(CRCSS), Mahidol University

6th Floor SiMR Building, 2 Prannok Road, Bangkoknoi, 10700, Bangkok,

Thailand

Phone: +66-2-4192882

E-mail: thongboonkerd@dr.com (or) vthongbo@yahoo.com

ABSTRACT

This study aims to apply a natural compound to prevent the process of epithelial mesenchymal transition (EMT) induced by oxalate treatment. Sodium oxalate was used to induce tubular cell injury and EMT in Mardin-Darby Canine kidney (MDCK) cell line. Oxalate exposure is known to induce cellular injury and presumed to be involved in the pathogenesis of calcium oxalate stone formation. Epigallocatechin gallate (EGCG) extracted from green tea (Camellia Sinensis) was assessed for its anti-fibrotic and anti-oxidative property. EGCG is the most abundant polyphenol compounds found in green tea with high potential anti-oxidative property. Microscopic examination revealed that oxalate could induce morphological change of MDCK from a cobble-stone like into fibroblast-like shap within 24 h. In addition, immunoblotting and indirect immunofluorescence assay confirmed that oxalate-treated cells gained mesenchymal phenotypes by increase expression of vimentin and fibronectin while decrease expression of epithelial markers including, E-cadherin, cytokeratin, occludin, and ZO-1. Interestingly, pretreatment of MDCK cells with 25 µM EGCG could prevent EMT induced by oxalate exposure as it could retain typical epithelial cell morphology as well as epithelial protein markers. The molecular mechanism underlying the prevention of EGCG is most likely by reduction of intracellular reactive oxygen species (ROS) production. Taken together, this study demonstrated a preventive effect of EGCG against oxalate-induced EMT in renal tubular cells which would shed light on the development of novel therapeutics of renal fibrosis in the near future.

Keywords: Epithelial mesenchymal transition, Oxalate, EGCG, Renal fibrosis

INTRODUCTION

Unsolved chronic kidney diseases (CKD) mostly leads to end-stage renal failure due to kidney fibrosis. Renal fibrosis or scar in the kidney requires a number of cellular events and mediators to act in concert that result in the deterioration of kidney function (1). The risk factors contributing to the development of fibrous kidney can be derived from various primary causes such as hypertension, diabetes mellitus, glomerulopathies and cell injury due to toxic substances, etc (1, 2). Recently, the epithelial plasticity known as epithelial mesenchymal transition (EMT) has been discovered to associate with renal fibrogenesis in injured kidney of adults (3-6). EMT indeed is the important process required during normal embryonic development. EMT process allows the anchored epithelial cells to rearrange into a developing organ (7). During EMT, typical morphology of epithelial cell turns into spindle-shape of fibroblast and the cell lose its polarity (7, 8). Importantly, cells lose their epithelial phenotypes while gain the mesenchymal characteristics. Those include down expression of E-cadherin and tight junction protein ZO-1, resulting in disintegration of cell-cell contact. Cells undergoing EMT up-regulate the mesenchymal marker, including fibroblast-specific protein 1 (FSP1) and vimentin. In addition, over production of extracellular matrix proteins (such as fibronectin and collagen) and metalloproteases was found during EMT induction (7, 9). Moreover, induction of EMT results in actin reorganization and formation of actin stress fiber. Expression of FSP1 was found in acute and chronic injured renal tubular cell, suggested the involvement of EMT in response to tissue repairing (10). Interestingly, study using transgenic mice model that allowed discrimination of the cell origin demonstrated that one third of renal interstitial fibroblasts were derived from tubular epithelial cells underwent EMT (11). Strong association between EMT and renal fibrosis was confirmed in the study provided by Rastaldi et al, (12). They demonstrated that EMT features were observed in 133 human renal biopsies and also correlated with a degree of

interstitial damage. In addition, it has been reported that kidney epithelial cells of collecting duct treated with insulin-like growth factors (IGFs) and transforming growth factor-beta 1 (TGB-beta1) were induced to undergo EMT (13). Most recently, EMT marker Twist was evidenced in renal biopsies from nephrolithiasis patients with large calculi (14). These aforementioned studies suggest that renal epithelial cells can transform through EMT mechanism in response to some stimuli and might participate in the pathogenesis of renal fibrosis.

At present, drinking of green tea is more widespread because of the beneficial effects to prevent from lifestyle-related diseases, including cancer and cardiovascular diseases (15-17). Medical studies have demonstrated that green tea contains not only an anti-oxidative but also anti-allergic, anti-carcinogenic and anti-bacterial effects (15, 18-20). Among the polyphenols found in green tea extract, (-)- epigallocatechin gallate (EGCG) is the major abundant catechins with high potential anti-oxidative property (21, 22). Anti-oxidative effect of green tea was demonstrated in rats with ethylene glycol-induced nephrolithiasis (23). Rats treated with green tea decreased excretion of urinary oxalate and calcium oxalate deposition while increased superoxide dismutase (SOD) activity. Moreover, lower number of cell apoptosis was found when compared to the control group. These findings suggest the inhibitory effect of green tea on calcium oxalate formation by its anti-oxidative property (23). Accordingly, green tea could attenuate the development of nephrolithiasis induced by oxalate treatment in rats. Green tea could protect the rats from oxalate-induced cytotoxic effect by reducing free radical production and lower number of crystal formation in the kidney (24). In addition, protective effect of green tea against nephrotoxicity of reserpine, the important anti-hypertensive drug was demonstrated in rat model. Administration of green tea extract in rats treated with reserpine showed a significant recovery of kidney proximal tubule cells when compared to the control groups (25). In addition, epigallocatechin gallate (EGCG) could protect human lens epithelial cells from H₂O₂-induced

apoptosis through the series of caspases and also modulation of the Bcl-2 family and the MAPK and Akt pathway (22). Recently, anti-fibrotic property of green tea has been demonstrated in an experimental hepatic fibrosis (26) and a pulmonary fibrosis (27). Experimental hepatic fibrosis in rats was induced by dimethylnitrosamine (DMN). However, administration of green tea extract could prevent the rats from development of fibrosis. The histophatological results of kidney tissues revealed that the lower hydroxyproline content was found in green tea treated rats. These results indicated the lower deposition of collagen and down expression of collagen type 1 (26). In addition, administration of EGCG in rat model of bleomycin-induced pulmonary fibrosis demonstrated the involvement of Nrf2-Keap1 signaling to enhance the anti-oxidative activities of phase II enzymes, including glutathione-S-transferase (GST) and NAD(P)H:quinine oxidoreductase 1 (NQO1). This cascade could attenuate the subsequent inflammation. These findings suggest that green tea extract contains the combination of beneficial effects on antiinflammation, anti-oxidative stress and anti-fibrosis (27). Therefore, better understanding in the progression of EMT and modulation on this pathogenic mechanism during renal epithelial cell damage would benefit a prevention of fibrosis. This study thus aims to apply a natural compound to reduce or prevent the process of EMT induced by oxalate treatment. In this study, sodium oxalate was used to induce tubular cell injury and EMT in Mardin-Darby Canine kidney (MDCK) cell line. Oxalate exposure is known to induce cellular injury and presumed to be involved in the pathogenesis of calcium oxalate stone formation (28-30). Epigallocatechin gallate (EGCG), the most abundant polyphenol compounds found in green tea (Camellia Sinensis) with high potential anti-oxidative property was assessed for its anti-fibrotic and anti-oxidative property.

MATERIALS AND METHODS

Cell culture

Mardin-Darby Canine kidney (MDCK), a distal tubular epithelial cell line was cultured in growth Eagle's minimum essential medium (MEM) (Gibco; Grand Island, NY) [MEM supplemented with 10% heat-inactivated fetal bovine serum (FBS) (Gibgo) in the presence of 100 U/ml penicillin G and 100 mg/ml streptomycin (Sigma, St.Louis, MO)]. Cells were maintained in a humidified incubator at 37°C with 5% CO₂.

Cytotoxicity test of EGCG by cell viability assay

MDCK cells were seeded in 24-well plate in growth medium 1 day prior to experiment. Cells were treated with 12, 25 and 50 μ M EGCG for 1 h. Cells left untreated were used as a control of treatment. Thereafter, treated cells were detached by trypsinization and determined cell viability by trypan blue exclusion assay.

Induction of epithelial mesenchymal transition (EMT)

MDCK cells were seeded into 6-well plate and cultured in a growth medium for 24 h. Prior to treatment, cells were washed with serum-free medium and then treated with 500 μ M sodium oxalate in maintenance MEM medium [MEM supplemented with 1% heat-inactivated FBS] for 24 h.

Morphological study and immunofluorescence microscopy

Cell morphology was observed under a phase contrast microscope (Olympus CKX41; Tokyo, Japan) at the beginning and 24 h after treatment. For immunofluorescence staining, cells were grown on coverslip and EMT was induced as previously described. Cells were processed for immunofluorescence staining of vimentin, fibronectin, cytokeratin, and ZO-1 using corresponding antibodies. In brief, cells were fixed with 3.7% (V/V) formaldehyde in PBS for 10

min and then permeabilized with 0.2% triton X-100 in PBS for 10 min. After washing step, cells were incubated overnight with primary antibody at dilution of 1:50 (in 1%BSA/PBS) at 4°C. Corresponding secondary antibody was used at dilution of 1:2000 (in 1%BSA/PBS) and incubated at RT for 1 h. The nuclei were counterstained with Hoechst dye (Invitrogen/Molecular Probes) at dilution of 1:1000. Thereafter, the cells were extensively washed with PBS and mounted onto a glass slide using ProLong Gold antifade reagent (Invitrogen). The images were captured under the Nikon Eclipse 80i fluorescence microscope (Nikon; Tokyo, Japan).

Prevention of EMT by epigallocatechin gallate (EGCG)

MDCK cells were cultured in growth medium for 24 h and were pretreated with 25 μ M EGCG in maintenance medium (MEM containing 1% heat inactivated FBS) for 1 h followed by sodium oxalate to complete 24 h-incubation. The cells treated with sodium oxalate without EGCG and those left untreated will serve as positive and negative controls, respectively.

Immunoblotting

The cells were induced to undergo EMT as previously described. Cell lysate was prepared in sample buffer (Leammli's buffer) and 30 µg of total protein were resolved by SDSPAGE under reducing and denaturing condition. The resolved protein bands were electrophoretically transferred onto a nitrocellulose membrane and non-specific bindings were blocked by 5% non-fat milk in PBS. The membrane was detected for the expression of vimentin, E-cadherin, occludin, catalase, and GAPDH (as a loading control) using specific antibodies (all was purchased from Santa Cruz Biotechnology, Santa Cruz, CA). After probing with corresponding secondary antibodies, the reactive protein bands were visualized by SuperSignal West Pico chemiluminescence substrate (Pierce Biotechnology, Inc., Rockford, IL) and autoradiography.

Detection of reactive oxygen species (ROS)

ROS production inside the cells was analyzed by flow cytometry. Briefly, the cells were collected as suspension by trypsinization and pretreated with 25 µM EGCG for 20 min. Thereafter, the cells were loaded with 50 µM dichlorofluorescein diacetate (DCFH-DA) for 30 min, followed by oxalate exposure for 30 min. The cells left untreated and treated with 0.02%H₂O₂ for were served as negative and positive control, respectively. After complete incubation period, the cells were kept on ice and immediately analyzed by FACScan equipped with CellQuest software (Benton Dickinson; Franklin Lake, NJ).

Statistical analysis

Data were presented as mean \pm SD. The significant difference among groups was performed by One-Way ANOVA with Tukey's HSD Post-hoc test using SPSS (version 11.5). Statistical significance was considered at P-value less than 0.05.

RESULTS

Sodium oxalate induced EMT in MDCK cells

MDCK cells were seeded into 6-well plate and cultured in a growth medium for 24 h prior to treat with 500 μM sodium oxalate for 24 h. As expected, Oxalate-treated MDCK cells underwent morphological change into more fibroblast-like in shape within 24 h compared to those left untreated (**Figure 1**). A number of calcium oxalate monohydrate crystals were observed in the treated condition. To examine whether oxalate exposure could induce EMT in renal epithelial cells, Western blot analysis and indirect immunofluorescence assay (IF) were performed to validate expression of epithelial and mesenchymal protein markers. The results by Western blot analysis revealed that oxalate-treated cells increased expression of vimentin (mesenchymal marker) whereas decreased expression of E-cadherin and occludin (epithelial markers) when compared to those of untreated cells (**Figure 2**). In according to Western blot results, IF revealed the increased level of vimentin and fibronectin (**Figure 3A**) while decreased level of cytokeratin, occludin and ZO-1 (**Figure 3B**). These findings suggest that MDCK were induced to undergo EMT by sodium oxalate exposure within 24 h.

Cytotoxicity test of EGCG in MDCK cells

To examine cytotoxicity of EGCG in MDCK cells, the cells were treated with various dose of EGCG for 1 h and cell viability was determined by trypan blue exclusion assay. The results showed that more than 95% cell viability could be observed in the control cells left untreated. Similar results were obtained when cells were treated with EGCG at 12.5 and 25 μ M. However, incubation with higher concentration of EGCG at 50 μ M could apparently reduce cell survival when compared to the control cells left untreated (92.5% compared to 98.48%; P=0.0543). Percentage of cell viability after EGCG treatment was shown in **Figure 4**. These

results suggest that low concentrations of EGCG at 12.5 and 25 μ M for 1 h did not significantly affect to MDCK cell survival. Therefore, pretreatment of cells with 25 μ M for 1 h was used in further experiments.

Preventive effect of EGCG against sodium oxalate-induced EMT

MDCK cells were pretreated with 25 µM EGCG in maintenance medium (MEM containing 1% heat inactivated FBS) for 1 h followed by 500 µM sodium oxalate to complete 24 h-incubation. Cells treated with 500 µM sodium oxalate without EGCG and cells left untreated were served as positive and negative control of EMT induction, respectively. Epithelial and EMT protein markers were evaluated by Western blot analysis and indirect immunofluorescence staining. Western blot analysis showed a slight increased vimentin expression, while E-cadherin and occludin were decrease when compared to the control cells. However, expression of vimentin, E-cadherin, and occludin was comparable to basal level when cells were pretreated with 25µM EGCG (Figure 5). In addition, immunofluorescence assay showed that EMT protein markers including vimentin, and fibronectin expression were obviously induced in MDCK cells treated with sodium oxalate for 24 h compared to control cells left untreated (Figure 6A). In contrast, epithelial protein markers including cytokeratin, occludin, and ZO-1 were downregulated in EMT-induced cells. However, expression of these protein markers were found comparable to those of control cells when cells were pretreated with 25 µM EGCG (Figure 6B). These results suggest that pretreatment of cells with 25 µM EGCG could prevent the cells from sodium oxalate-induced EMT process.

Reduction of reactive oxygen species (ROS) by EGCG

Intracellular ROS production was analyzed by flow cytometry. The cells were collected as suspension and incubated with or without EGCG. Thereafter, the cells were loaded with

dichlorofluorescein diacetate (DCFH-DA) for 30 min, followed by oxalate exposure. Cells treated with H_2O_2 were served as positive control. Cells left untreated were served as negative control.

Intracellular ROS production was basically found in the control cells (less that 5%); however, it was markedly increased when cells were treated with H₂O₂. Cells underwent EMT process by sodium oxalate induction significantly produced more ROS inside the cells compared to those of control cells. As expected, pretreated the cells with 25 μ M EGCG before sodium oxalate treatment can significantly lower intracellular ROS production (**Figure 7**). The results confirmed the anti-oxidant property of EGCG and it is possible that EGCG might prevent the cells from undergoing EMT by mediated through intracellular ROS production.

DISCUSSION

There is an increasing evidence for EMT and renal fibrosis over time. Strutz *et al*, firstly reported the expression of fibroblast-specific protein 1 (FSP-1), which suggest the conversion of epithelial cells into fibroblast type in murine fibrotic kidney (10). In the context of renal stone diseases and EMT, Boonla *et al*, demonstrated that signs of tubular EMT can be found in nephrolithiasis patients with staghorn calculi. The plausible cause of tubular EMT might be the production of a well-know fibrotic factor TGF-beta 1, which was strongly positive in fibrotic kidney tissues (31). Most recent study in nephrolithiasis patients with large calculi evidenced that the EMT marker Twist was markedly expressed in tubular epithelial cells of kidney biopsies from patients compared to those obtained from normal kidneys. The researchers also demonstrated the inverse correlation of Twist and E-cadherin (epithelial marker) expression and suggested that Twist might be used as an index to predict the progression of renal fibrosis in patients (14). For this reason, it is in need of seeking for the effective therapeutics to prevent the progression of renal fibrosis.

In this study, we thus test the anti-fibrotic property of EGCG against EMT induction by high sodium oxalate. We demonstrated that high concentration of oxalate can induce fibroblast-like feature as shown in **Figure 1**. Treatment with 500 µM sodium oxalate for 24 h could induce morphological changes of the cells from cobble stone-like into more spindle of fibroblast-like compared to the control cells with unchanged. Interestingly, pretreatment of 25 µM EGCG follow by sodium oxalate could prevent the cells from deteriorate effect. Higher concentration of EGCG at 50 µM; however, did not show protective effect but rather provided cytotoxic effect (data not shown) supporting a number of studies that revealed the pro-oxidative property of EGCG in inbition of cell proliferation and induction of apoptosis (32-34). Previous study reported that EGCG supplementation could attenuate the development of nephrolithiasis in rat by

lower number of crystal formation in kidney (23, 35). We also observed a lower number of COM crystals formed under EGCG treated condition compared to those treated with oxalate alone. Interestingly, typical calcium oxalate dihydrate (COD) crystals with octahedral shape could be observed in MDCK cells pretreated with EGCG before oxalate treatment (data not shown). The results suggest that EGCG treatment favors COD crystallization after treatment with high concentration of oxalate. It might be possible that EGCG affect COM crystal formation by shifting pH of the solution to become higher (more basic pH). Retrospective study in renal stone patients revealed that urinary pH could influence the type of crystals formed. They found that COD crystals were common in patients with higher urine pH (36). We observed that MEM containing 25 µM EGCG has higher pH (approx. pH 8) compared to that of MEM (pH 7.4) alone. It is also possible that the formation of COD crystals might a direct consequent of the physicochemical property of EGCG when interacts with ions. The precise mechanism underlying this phenomenon requires further investigations.

We sought to determine whether the change in cell morphology in response to high oxalate was implicated with EMT through examination of mesenchymal and epithelial markers. In according to other studies, oxalate-treated cells lost their epithelial features while gained mesenchymal characteristics. We found decreased expression of E-cadherin the hallmark of EMT in cells treated with oxalate; however E-cadherin expression was retained at basal level when cells were pretreated with EGCG (**Figure 5**). In addition, the results by indirect immunofluorescence revealed that oxalate-treated cells increased expression of vimentin as well as fibronectin, whilst decreased expression of tight junction proteins, occludin and ZO-1. In addition, occludin and ZO-1 redistribution was observed significantly in oxalate-treated cells. Occludin and ZO-1 were markedly disappeared from the TJ locating at the cell borders into the cytoplasm (**Figure 3**). Expression of vimentin was up-regulated in oxalate-treated cells but

decreased into basal level when cells were pretreated with EGCG followed by oxalate (**Figure 6**). These findings suggest that TJ disruption occurred when cells were underwent EMT-induced by oxalate. Role of EGCG in protection of tight junction (TJ) barrier has been reported. EGCG can preserve the TJ integrity of the colonic epithelial cells induced by IFN-γ via STAT1 independent manner (37, 38). In addition, EGCG could reduce ritonavir-induced endothelial permeability through its effective anti-oxidative property (39). In the present study, both immunofluorescence microscopy and Western blot analysis indicated that EGCG could effectively prevent TJ disassembly induced by oxalate.

Several lines of evidence revealed that oxalate could induce reactive oxygen species (ROS) production in renal epithelial cells. Thamilselvan S, et al. demonstrated that peroxidatve injury initiated by oxalate was involved with the induction of TGF-beta1 and the imbalance of redox reaction by glutathione (GSH) system (40). However, GSH redox status as well as the level of TGF-beta1 was restored to the basal stage by addition of antioxidants, including vitamin E and catalase (40). Evidence from clinical studies indicates that oxidative injury was found in kidney of stone patients with hyperoxaluria (41-43). Several markers indicating the occurrence of oxidative stress and epithelial cell injury were found in the urine of the patients, including higher level of malondialdehyde (MDA), glutathione (GSH), beta-galactosidase (GAL) and Nacetyl-beta-glucosaminidase (NAG) (41, 44, 45). Recent study revealed that administration of green tea can prevent renal tubular microstructure change and oxidative stress induced by glyoxylate in mice (46). One of a molecular mechanism of oxalate-induced oxidative stress is a production of reactive oxygen species (ROS). Anti-oxidant property of EGCG could protect cell injury by hypoxia-induced oxidative stress in MDCK cells (47). Recent studies showed that regulation of NADPH oxidase, a plasma membrane enzyme generated ROS by the activation of protein kinase C (PKC)-alpha and –delta (48). Importantly, TGF-beta1 a potent fibrotic factor

that triggers EMT could also induce a production of intracellular ROS of the rat proximal tubular epithelial cells (49) and MDCK cells (50).

Based on these aforementioned studies, ROS and alterations in redox homeostasis potentially contribute to EMT process. Theoretically, EGCG with highly anti-oxidative activity might control the progression of EMT through the action of ROS scavenger. However, there was no direct evidence to show that ROS generation-induced by oxalate could trigger the process of EMT. In attempt to address this issue, we then assayed for the intracellular ROS after oxalate treatment by pulsing with DCFH-DA and analyzed by flow cytometer. As expected, the results clearly showed that intracellular ROS was significantly elevated when cells were induced to undergo EMT by high oxalate concentration compared to the control cells left untreated. Pretreatment with EGCG markedly reduced ROS production induced by oxalate (Figure 7). In consistent with study of peritoneal fibrosis in a mouse model, EGCG could suppress NF-kB activation and ROS generation and thus prevent from progression of peritoneal fibrosis (51). In addition, although we did not investigate whether TGF-beta1 is mediated in ROS generation and the consequent activation/inactivation of the well-known pathways (i.e. SNAII, GSK-3β and Wnt/βcatenin) to trigger EMT (49, 52), we showed that oxalate could induce EMT phenotype concomitantly with the increased ROS production. EGCG pretreatment could prevent the conversion of epithelial cells into fibroblast-like cells and reduce intracellular ROS to a greater extent that comparable to the basal level.

To our knowledge, this is the first report to demonstrate that high oxalate concentration could induce alteration in epithelial cell shape to become fibroblast-like morphology through the process so-called EMT and a major component of natural green tea extract, EGCG significantly prevents induction of EMT at least by maintaining cell junctional integrity as well as through its antioxidant property to counteract intracellular ROS production. At present, we provide ongoing

effort to study the signaling pathways triggered by EGCG in prevention of oxalate-induced EMT. This would pave the way to the understanding of renal fibrogenesis and ultimate goal in therapeutics of renal fibrosis in chronic kidney diseases.

ACKNOWLEDGEMENTS

This study was supported by Office of the Higher Education Commission and Mahidol University under the National Research Universities Initiative, The Thailand Research Funds (RTA5380005 and TRG5480005), and Mahidol University. VT is also supported by the "Chalermphrakiat" Grant, Faculty of Medicine Siriraj Hospital

REFERENCES

- 1. Vilayur E, Harris DC. Emerging therapies for chronic kidney disease: what is their role? Nat Rev Nephrol. 2009;5(7):375-83.
- 2. Brosnahan G, Fraer M. Chronic kidney disease: whom to screen and how to treat, part 1: definition, epidemiology, and laboratory testing. South Med J. 2010;103(2):140-6.
- 3. Guarino M, Tosoni A, Nebuloni M. Direct contribution of epithelium to organ fibrosis: epithelial-mesenchymal transition. Hum Pathol. 2009;40(10):1365-76.
- 4. Kalluri R, Neilson EG. Epithelial-mesenchymal transition and its implications for fibrosis. J Clin Invest. 2003;112(12):1776-84.
- 5. Zeisberg M, Kalluri R. The role of epithelial-to-mesenchymal transition in renal fibrosis. J Mol Med (Berl). 2004;82(3):175-81.
- 6. Flier SN, Tanjore H, Kokkotou EG, Sugimoto H, Zeisberg M, Kalluri R. Identification of epithelial to mesenchymal transition as a novel source of fibroblasts in intestinal fibrosis. J Biol Chem. 2010;285(26):20202-12.
- 7. Zeisberg M, Neilson EG. Biomarkers for epithelial-mesenchymal transitions. J Clin Invest. 2009;119(6):1429-37.

- 8. Liu Y. Epithelial to mesenchymal transition in renal fibrogenesis: pathologic significance, molecular mechanism, and therapeutic intervention. J Am Soc Nephrol. 2004;15(1):1-12.
- 9. Xu J, Lamouille S, Derynck R. TGF-beta-induced epithelial to mesenchymal transition. Cell Res. 2009;19(2):156-72.
- 10. Strutz F, Okada H, Lo CW, Danoff T, Carone RL, Tomaszewski JE, et al. Identification and characterization of a fibroblast marker: FSP1. J Cell Biol. 1995;130(2):393-405.
- 11. Iwano M, Plieth D, Danoff TM, Xue C, Okada H, Neilson EG. Evidence that fibroblasts derive from epithelium during tissue fibrosis. J Clin Invest. 2002;110(3):341-50.
- 12. Rastaldi MP, Ferrario F, Giardino L, Dell'Antonio G, Grillo C, Grillo P, et al. Epithelial-mesenchymal transition of tubular epithelial cells in human renal biopsies. Kidney Int. 2002;62(1):137-46.
- Ivanova L, Butt MJ, Matsell DG. Mesenchymal transition in kidney collecting duct epithelial cells. Am J Physiol Renal Physiol. 2008;294(5):F1238-48.
- Liu M, Liu YZ, Feng Y, Xu YF, Che JP, Wang GC, et al. Novel evidence demonstrates that epithelial-mesenchymal transition contributes to nephrolithiasis-induced renal fibrosis.
 J Surg Res. 2013;182(1):146-52.
- Ferrazzano GF, Amato I, Ingenito A, De Natale A, Pollio A. Anti-cariogenic effects of polyphenols from plant stimulant beverages (cocoa, coffee, tea). Fitoterapia.
 2009;80(5):255-62.
- Inoue M, Sasazuki S, Wakai K, Suzuki T, Matsuo K, Shimazu T, et al. Green tea consumption and gastric cancer in Japanese: a pooled analysis of six cohort studies. Gut. 2009;58(10):1323-32.

- 17. Lorenz M, Urban J, Engelhardt U, Baumann G, Stangl K, Stangl V. Green and black tea are equally potent stimuli of NO production and vasodilation: new insights into tea ingredients involved. Basic Res Cardiol. 2009;104(1):100-10.
- 18. Hannig C, Sorg J, Spitzmuller B, Hannig M, Al-Ahmad A. Polyphenolic beverages reduce initial bacterial adherence to enamel in situ. J Dent. 2009;37(7):560-6.
- Melgarejo E, Medina MA, Sanchez-Jimenez F, Urdiales JL. Epigallocatechin gallate reduces human monocyte mobility and adhesion in vitro. Br J Pharmacol. 2009;158(7):1705-12.
- 20. Osterburg A, Gardner J, Hyon SH, Neely A, Babcock G. Highly antibiotic-resistant Acinetobacter baumannii clinical isolates are killed by the green tea polyphenol (-)-epigallocatechin-3-gallate (EGCG). Clin Microbiol Infect. 2009;15(4):341-6.
- 21. Arts IC, van De Putte B, Hollman PC. Catechin contents of foods commonly consumed in The Netherlands. 2. Tea, wine, fruit juices, and chocolate milk. J Agric Food Chem. 2000;48(5):1752-7.
- 22. Yao K, Ye P, Zhang L, Tan J, Tang X, Zhang Y. Epigallocatechin gallate protects against oxidative stress-induced mitochondria-dependent apoptosis in human lens epithelial cells. Mol Vis. 2008;14:217-23.
- 23. Itoh Y, Yasui T, Okada A, Tozawa K, Hayashi Y, Kohri K. Preventive effects of green tea on renal stone formation and the role of oxidative stress in nephrolithiasis. J Urol. 2005;173(1):271-5.
- 24. Jeong BC, Kim BS, Kim JI, Kim HH. Effects of green tea on urinary stone formation: an in vivo and in vitro study. J Endourol. 2006;20(5):356-61.
- 25. Abdel-Majeed S, Mohammad A, Shaima AB, Mohammad R, Mousa SA. Inhibition property of green tea extract in relation to reserpine-induced ribosomal strips of rough

- endoplasmic reticulum (rER) of the rat kidney proximal tubule cells. J Toxicol Sci. 2009;34(6):637-45.
- 26. Kim HK, Yang TH, Cho HY. Antifibrotic effects of green tea on in vitro and in vivo models of liver fibrosis. World J Gastroenterol. 2009;15(41):5200-5.
- 27. Sriram N, Kalayarasan S, Sudhandiran G. Epigallocatechin-3-gallate augments antioxidant activities and inhibits inflammation during bleomycin-induced experimental pulmonary fibrosis through Nrf2-Keap1 signaling. Pulm Pharmacol Ther. 2009;22(3):221-36.
- 28. Jonassen JA, Cao LC, Honeyman T, Scheid CR. Mechanisms mediating oxalate-induced alterations in renal cell functions. Crit Rev Eukaryot Gene Expr. 2003;13(1):55-72.
- 29. Khan SR, Shevock PN, Hackett RL. Acute hyperoxaluria, renal injury and calcium oxalate urolithiasis. J Urol. 1992;147(1):226-30.
- 30. Veena CK, Josephine A, Preetha SP, Varalakshmi P, Sundarapandiyan R. Renal peroxidative changes mediated by oxalate: the protective role of fucoidan. Life Sci. 2006;79(19):1789-95.
- 31. Boonla C, Krieglstein K, Bovornpadungkitti S, Strutz F, Spittau B, Predanon C, et al. Fibrosis and evidence for epithelial-mesenchymal transition in the kidneys of patients with staghorn calculi. BJU Int. 2011;108(8):1336-45.
- 32. Chen R, Wang JB, Zhang XQ, Ren J, Zeng CM. Green tea polyphenol epigallocatechin-3-gallate (EGCG) induced intermolecular cross-linking of membrane proteins. Arch Biochem Biophys. 2011;507(2):343-9.
- 33. Miyamoto Y, Haylor JL, El Nahas AM. Cellular toxicity of catechin analogues containing gallate in opossum kidney proximal tubular (OK) cells. J Toxicol Sci. 2004;29(1):47-52.

- 34. Miyamoto Y, Sano M, Haylor JL, El Nahas AM. (-)-Epigallocatechin 3-O-gallate (EGCG)-induced apoptosis in normal rat kidney interstitial fibroblast (NRK-49F) cells. J Toxicol Sci. 2008;33(3):367-70.
- 35. Jiang YS, Jiang T, Huang B, Chen PS, Ouyang J. Epithelial-mesenchymal transition of renal tubules: Divergent processes of repairing in acute or chronic injury? Med Hypotheses. 2013;81(1):73-5.
- 36. Pierratos AE, Khalaff H, Cheng PT, Psihramis K, Jewett MA. Clinical and biochemical differences in patients with pure calcium oxalate monohydrate and calcium oxalate dihydrate kidney stones. J Urol. 1994;151(3):571-4.
- 37. Watson JL, Ansari S, Cameron H, Wang A, Akhtar M, McKay DM. Green tea polyphenol (-)-epigallocatechin gallate blocks epithelial barrier dysfunction provoked by IFN-gamma but not by IL-4. Am J Physiol Gastrointest Liver Physiol. 2004;287(5):G954-61.
- 38. Suzuki T, Hara H. Role of flavonoids in intestinal tight junction regulation. J Nutr Biochem. 2011;22(5):401-8.
- 39. Chen C, Lu XH, Yan S, Chai H, Yao Q. HIV protease inhibitor ritonavir increases endothelial monolayer permeability. Biochem Biophys Res Commun. 2005;335(3):874-82.
- 40. Rashed T, Menon M, Thamilselvan S. Molecular mechanism of oxalate-induced free radical production and glutathione redox imbalance in renal epithelial cells: effect of antioxidants. Am J Nephrol. 2004;24(5):557-68.
- 41. Khan SR. Hyperoxaluria-induced oxidative stress and antioxidants for renal protection. Urol Res. 2005;33(5):349-57.
- 42. Khan SR. Stress oxidative: nephrolithiasis and chronic kidney diseases. Minerva Med. 2013;104(1):23-30.

- 43. Evan AP, Lingeman JE, Worcester EM, Bledsoe SB, Sommer AJ, Williams JC, Jr., et al. Renal histopathology and crystal deposits in patients with small bowel resection and calcium oxalate stone disease. Kidney Int. 2010;78(3):310-7.
- 44. Huang HS, Ma MC, Chen CF, Chen J. Lipid peroxidation and its correlations with urinary levels of oxalate, citric acid, and osteopontin in patients with renal calcium oxalate stones. Urology. 2003;62(6):1123-8.
- 45. Tungsanga K, Sriboonlue P, Futrakul P, Yachantha C, Tosukhowong P. Renal tubular cell damage and oxidative stress in renal stone patients and the effect of potassium citrate treatment. Urol Res. 2005;33(1):65-9.
- 46. Hirose M, Yasui T, Okada A, Hamamoto S, Shimizu H, Itoh Y, et al. Renal tubular epithelial cell injury and oxidative stress induce calcium oxalate crystal formation in mouse kidney. Int J Urol. 2010;17(1):83-92.
- 47. Itoh Y, Yasui T, Okada A, Tozawa K, Hayashi Y, Kohri K. Examination of the antioxidative effect in renal tubular cells and apoptosis by oxidative stress. Urol Res. 2005;33(4):261-6.
- 48. Thamilselvan V, Menon M, Thamilselvan S. Oxalate-induced activation of PKC-alpha and -delta regulates NADPH oxidase-mediated oxidative injury in renal tubular epithelial cells. Am J Physiol Renal Physiol. 2009;297(5):F1399-410.
- 49. Rhyu DY, Yang Y, Ha H, Lee GT, Song JS, Uh ST, et al. Role of reactive oxygen species in TGF-beta1-induced mitogen-activated protein kinase activation and epithelial-mesenchymal transition in renal tubular epithelial cells. J Am Soc Nephrol. 2005;16(3):667-75.

- 50. Zhang A, Dong Z, Yang T. Prostaglandin D2 inhibits TGF-beta1-induced epithelial-to-mesenchymal transition in MDCK cells. Am J Physiol Renal Physiol. 2006;291(6):F1332-42.
- 51. Kitamura M, Nishino T, Obata Y, Furusu A, Hishikawa Y, Koji T, et al. Epigallocatechin gallate suppresses peritoneal fibrosis in mice. Chem Biol Interact. 2012;195(1):95-104.
- 52. Cannito S, Novo E, di Bonzo LV, Busletta C, Colombatto S, Parola M. Epithelial-mesenchymal transition: from molecular mechanisms, redox regulation to implications in human health and disease. Antioxid Redox Signal. 2010;12(12):1383-430.

Figure legends

Figure 1. Morphological change induced by oxalate exposure. A) Control MDCK cells left untreated was appeared as a cobble-stone like morphology whereas B) the cells treated with 500 μ M sodium oxalate were induced to undergo morphological change within 24 h as more fibroblast-like in shape have been observed. Calcium oxalate monohydrate crystals (COM), the pathologic crystals were observed under treatment with 500 μ M sodium oxalate as indicated by arrows in B). Original magnification = 400X.

Figure 2. Western blot analysis to detect expression of vimentin (EMT marker), E-cadherin and occludin (epithelial markers). Vimentin was increase while E-cadherin and occludin were decreased in sodium oxalate-treated MDCK cells. GAPDH expression was used to control equal protein loading.

Figure 3. Alterations in expression level of EMT and epithelial markers by indirect immunofluorescence after sodium oxalate exposure. A) Increased level of vimentin and fibronectin (EMT protein markers while B) decreased level of cytokeratin, occludin, and ZO-1 (epithelial protein markers) were observed in sodium oxalate-treated MDCK cells.

Figure 4. Cytotoxic effect of EGCG to MDCK cells. Cells were treated with various dose of EGCG for 1 h and then trypsinized for determination of cell viability by trypan blue exclusion assay.

Figure 5. Western blot analysis of EMT and epithelial markers after pretreatment with EGCG. Western blot analysis showed a slight increased vimentin expression, while E-cadherin and occludin were decreased expression when compared to the control cells. Basal level of vimentin, E-cadherin, and occludin was found when cells were pretreated with EGCG. GAPDH expression was used to control equal protein loading

Figure 6. Expression of A) vimentin, fibronectin, B) cytokeratin, occludin, and ZO-1 was comparable to that of control cells when MDCK cells were pretreated with 25μM EGCG for 1 h before sodium oxalate exposure.

Figure 7. Preventive effect of EGCG by lower production of intracellular reactive oxygen species (ROS). ROS production was measured by DCFH-DA loading and analyzed by flow cytometry. MDCK cells left untreated and treated with hydrogen peroxide were serve as negative and positive control, respectively. Sodium oxalate treatment could induce ROS production significantly compared to the basal stage (P < 0.0001). Pretreatment with EGCG before sodium oxalate treatment could markedly reduce production of ROS (Oxalate VS EGCG+oxalate, P < 0.0002). P<0.05 was considered statistical significant. Symbols: §, statistically significant versus control; ¥, statistically significant versus oxalate.

Figure1.

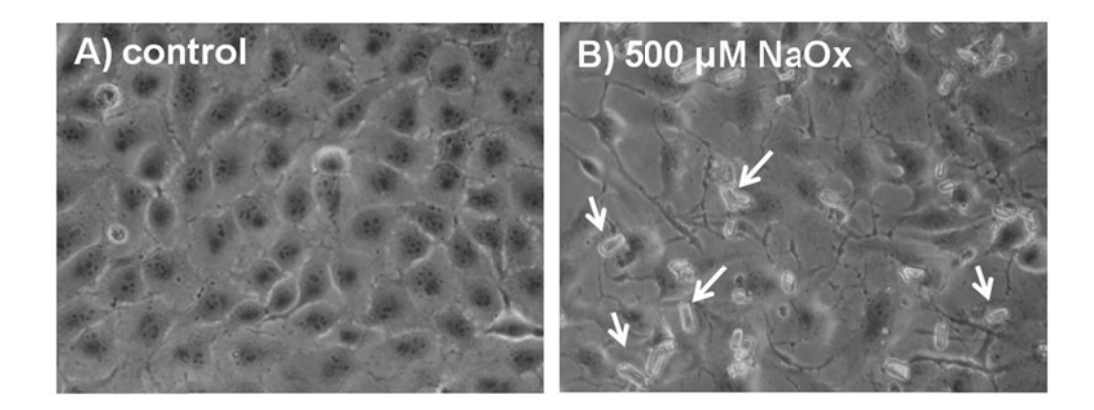


Figure 2.

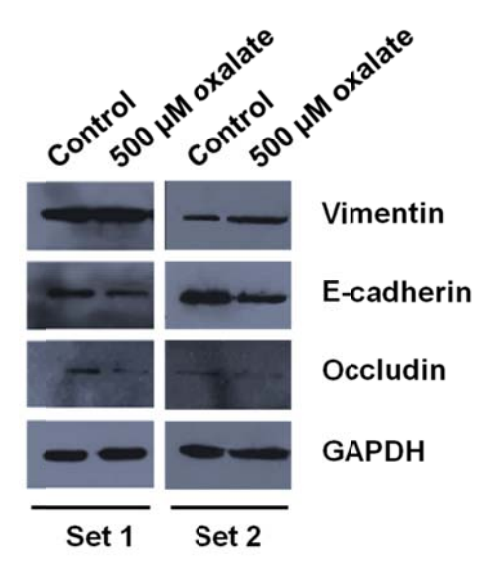


Figure 3.

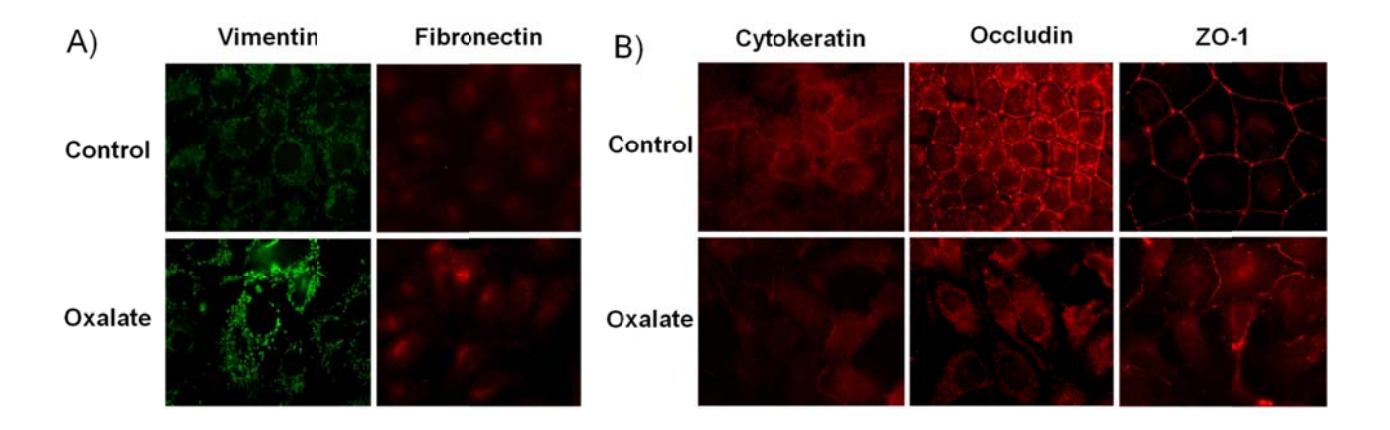


Figure 4.

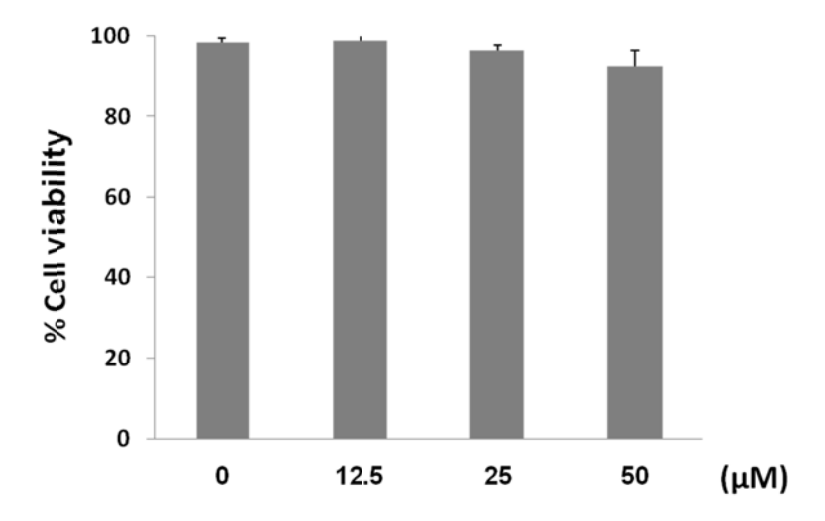


Figure 5.

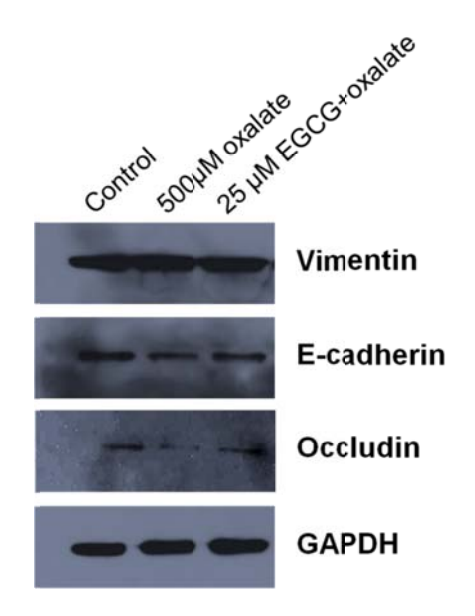


Figure6.

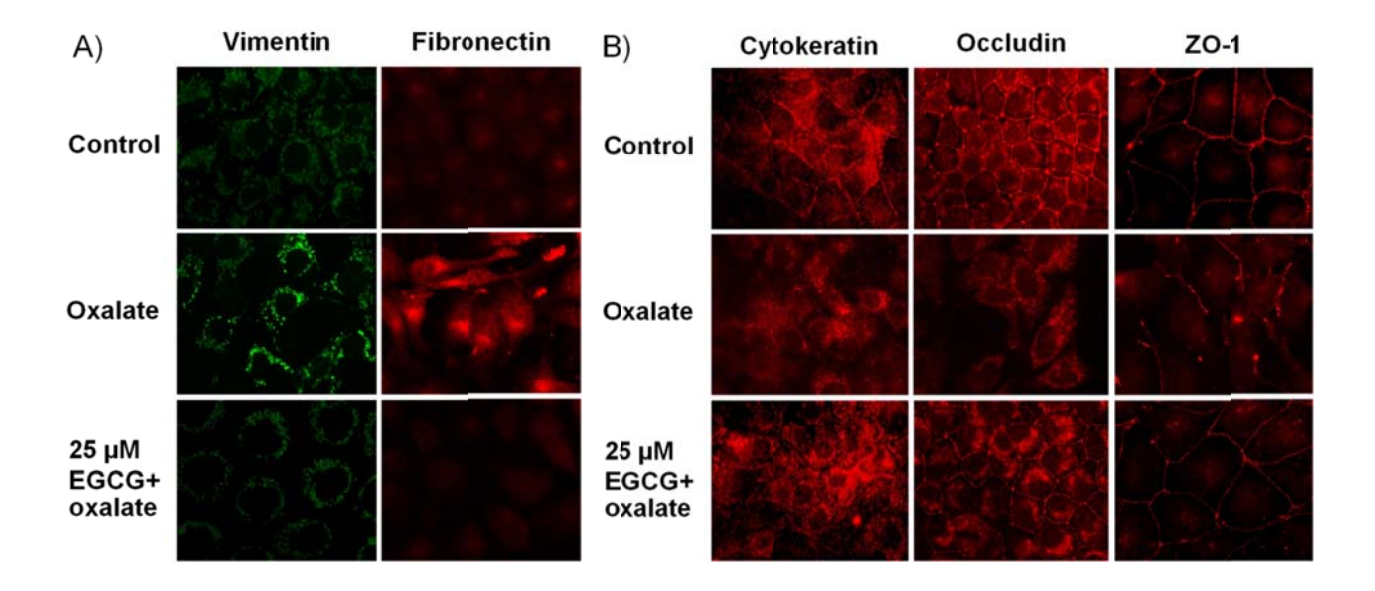


Figure7.

